5 8

NASA Contractor Report NASA/CR-2000-208582

Delta II Explosion Plume Analysis Report

Prepared by:
Applied Meteorology Unit

Prepared for:
Kennedy Space Center
Under Contract NAS10-96018

NASA
National Aeronautics and
Space Administration

Office of Management

Scientific and Technical
Information Program

2000

ATTRIBUTES AND ACKNOWLEDGMENTS:

NASA/KSC POC:
Dr. Francis J. Merceret
YA-D

Applied Meteorology Unit (AMU):

Randolph J. Evans

Executive Summary

A Delta II rocket exploded seconds after liftoff from Cape Canaveral Air Force Station (CCAFS) on 17 January 1997. The cloud produced by the explosion provided an opportunity to evaluate the models which are used to track potentially toxic dispersing plumes and clouds at CCAFS. The primary goal of this project was to conduct a case study of the dispersing cloud and the models used to predict the dispersion resulting from the explosion. The case study was conducted by comparing mesoscale and dispersion model results with available meteorological and plume observations. This study was funded by KSC under Applied Meteorology Unit (AMU) option hours.

The models used in the study are part of the Eastern Range Dispersion Assessment System (ERDAS) and include the Regional Atmospheric Modeling System (RAMS), HYbrid Particle And Concentration Transport (HYPACT), and Rocket Exhaust Effluent Dispersion Model (REEDM). Two different versions of RAMS were used in this study: RAMS version 3a from the ERDAS prototype system and RAMS version 4a from the Parallelized RAMS Operational Weather Simulation System (PROWESS).

The primary observations used for explosion cloud verification of the study were from the National Weather Service's Weather Surveillance Radar 1988-Doppler (WSR-88D). Radar reflectivity measurements of the resulting cloud provided good estimates of the location and dimensions of the cloud over a four-hour period after the explosion.

Meteorological data from local observations and sensors provided a basis for comparison with meteorological model output. The meteorological conditions on this day were strongly influenced by synoptic rather than local forcing. Observed data were obtained from the WINDS tower network at CCAFS/Kennedy Space Center (KSC), rawinsonde data from CCAFS, 915 MHz and 50 MHz radar wind profilers at CCAFS/KSC, and standard local station and buoy observations.

In this report, the terms plume and cloud are used interchangeably. In dispersion meteorology, a plume is usually thought of as an elongated mass of gaseous or particulate material that emanates from a source and widens and disperses with the flow of the wind. A cloud is usually referred to as visible mass of gas or particles shaped like a sphere. When the Delta II exploded, it initially produced a large cloud that dispersed and moved downwind in a plume-like fashion.

The conclusions of this study can be categorized according to the plume observation technique and according to the models used in the analysis. The findings of this study are:

WSR-88D radar as a plume observation tool

- The WSR-88D is a good tool for providing plume tracks from rocket explosion plumes. The radar provided excellent data on the location and track of the resulting potentially toxic cloud. The data were extremely useful for model verification since no ongoing program is in place to measure plume track or concentrations. Bud Parks of ACTA, Inc. is conducting a study to capture data from nominal and abort launch clouds and has captured radar data from three Eastern Range abort clouds and 36 of 46 (78%) nominal launch clouds (Parks and Evans 1998).

- The WSR-88D does not provide concentration data. The only data obtained by the radar is the reflectivity value measured in dBZ. While this measurement gives an estimate on the relative density of material (smoke particles, water, dust, or other particulate matter), a methodology is needed to convert dBZ to concentrations of hydrochloric acid (HCl), nitrogen tetroxide (N_2O_4), or other materials of interest. One of Range Safety's main concerns is determining the exposure limit (concentration over a specified time) of certain toxic materials.

  A dark orange cloud at the very top of the large lower cloud was initially visible. The dark orange cloud most likely contained some amount of nitrogen tetroxide. Because it was located near the top of the cloud, it is unsure how much, if any, of the N_2O_4 mixed within the cloud and made it to the surface. Our analysis was not able to determine the concentration of N_2O_4 in the explosion cloud.

- Vertical plume height data for this case was not very accurate. The radar appeared to accurately track the clouds' trajectories in the x-y dimension. However, the vertical measurements appeared to be inaccurate for two reasons. The first reason was that for long distances from the radar, such as the 35+ kilometers distance from Melbourne to Cape Canaveral, the radar beam widened enough to introduce inaccuracies in the vertical plume height measurements. The second reason for inaccurate vertical measurements was because of the strong inversion causing the radar beam to bend and bring about measurement inaccuracies.

RAMS model

- The vertical wind profile predictions in this case show agreement with observations. Both ERDAS and PROWESS configurations of RAMS produced wind flow measurements that matched closely with rawinsonde and profiler measurements and seemed to provide adequate input to HYPACT.
- RAMS under-predicted onshore flow at the level of the Delta II cloud. Both versions of RAMS predicted onshore flow in the 600- to 900-meter layer in the area south of Cape Canaveral. However, the observed winds had more of a northeast, onshore component than the RAMS-predicted winds. The movement of the actual explosion cloud tracked onshore north of the model-predicted cloud. The prototype ERDAS RAMS predicted winds with more of an onshore component than PROWESS RAMS.
- RAMS accurately predicted the strength and height of inversion for this case. The well-defined inversion that was measured by rawinsonde and based at approximately 800 meters above the ground was predicted by RAMS to be based at approximately 750 meters above the ground. The inversion, as determined by the vertical temperature profile, had a significant influence on the explosion cloud.

REEDM source term

- Characterizing the source term of unique explosions is difficult. If a rocket explosion occurs, the circumstances will be different each time it happens. For example: What was the flight time? How much fuel was consumed? What were the height, location and distribution of the explosion products? Were the hazardous and toxic materials separated or mixed within the cloud? Did the second stage ascend and then explode as with the Delta II? Did the solid rocket motors explode immediately or did they follow an errant path before they exploded? All of these questions make it difficult to develop a model that will accurately assess and characterize the source term. We were able to use information obtained after-the-fact from radar and video to characterize the source term but in a real-time scenario only estimates of the source term characterization can be made.
- Splitting the source into two sources for HYPACT model was a reasonable approximation. In the post-explosion mode of this analysis, we split the source into two sources for the HYPACT model based on observations. This methodology proved better for this case as opposed to using the single column source term that was generated by REEDM. In real-time, REEDM currently does not split the source term.

HYPACT model

- Plume came onshore further to the north and earlier than predicted. HYPACT moved the large lower cloud resulting from the Delta II explosion onshore at a point that was approximately 12 kilometers south of where it actually came onshore. HYPACT predicted the plume would come across the coastline in the Satellite Beach/Indian Harbor Beach area when it actually crossed the coastline in the Cocoa Beach area. The observed winds at the level moving the cloud at 600-900 m were northerly prior to the explosion but then shifted to northeasterly during the 1-2 hours following the explosion. RAMS predicted the shift of these winds from northerly to northeasterly but did not predict the shift as quickly as observed. RAMS supplies wind and meteorological data to HYPACT. Because of RAMS' gradual response to shift the winds, HYPACT missed the location and timing of the plume impact on the coastline.

- Trajectory, diffusion and timing of HYPACT plumes showed similarities to observed plume. Except for the problem mentioned above, the trajectory, diffusion, and the timing of the HYPACT plumes were similar to the plumes observed by radar. One favorable result was noted in the spread and diffusion of the lower cloud as it moved south. The cloud spread in the crosswind direction at a rate and in distance similar to observed.
- Range Safety's REEDM predicted the movement of plume to the south (176 degrees). REEDM using the 1613 UTC rawinsonde from Cape Canaveral moved the plume to the south and kept it offshore until it reached the Melbourne Beach area. REEDM did not account for the winds with an easterly component that existed at a height of 700-800 meters in the area over the ocean to the south of Cape Canaveral.

Recommendations

- Develop methodology to correlate concentrations with radar reflectivity measurements. The WSR-88D proved to be a valuable tool in tracking nominal and abort rocket plumes. However, the radar provides no information on the concentrations within the clouds. What is needed is measurement of concentrations within the plumes using a sample collection method or another remote sensing technique such as lidar. This data could then be correlated with radar measurements of reflectivity in dBZ.
- Improvements are needed in HYPACT plume dynamics algorithms. HYPACT currently treats plumes as non-buoyant, non-depositing entities. We recommend that future enhancements should be made to HYPACT to improve its ability to handle buoyant plumes and particle deposition. These improvements would allow HYPACT to model rocket exhaust plumes better than the current version of HYPACT.
- Conduct other studies of rocket explosion plumes. Since the explosion of the Delta II, two other rockets have exploded after launch from Cape Canaveral-Titan IV on 12 August 1998 and Delta III on 26 August 1998. In both cases the explosion clouds were tracked by WSR-88D radar. Detailed studies should be conducted to verify mesoscale models, diffusion models, and radar tracking techniques.

Table of Contents

Executive Summary ... iii
Table of Contents ... vi
List of Tables ... xii
List of Acronyms ... xiii
1. Introduction ... 1
2. Background and Study Procedures ... 2
2.1. Delta II Explosion Event ... 2
2.2. Data Sources ... 3
2.2.1. Radar data ... 3
2.2.2. Meteorological data ... 6
2.2.3. Satellite data ... 7
2.3. Model description/configuration ... 7
2.3.1. ERDAS/PROWESS development ... 7
2.3.2. RAMS-ERDAS ... 8
2.3.3. RAMS-PROWESS ... 8
2.3.4. HYPACT-ERDAS and HYPACT-PROWESS ... 9
2.3.5. REEDM ... 9
3. Results ... 11
3.1. Observed data ... 11
3.1.1. Meteorology on 17 January 1997 ... 11
3.1.2. Visual observations ... 14
3.1.3. Satellite data ... 17
3.1.4. Radar data ... 18
3.1.4.1. Cloud 1 ... 22
3.1.4.2. Cloud 2 ... 23
3.2. Model data ... 32
3.2.1. REEDM results ... 32
3.2.2. RAMS results from ERDAS and PROWESS ... 33
3.2.3. HYPACT results from ERDAS and PROWESS ... 43
3.2.3.1. HYPACT Configuration ... 43
3.2.3.2. HYPACT runs ... 44
3.2.3.3. HYPACT results ... 44
3.2.3.4. HYPACT results summary ... 45
3.2.4. ERDAS HYPACT trajectory analysis ... 57
4. Conclusions and Recommendations ... 59

5. References 62
APPENDIX A ERDAS RAMSIN file 64
APPENDIX B PROWESS RAMSIN file 74
APPENDIX C ERDAS HYPACT_IN file 84
APPENDIX D PROWESS HYPACT_IN file 88

List of Figures

Figure 1. Photograph of Delta II explosion at 1628 UTC on 17 January 1997. 2
Figure 2. Damage crater resulting from falling debris from Delta II on 17 January 1997. 3
Figure 3. WSR-88D image from National Weather Service captured at 1625-1635 UTC on 17 January 1997. Launch occurred at 1628 UTC. 4
Figure 4. WSR-88D image from National Weather Service captured at 1655-1706 UTC on 17 January 1997. 5
Figure 5. Surface map of eastern United States at 1800 UTC on 17 January 1997. 12
Figure 6. Graph of potential temperature profile versus height for three rawinsondes on 17 Jan 1997. 13
Figure 7. Graph of wind speed (WS) and wind direction (WD) versus height from rawinsonde at 1815 UTC on 17 January 1997. 13
Figure 8. The two clouds produced from the explosion of the vehicle a few seconds after the explosion on 17 January 1997. This picture was captured from amateur video taken along Cocoa Beach. 15
Figure 9. The two explosion clouds at approximately 16 seconds after the explosion. Note the orange area located at the top of Plume 1. 16
Figure 10. Zoomed in view of explosion clouds at approximately 12 seconds after the explosion. The small orange cloud at the top of the lower cloud most likely contains nitrogen tetroxide. 16
Figure 11. GOES satellite image of Delta II explosion cloud at 1645 UTC 17 January 1997. (from Brandli 1997). 17
Figure 12. GOES satellite image of Delta II explosion cloud at 1715 UTC 17 January 1997. (from Brandli 1997). 18
Figure 13. Composite radar image from Melbourne WSR-88D for 10-minute scan beginning at 1635 UTC. A-B line indicates cross section shown in Figure 14. 20
Figure 14. Cross section of composite radar image for 1635 UTC. East-west cross section location shown in Figure 13. 20
Figure 15. Composite radar image from Melbourne WSR-88D for 10-minute scan beginning at 1833 UTC. A-B line indicates cross section shown in Figure 16. 21
Figure 16. Cross section of composite radar image for 1833 UTC. East-west cross section location shown in Figure 15. 21
Figure 17. WSR-88D composite scan beginning at 1616 UTC. 24
Figure 19. WSR-88D composite scan beginning at 1635 UTC. 24
Figure 18. WSR-88D composite scan beginning at 1625 UTC. 24
Figure 20. WSR-88D composite scan beginning at 1645 UTC. 24
Figure 21. WSR-88D composite scan beginning at 1655 UTC. 25
Figure 23. WSR-88D composite scan beginning at 1715 UTC. 25
Figure 22. WSR-88D composite scan beginning at 1705 UTC. 25
Figure 24. WSR-88D composite scan beginning at 1725 UTC. 25
Figure 25. WSR-88D composite scan beginning at 1735 UTC. 26
Figure 27. WSR-88D composite scan beginning at 1754 UTC. 26
Figure 26. WSR-88D composite scan beginning at 1745 UTC. 26

Figure 28. WSR-88D composite scan beginning at 1804 UTC. 26
Figure 29. WSR-88D composite scan beginning at 1814 UTC. 27
Figure 31. WSR-88D composite scan beginning at 1833 UTC. 27
Figure 30. WSR-88D composite scan beginning at 1824 UTC. 27
Figure 32. WSR-88D composite scan beginning at 1843 UTC. 27
Figure 33. WSR-88D composite scan beginning at 1853 UTC. 28
Figure 35. WSR-88D composite scan beginning at 1913 UTC. 28
Figure 34. WSR-88D composite scan beginning at 1903 UTC. 28
Figure 36. WSR-88D composite scan beginning at 1922 UTC. 28
Figure 37. WSR-88D composite scan beginning at 1932 UTC. 29
Figure 39. WSR-88D composite scan beginning at 1952 UTC. 29
Figure 38. WSR-88D composite scan beginning at 1942 UTC. 29
Figure 40. WSR-88D composite scan beginning at 2002 UTC. 29
Figure 41. WSR-88D composite scan beginning at 2011 UTC. 30
Figure 42. WSR-88D composite scan beginning at 2021 UTC. 30
Figure 43. The plume height of the lower cloud (Plume 1) over the 4-h period. Heights were determined using the 88Display software tool.. 31
Figure 44. The plume height of the upper cloud (Plume 2) over the 4-h period. Heights were determined using the 88Display software tool. 31
Figure 45. REEDM plots from the 1613 UTC rawinsonde just prior to the Delta II rocket failure on 17 January 1997. 32
Figure 46. REEDM cross-section plot showing rawinsonde data from 1613 UTC on the left and REEDM source term predictions on the right. 33
Figure 47. Observed wind speed and direction from rawinsonde at 1613 UTC. Note that the observed wind directions from 0 - 15° are shown on the graph as greater than 360°. 34
Figure 48. Predicted wind speed and direction from ERDAS RAMS at 1600 UTC. Note that the observed wind directions from 0 - 15° are shown on the graph as greater than 360°. 34
Figure 49. Rawinsonde-observed potential temperature at 1613 UTC compared to model-predicted potential temperature at 1600 UTC. The model predictions were from ERDAS RAMS. 35
Figure 50. Streamline forecasts comparing output from ERDAS and PROWESS on 17 January 1997. Each figure is marked with its model configuration, time, and height. 37
Figure 51. Streamline forecasts comparing output from ERDAS and PROWESS on 17 January 1997. Each figure is marked with its model configuration, time, and height. 38
Figure 52. Streamline forecasts comparing output from ERDAS and PROWESS on 17 January 1997. Each figure is marked with its model configuration, time, and height. 39
Figure 53. Streamline forecasts comparing output from ERDAS and PROWESS on 17 January 1997. Each figure is marked with its model configuration, time, and height. 40
Figure 54. Surface temperature (F) forecasts comparing output from the lowest levels of ERDAS (10 m) and PROWESS (35 m) on 17 January 1997. 41
Figure 55. Potential temperature (K) cross section forecasts comparing output from ERDAS and PROWESS on 17 January 1997. 42

Figure 56. ERDAS HYPACT, 1630 UTC, 17 Jan 1997. 47
Figure 57. Same as Figure 56, vertical view from south. 47
Figure 58. ERDAS HYPACT, 1640 UTC, 17 Jan 1997. 47
Figure 59. Same as Figure 58, vertical view from south. 47
Figure 60. ERDAS HYPACT, 1650 UTC, 17 Jan 1997. 47
Figure 61. Same as Figure 60, vertical view from south. 47
Figure 62. ERDAS HYPACT, 1700 UTC, 17 Jan 1997. 48
Figure 63. Same as Figure 62, vertical view from south. 48
Figure 64. ERDAS HYPACT, 1710 UTC, 17 Jan 1997. 48
Figure 65. Same as Figure 64, vertical view from south. 48
Figure 66. ERDAS HYPACT, 1720 UTC, 17 Jan 1997. 48
Figure 67. Same as Figure 66, vertical view from south. 48
Figure 68. ERDAS HYPACT, 1730 UTC, 17 Jan 1997. 49
Figure 69. Same as Figure 68, vertical view from south. 49
Figure 70. ERDAS HYPACT, 1740 UTC, 17 Jan 1997. 49
Figure 71. Same as Figure 70, vertical view from south. 49
Figure 72. ERDAS HYPACT, 1800 UTC, 17 Jan 1997. 49
Figure 73. Same as Figure 72, vertical view from south. 49
Figure 74. ERDAS HYPACT, 1820 UTC, 17 Jan 1997. 50
Figure 75. Same as Figure 74, vertical view from south. 50
Figure 76. ERDAS HYPACT, 1840 UTC, 17 Jan 1997. 50
Figure 77. Same as Figure 76, vertical view from south. 50
Figure 78. ERDAS HYPACT, 1900 UTC, 17 Jan 1997. 50
Figure 79. Same as Figure 78, vertical view from south. 50
Figure 80. ERDAS HYPACT, 1930 UTC, 17 Jan 1997. 51
Figure 81. Same as Figure 80, vertical view from south. 51
Figure 82. ERDAS HYPACT, 2000 UTC, 17 Jan 1997. 51
Figure 83. Same as Figure 82, vertical view from south. 51
Figure 84. ERDAS HYPACT, 2030 UTC, 17 Jan 1997. 51
Figure 85. Same as Figure 84, vertical view from south. 51
Figure 86. PROWESS HYPACT, 1630 UTC, 17 Jan 1997. 52
Figure 87. Same as Figure 86, vertical view from south. 52
Figure 88. PROWESS HYPACT, 1640 UTC, 17 Jan 1997. 52
Figure 89. Same as Figure 88, vertical view from south. 52
Figure 90. PROWESS HYPACT, 1650 UTC, 17 Jan 1997. 52
Figure 91. Same as Figure 90, vertical view from south. 52

Figure 92. PROWESS HYPACT, 1700 UTC, 17 Jan 1997. 53
Figure 93. Same as Figure 92, vertical view from south. 53
Figure 94. PROWESS HYPACT, 1710 UTC, 17 Jan 1997. 53
Figure 95. Same as Figure 94, vertical view from south. 53
Figure 96. PROWESS HYPACT, 1720 UTC, 17 Jan 1997. 53
Figure 97. Same as Figure 96, vertical view from south. 53
Figure 98. PROWESS HYPACT, 1730 UTC, 17 Jan 1997. 54
Figure 99. Same as Figure 98, vertical view from south. 54
Figure 100. PROWESS HYPACT, 1740 UTC, 17 Jan 1997. 54
Figure 101. Same as Figure 100, vertical view from south. 54
Figure 102. PROWESS HYPACT, 1800 UTC, 17 Jan 1997. 54
Figure 103. Same as Figure 102, vertical view from south. 54
Figure 104. PROWESS HYPACT, 1820 UTC, 17 Jan 1997. 55
Figure 105. Same as Figure 104, vertical view from south. 55
Figure 106. PROWESS HYPACT, 1840 UTC, 17 Jan 1997. 55
Figure 107. Same as Figure 106, vertical view from south. 55
Figure 108. PROWESS HYPACT, 1900 UTC, 17 Jan 1997. 55
Figure 109. Same as Figure 108, vertical view from south. 55
Figure 110. PROWESS HYPACT, 1930, UTC, 17 Jan 1997. 56
Figure 111. Same as Figure 110, vertical view from south. 56
Figure 112. PROWESS HYPACT, 2000 UTC, 17 Jan 97. 56
Figure 113. Same as Figure 112, vertical view from south. 56
Figure 114. PROWESS HYPACT, 2030 UTC, 17 Jan 97. 56
Figure 115. Same as Figure 114, vertical view from south. 56
Figure 116. Data of observed vs. predicted plume location for lower plume resulting from Delta II explosion at 1628 UTC on 17 January 1997. 58

List of Tables

Table 1. Wind speed and direction from the 50-MHz profiler at KSC on 17 January 1997. 14

Table 2. Data obtained from WSR-88D Level II archive for 17 January 1997 using the 88Display software. Data in this table show Plume 1 (lower cloud) information. 19

Table 3. Data obtained from WSR-88D Level II archive for 17 January 1997 using the 88Display software. Data in this table show Plume 2 (upper cloud) information. 19

Table 4. Location and dimensions of plume determined by REEDM and modeled by HYPACT. These plume dimensions were used in the ERDAS HYPACT simulation. 43

Table 5. Location and dimensions of plume determined from visual and radar observations and modeled by HYPACT. These plume dimensions were used in the PROWESS HYPACT simulation. 43

List of Acronyms

Term	Description
45 WS	45th Weather Squadron
AMU	Applied Meteorology Unit
CCAFS	Cape Canaveral Air Force Station
LC-17	Launch complex 17A
DRWP	Doppler Radar Wind Profiler
EHS	Extremely Hazardous Substances
ERDAS	Eastern Range Dispersion Assessment System
GOES	Geostationary Operational Environmental Satellite
HCl	Hydrochloric acid
HYPACT	HYbrid Particle And Concentration Transport
IRIS	Interactive Radar Information System
KSC	Kennedy Space Center
LAN	Local Area Network
MARSS	Meteorological And Range Safety Support
MARSS-REPL	MARSS Replacement
MRC	Mission Research Corporation
MIDDS	Meteorological Interactive Data Display System
MLB	Melbourne, Florida
N_2O_4	Nitrogen tetroxide
NCEP	National Centers for Environmental Prediction
NEXRAD	NEXt generation RADar
NGM	Nested Grid Model
NWS	National Weather Service
OBDG	Ocean Breeze/Dry Gulch
PROWESS	Parallelized RAMS Operational Weather Simulation System
REEDM	Rocket Exhaust Effluent Dispersion Model
RAMS	Regional Atmospheric Modeling System
ROCC	Range Operations Control Center
UDMH	Unsymmetrical dimethyl hydrazine
VCP	Volume Coverage Pattern
WINDS	Weather Information Network Display System
WSR-88D	Weather Surveillance Radar-1988 Doppler

1. Introduction

The primary goal of this study was to conduct a case study of the dispersing plume and cloud resulting from the Delta II explosion on 17 January 1997 at Cape Canaveral Air Force Station (CCAFS). The case study was conducted by comparing mesoscale and dispersion model results with available meteorological and plume observations. This study was funded by KSC under Applied Meteorology Unit (AMU) option hours.

The models used in the study are part of the Eastern Range Dispersion Assessment System (ERDAS). These models include:

- Regional Atmospheric Modeling System (RAMS) - A nested primitive equation mesoscale meteorological prediction model.
- HYbrid Particle And Concentration Transport (HYPACT) model - A Lagrangian particle diffusion model.
- Rocket Exhaust Effluent Dispersion Model (REEDM).

A description of ERDAS and its models is found in Lyons and Tremback (1994), Evans (1996), and Evans et al. (1996).

The primary observations used for plume verification of the study were from the National Weather Service's Weather Surveillance Radar 1988-Doppler (WSR-88D). Radar reflectivity measurements of the resulting cloud provided good estimates of the location and dimensions of the cloud over a four-hour period after the explosion.

Meteorological data from local observations and sensors provided a basis for comparison with meteorological model output. The meteorological conditions on this day were strongly influenced by synoptic rather than local forcing. Observed data were obtained from the WINDS tower network at CCAFS/Kennedy Space Center (KSC), rawinsonde data from CCAFS, 915 MHz and 50 MHz radar wind profilers at CCAFS/KSC, and standard local station and buoy observations.

This report describes the modeling analysis which was conducted using the ERDAS models. Section 2 provides background information on the ERDAS system, the observed radar and meteorological data, the explosion and provides some references to analyses conducted by others on the Delta II explosion. Section 3 presents results of the radar data reduction effort and the mesoscale and dispersion modeling analyses. Section 4 presents conclusions of the study and recommendations for future operational analyses.

2. Background and Study Procedures

2.1. Delta II Explosion Event

The Delta II rocket was launched from Launch Complex 17 (LC-17) at CCAFS at 1628 UTC on 17 January 1997. It exploded 12.5 seconds after liftoff at a height of approximately 438 meters. Figure 1 shows a photograph of the explosion. This initial explosion destroyed only the first stage and the boosters and produced a large cloud extending from the ground upward. The Delta II is a three-stage liquid-propellant vehicle with nine solid-propellant strap-on booster motors. The second and third stages and payload survived the initial explosion and continued upward to about 760 meters at 22.4 seconds. Destruct signals were sent at this point, and the exploding second-stage formed a buoyant cloud that rose above and separated from the lower cloud. Detailed information on the rocket and explosion scenario is found in Ha and Deane (1998). An example of damage caused by the falling debris is presented in Figure 2.

Figure 1. Photograph of Delta II explosion at 1628 UTC on 17 January 1997.

The clouds drifted in two primary directions. The lower cloud drifted to the south over the next few hours passing over the Atlantic Ocean south of Cape Canaveral, over Cocoa Beach and Melbourne and continued south through Indian River County. The upper cloud moved toward the east remaining over the ocean. The cause of the formation of two separate plumes was strong wind shear across a temperature inversion at about 910 m. Winds below the inversion were on the order of 11 m sec^{-1} from the north and north-northwest. Immediately above the base of the inversion the observed winds were within a few degrees of due northerly, then backed rapidly with height, and became northwesterly above 1350 m and westerly above about 2400 meters. Descriptions of the meteorology and plume track for this event are discussed in Pace et al. (1998), Parks and Evans (1998), and Ha and Deane (1998).

Figure 2. Damage crater resulting from falling debris from Delta II on 17 January 1997.

2.2. Data Sources

2.2.1. Radar data

The Weather Surveillance Radar 1988-Doppler (WSR-88D), also known as NEXt generation RADar (NEXRAD), is a powerful, modern radar with advanced computer processing to provide a wealth of atmospheric data with high accuracy and resolution. The radar operates at an S-band wavelength of approximately 10.7 centimeters with an operating power of 750 kilowatts and a peak power of 1 megawatt. The WSR-88D antenna is a parabolic dish 28 feet (8.5 m) in diameter, which produces a 1-degree diameter conical beam. The antenna rotates continuously in azimuth at a maximum speed of 5 rotations per minute and moves in predetermined incremental steps in elevation from 0.5 to 19.5 degrees. The elevation steps are determined by the volume coverage pattern (VCP) being used. The radar can operate in storm-mode to detect precipitation or in clear-air mode when no precipitation is within range. In storm mode the antenna turns rapidly and completes a full volume scan cycle in 5 or 6 minutes. In clear-air mode the radar antenna turns more slowly and transmits a more powerful pulse of energy to detect targets weaker than precipitation. In this mode the volume scan pattern is limited to scans at 0.5, 1.5, 2.5, 3.5, and 4.5-degree elevation angles. The antenna rotates full circle in the horizontal for approximately 2 minutes at each elevation angle before stepping up to scan the next higher angle, completing the full volume scan cycle in 10 minutes.

It has been known for some time that the WSR-88D can detect a wide variety of phenomena. These include raindrops, dust, insects, birds, smoke, and refractive gradients. Other studies have used Doppler radars to detect smoke plumes. Rogers and Brown (1997) used an S-band (10-cm wavelength) scanning radar to track the advection and spread of a smoke plume generated by a large industrial fire in Montreal, Canada. They concluded that radar observations may be useful in monitoring plume behavior and estimating the amount of particulate material in plumes, although such estimates require better knowledge of the refractive index of the material than now seems to be available. Banta et al (1992) observed smoke plumes from forest fires using Doppler radar.

It wasn't known how well the radar could detect the abort cloud from a launch vehicle failure until the Delta II explosion at Cape Canaveral was observed on 17 January 1997. A detailed analysis of the Delta II abort cloud will be described in Section 3.1.4.

At the time of the explosion, the National Weather Service in Melbourne monitored the track of the plume using the WSR-88D. The Melbourne WSR-88D radar is the closest one to Cape Canaveral. Images obtained from their archives are presented in Figures 3 and 4. These images show how clearly the radar detects the smoke, water, and other particles contained in the cloud. Local television stations also tracked the movement of the cloud using their weather radar and then broadcast these images to the public.

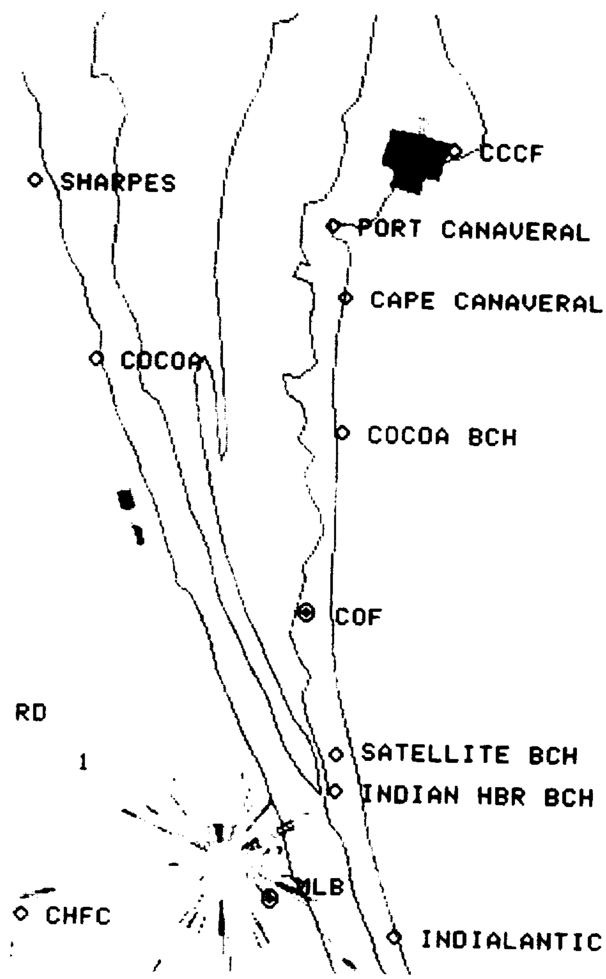

Figure 3. WSR-88D image from National Weather Service captured at 1625-1635 UTC on 17 January 1997. Launch occurred at 1628 UTC.

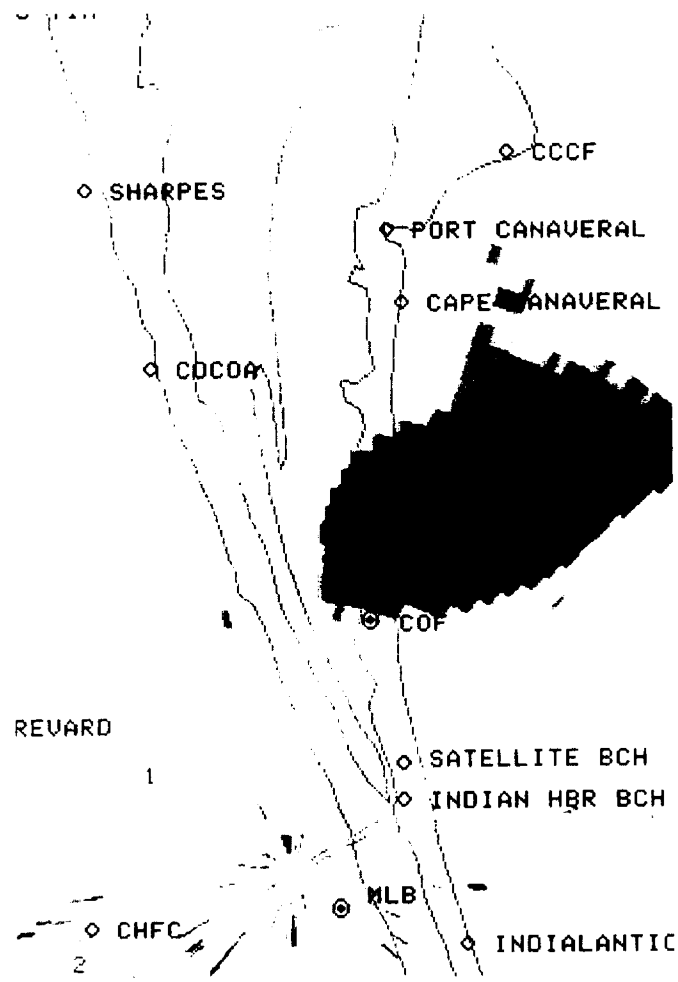

Figure 4. WSR-88D image from National Weather Service captured at 1655-1706 UTC on 17 January 1997.

The WSR-88D was a very good tool for tracking the location of the Delta II abort cloud. However, it was not able to provide concentrations of the toxic emissions resulting from the abort. The Delta launch complex is located 37 km from the radar antenna at an azimuth of 14 degrees from north. On 17 January, the radar was operating in clear-air mode and had begun a new volume scan series at 1626 UTC. The lowest elevation scan at 0.5 degrees would have ended and the 1.5-degree elevation scan just begun when the Delta II rocket lifted off at 1628 UTC. Therefore, the 0.5-degree scan showed no return from the LC-17 area. However, the 1.5-degree scan detected a strong echo directly over LC-17. The radar beam centerline was 1123 m above the ground and the beam was more than 610 m in diameter at this point. The strength of the echo was 46 dBZ as determined by the Level-2 data archive.

The radar also could not provide a precise height of the base or top of the cloud. An error on the order of 600 meters can result from the diameter of the beam at these ranges. An echo-free elevation slice above and below the cloud is also needed to bound the error. No slice was ever completely under the cloud, and with the maximum scan angle only 4.5 degrees, the cloud tops were only estimated as well. An even greater error in cloud altitude is likely because of the 5 degree Celsius temperature inversion near 900 meters. The height of the radar beam is calculated on the basis of normal atmospheric refraction of the beam. However, when temperature increases and humidity decreases as in this inversion, the radar beam is bent downward from it's normal path (Doviak and Zrnic 1993). Therefore, all radar measurements of cloud heights above 900 m are almost certainly too high by a significant amount due to superrefraction of the radar beam.

After the explosion, the Melbourne WSR-88D data for 17 January were obtained for analysis. The analyses were conducted using the software package 88Display (Hoffert and Pearce 1996). 88Display contains features which allow users to display detailed Level II data and to obtain various parameters associated with the radar echoes. Level II data are base data which include base reflectivity, mean radial velocity, and spectrum width.

The features of 88Display include displaying composite reflectivity for all elevation angles, display base reflectivity for each elevation angle, building animated time loops, and also displaying vertical cross-sections. The cross sections can be built using any two user-selected points from a map of the composite or base reflectivities. Another very useful feature of the software is the information query function. When a user clicks the mouse on an echo feature on the map, the program returns data on elevation, azimuth, ground range (distance from radar), latitude, longitude, and height above ground. This information is based on elevation angle of the currently selected scan.

The data collected by the WSR-74C located at Patrick AFB were not available for these analyses (Herring 1999). The tape containing the data was produced using the McGill processor and its associated software. When the WSR-74C was upgraded to the Interactive Radar Information System (IRIS) SIGMET software in 1997, the new system would not read the tapes created on the older machine. Having no requirement to retain these tapes, the contractor recycled them for other use.

2.2.2. Meteorological data

The meteorological data used for this study consisted of the data which are routinely available within the Meteorological Interactive Data Display System (MIDDS). The RAMS model runs which were made for 1200 UTC on 17 January 1997 were initialized with the following data:

- 1200 UTC Weather Information Network Display System (WINDS) tower data (39 stations)
- 1200 UTC surface and buoy observations (484 stations)
- 1200 UTC rawinsonde data (37 stations)
- NCEP Eta grids generated from the analysis at 1200 UTC 17 January 1998 for the following forecast times:
    - 1800 UTC 17 January,
    - 0000 UTC 18 January,
    - 0600 UTC 18 January,
    - 1200 UTC 18 January,

The 12-hr forecast grid (0000 UTC 18 January) used for boundary conditions was found to contain bad data that caused RAMS to stop running at the 7-h forecast time (1900 UTC). To fix the problem, we substituted the 24-h Eta forecast grid from the previous forecast cycle. RAMS ran to completion with these data.

Other meteorological data were available to characterize the weather conditions at the time of the accident. This data included the following:

- WINDS tower data (available at 5-minute intervals)
- Surface and buoy observations (available hourly)
- Rawinsonde data (available at 1128, 1243, 1453, 1548, 1613, and 1815 UTC)
- 50 MHz profiler data (available hourly)
- 915 MHz profiler data (including Radio Acoustic Sounding Systems virtual temperature data)

2.2.3. Satellite data

Satellite data from the GOES-8-east satellite data was available for 17 January 1997. The satellite photos were used to show the clouds present on this day. The satellite data was also used to show the location of the explosion clouds as they advected downwind.

2.3. Model description/configuration

2.3.1. ERDAS/PROWESS development

ERDAS was developed by Mission Research Corporation (MRC)/ASTER division for the Air Force as a prototype system to provide emergency response guidance for operations at KSC/CCAFS in case of an accidental hazardous material release or an aborted vehicle launch. The ERDAS development occurred during the period 1989 to 1994 under Phase I and II Small Business Innovative Research contracts with the Air Force Space and Missile Systems Center, Los Angeles, CA. ERDAS was delivered to the Air Force's Range Operations Control Center (ROCC) in March 1994. The AMU was tasked with keeping the prototype ERDAS running and with evaluating ERDAS during the period March 1994 to December 1995. The AMU evaluation report concluded that ERDAS provided significant improvement over current toxic dispersion modeling capabilities but the system contained deficiencies which needed addressing before the ERDAS could become operational (Evans 1996).

The Parallelized RAMS Operational Weather Simulation System (PROWESS) was developed by MRC during the period 1993 to 1996 for NASA (Tremback et al. 1996). The goals of the PROWESS project were to demonstrate capability of the parallelized RAMS code to run on a cluster of low-cost workstations. The model was configured to forecast the initiation, development, interaction and dissipation of sea breeze and river breeze-generated thunderstorms during initially undisturbed conditions on scales as small as several kilometers. The differences between PROWESS and ERDAS are described in Sections 2.3.2 and 2.3.3. PROWESS was installed in the AMU and has run on a routine basis but was not evaluated by the AMU. PROWESS was not evaluated because the AMU tasking committee selected other projects for the AMU at the time PROWESS was delivered.

The next generation of ERDAS was rehosted into the newly upgraded Meteorological And Range Safety Support Replacement (MARSS-REPL) system. MARSS-REPL was installed in 1997 at CCAFS/KSC as the primary toxic/hazard diffusion prediction system. An earlier version of MARSS and a prototype of the MARSS-REPL, the Meteorological Monitoring System (MMS) are described in Lane and Evans (1989) and Evans et al. (1994). The MARSS-REPL consists of 13 Hewlett-Packard C100 and C110 workstations. The workstations are connected by a Local Area Network (LAN) that allows users at CCAFS and KSC to run and display the diffusion model Ocean Breeze/Dry Gulch. Users can also display various meteorological displays.

Some of the primary features of the upgraded and certified system (called ERDAS-REPL), delivered in late 1998, are:

- An upgraded LAN using a higher speed distribution mechanism known as Fiber Distributed Data Interface to support the larger data transfers.
- A series of Hewlett-Packard K460 workstations used as dedicated RAMS processors utilizing a Symmetric Multi-Processor architecture.
- RAMS with:
  - Full microphysics activated,
  - Four nested grids with the largest grid covering the southeast United States, and
  - 1.25-km grid spacing on the fine grid covering approximately 100 km by 80 km centered on CCAFS/KSC.
- Additional meteorological data sources now include 50 MHz Doppler radar wind profiler, 915 MHz radar wind profilers, rawinsondes, coastal buoys, surface stations, wind towers, and gridded

National Centers for Environmental Prediction (NCEP) ETA model grids. New data quality control procedures were implemented for observational data.

- The system will now run Rocket Exhaust Effluent Diffusion Model (REEDM) and BLASTX models, along with Ocean Breeze/Dry Gulch (OB/DG), HYPACT/RAMS.

2.3.2. RAMS-ERDAS

The AMU conducted the Delta II modeling analysis by running RAMS for 17 January 1997 and using the forecast meteorological data to drive the diffusion model HYPACT. The RAMS-ERDAS configuration was the same as the configuration used for the daily operation of RAMS in the prototype ERDAS. This configuration has been set since the prototype ERDAS was installed in the ROCC in 1994. The key points of this configuration are:

- RAMS version 3a
- Microphysics inactive (NLEVEL=1)
- 3 nested grids
  - Coarse grid: 60 km spacing, 2220 x 2100 km domain
  - Medium grid: 15 km spacing, 495 x 555 km domain
  - Fine grid: 3 km spacing, 108 x 108 km domain
- Vertical grid with 10-m lowest grid point on fine grid and expanding in depth upward
- Twice-daily RAMS runs initialized at 0000 and 1200 UTC with hourly forecast output
- Input data used to initialize the model are obtained from MIDDS and include:
  - NCEP ETA data
  - rawinsondes
  - surface and buoy data
  - local CCAFS/KSC WINDS tower data

A complete listing of the file RAMSIN containing the input parameters for running RAMS is provided in Appendix A.

2.3.3. RAMS-PROWESS

The RAMS-PROWESS runs were made using the version of RAMS on the PROWESS workstations. The PROWESS workstations consist of one IBM RS/6000-370 and seven IBM RS/6000-250 workstations which run the parallel version of RAMS. The key points of this configuration are:

- RAMS version 4a
- Microphysics active (NLEVEL=3)
- 4 nested grids
  - Coarse grid: 72 km spacing, 2376 x 2088 km domain
  - Medium grid: 18 km spacing, 594 x 666 km domain
  - Fine grid: 6 km spacing, 222 x 222 km domain
  - Finest grid: 1.5 km spacing, 61.5 x 85.5 km domain
- Vertical grid with 38-m lowest grid point
- Twice-daily RAMS runs initialized at 0000 and 1200 UTC with hourly forecast output

- Hourly output beginning at initialization time of 1200 UTC
- Input data used to initialize the model is obtained from MIDDS and includes
  - NCEP ETA data
  - Rawinsondes
  - Surface and buoy data
  - Local CCAFS/KSC WINDS tower data

A complete listing of the file RAMSIN containing the input parameters for running RAMS is provided in Appendix B.

2.3.4. HYPACT-ERDAS and HYPACT-PROWESS

The primary model used for computing dispersion estimates in ERDAS is HYPACT. HYPACT is an advanced Lagrangian particle dispersion model. Dispersion in the Lagrangian mode of HYPACT is simulated by tracking a large set of particles. Subsequent positions of each particle are computed from the relation:

$$X[t + \Delta t] = X[t] + [u + u'] \Delta t$$

$$Y[t + \Delta t] = Y[t] + [v + v'] \Delta t$$

$$Z[t + \Delta t] = Z[t] + [w + w' + w_p] \Delta t$$

where u, v and w are the resolvable scale wind components which are derived from the RAMS wind field, and u', v', and w' are the random subgrid turbulent wind components deduced from RAMS. The w_p term is the terminal velocity resulting from external forces such as gravitational settling.

REEDM predicts plume rise and downwind concentrations resulting from nominal or aborted launches. In ERDAS, REEDM produces the source term which is used by HYPACT to predict plume dispersion and resulting downwind concentrations.

For modeling launch scenarios, HYPACT obtains the source term data (release rate) from the REEDM launch plume data. HYPACT then diffuses the plume using the RAMS-predicted wind fields and potential temperature fields to advect and disperse the particles vertically and horizontally downwind from the source.

HYPACT can model any number of sources which are specified anywhere in the domain and configured as point, line, area, or volume sources. The emissions from these sources can be instantaneous, intermittent, or continuous and the pollutants can be treated as gases or aerosols.

To simulate the Delta II explosion plume using HYPACT required that we modify the HYPACT input configuration file produced within the ERDAS dispersion function. For launch plume dispersion scenarios, ERDAS uses REEDM to produce a source term for a rocket exhaust plume. This source term, which is actually a series of source terms in a vertical column, represents the mass of an emitted launch plume product. REEDM computes the source term based on a number of factors such as:

- type of launch (e.g. nominal, abort conflagration, or abort deflagration)
- type of vehicle (e.g. Atlas, Delta II, Titan IV, Shuttle, etc.)
- vertical stability (i.e. stabilization height).

2.3.5. REEDM

Prior to each land-based launch, Range Safety, in conjunction with their support contractor, ACTA Inc., runs REEDM to predict the location and concentration of the toxic cloud arising from the normal launch or abort plumes. REEDM is currently the model of choice and the only certified model which Range Safety personnel can use to evaluate launch cloud dispersion. At the time of the Delta II explosion, REEDM 7.07 was the version of REEDM in use at the time. Range Safety has continued to upgrade REEDM and uses the latest version available to evaluate launch cloud dispersion.

Toxic substances are identified on the EPA list of Extremely Hazardous Substances (EHS). The Delta II contained or produced the following EHS chemicals as propellants or products of solid rocket propellant combustion.

- Hydrazine
- Unsymmetrical dimethyl hydrazine (UDMH)
- Nitrogen tetroxide
- Hydrogen chloride

Aerozine-50 is the Delta II second stage hypergolic fuel and is a 50-50 mixture of hydrazine and UDMH. Nitrogen tetroxide is the Delta II second stage hypergolic oxidizer. The reaction of the solid propellant involves aluminum oxide as the oxidizer and ammonium perchlorate as the fuel to produce hydrogen chloride along with other non-EHS reaction products.

REEDM models the toxic cloud formation process in four significant steps:

- cloud formation
- cloud rise (buoyant cloud rise)
- cloud stabilization (at neutral buoyancy after heat exchange with the atmosphere)
- cloud transport and dispersion

A single rawinsonde sounding provides the input meteorological data for REEDM, which incorporates vertical but not horizontal wind shear. Thus the sounding is assumed to represent the flow across the entire area-wide model domain.

REEDM predicts the ground trace or net ground level concentration of hazardous material arising due to its dispersion from the elevated cloud. This ground-level isopleth does not portray the cloud's passage in terms of time, but lists range and bearing from the source, peak concentration at that range and bearing, and, cloud arrival and departure times at that range and bearing. REEDM results for the Delta II scenario are presented in Section 3.2.1.

3. Results

The results of the Delta II explosion plume analysis are presented in this section. The observations which provided the verification and which were used to compare with modeled data are presented first. These data included meteorological, visual (video tape) observations, satellite and WSR-88D radar data. The model data used in this analysis are presented next. These data included the predictions produced by REEDM, RAMS, and HYPACT.

3.1. Observed data

3.1.1. Meteorology on 17 January 1997

A cold front had passed through the Cape Canaveral area approximately 24 hours prior to the Delta II launch and had pushed through all of Florida, most of the Bahamas, and through the eastern two-thirds of Cuba (Figure 5). Therefore, the prevailing weather conditions at Cape Canaveral on 17 January were post-frontal in nature. Across the Florida peninsula, the winds at the surface were generally from the north and northwest as the cold dense air moved southward. A high pressure area centered over the Louisiana area was building eastward into Florida. The colder air mass was relatively shallow at launch time as subsiding air behind the front formed a well-defined temperature inversion near 900 m. Skies were clear over the launch site while scattered to broken stratocumulus clouds were located over the ocean further east. Low temperatures in the area that morning were in the upper 30's. The Shuttle Landing Facility reported a low temperature of 36° F.

A graph showing the potential temperature profile from the three Cape Canaveral rawinsondes on 17 January are presented in Figure 6. The graphs show the very strong inversion based at approximately 750 meters at 1128 UTC. Also shown are the potential temperature profiles from 1613 and 1815 UTC. At these times, the inversion base had risen to approximately 900 meters as the surface warmed 5 to 7 K. A graph showing the wind speed and wind direction at 1815 UTC show the marked difference in the winds above and below the inversion (Figure 7). The northwesterly winds below the inversion were fairly strong at 8 to 10 m s^{-1} but increased in speed and then backed to become more westerly above the inversion.

Table 1 presents the hourly wind speed and direction data at 150-meter increments from 2000 to 5000 m as collected by the 50 MHz profiler at KSC. The profiler data indicate the winds at the 2000-meter level were northwesterly with speeds of 13 to 18 knots at 1600 UTC but then became westerly and north-northwesterly during the next five hours. The winds above 2700 m were westerly with speeds of 20 to 30 knots during the period 1600 to 2100 UTC.

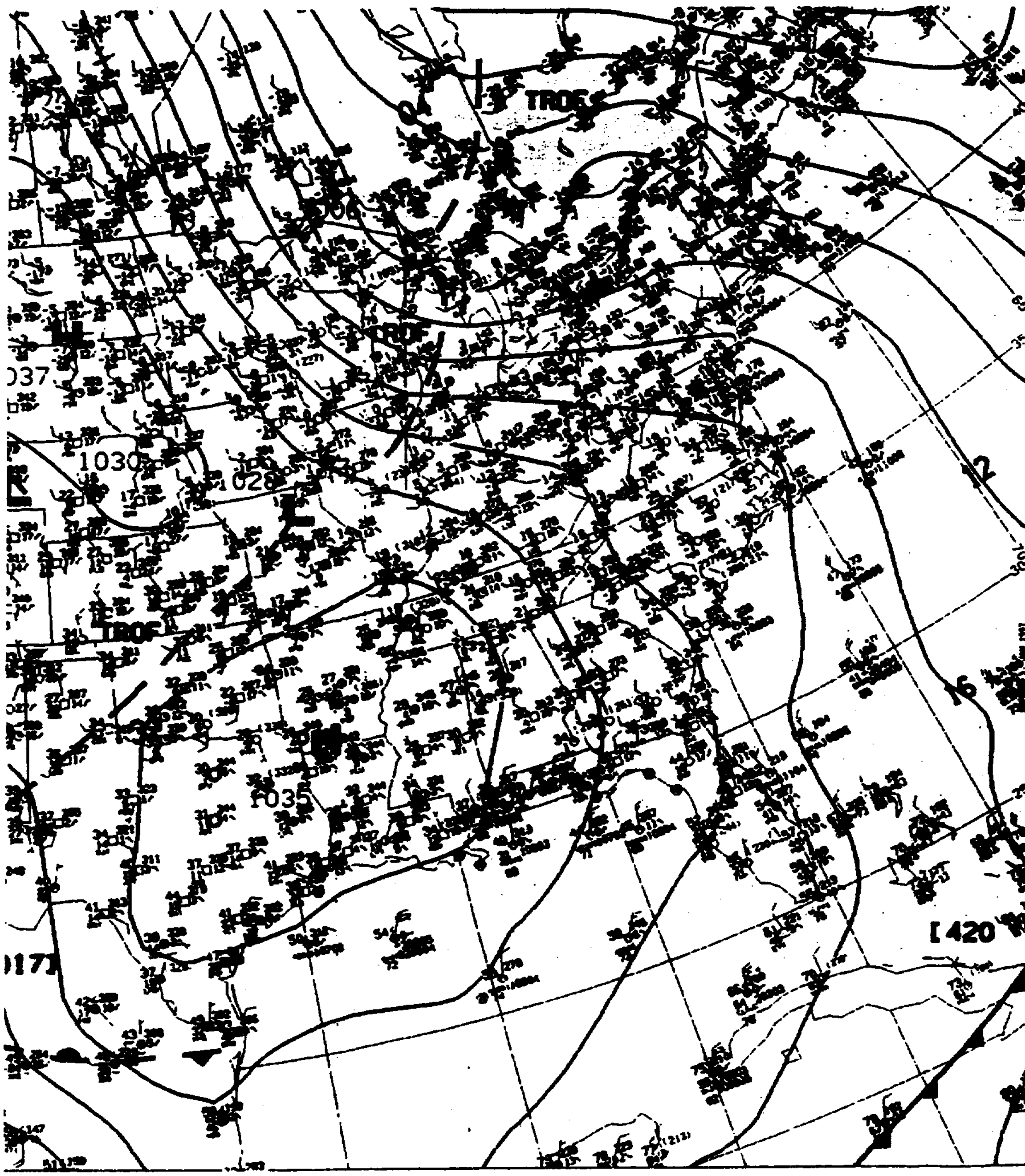

Figure 5. Surface map of eastern United States at 1800 UTC on 17 January 1997.

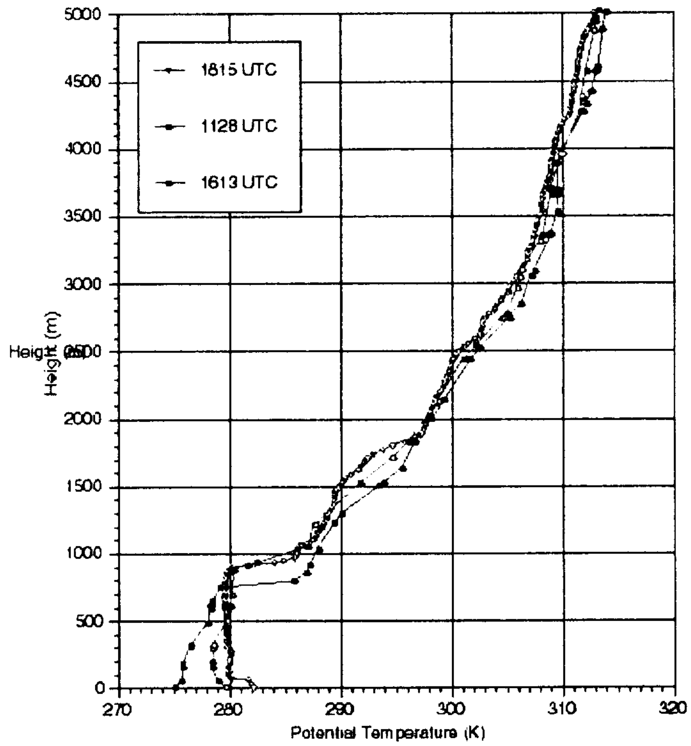

Figure 6. Graph of potential temperature profile versus height for three rawinsondes on 17 Jan 1997.

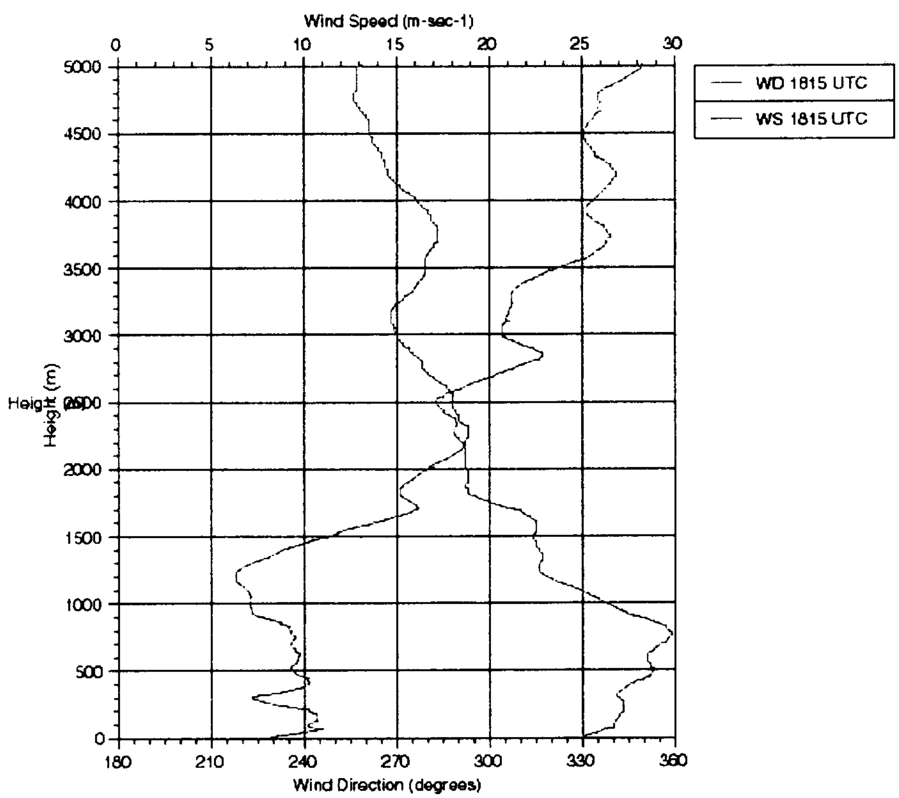

Figure 7. Graph of wind speed (WS) and wind direction (WD) versus height from rawinsonde at 1815 UTC on 17 January 1997.

Table 1. Wind speed and direction from the 50-MHz profiler at KSC on 17 January 1997.

Time (UTC)	1600		1700		1800		1900		2000		2100	
Height (m)	Direct. (deg)	Speed (kts)	Direct. (deg)	Speed (kts)	Direct. (deg)	Speed (kts)	Direct. (deg)	Speed (kts)	Direct. (deg)	Speed (kts)	Direct. (deg)	Speed (kts)
2011.0	318	13.5	268	20.2	272	20	284	18.7	285	17.4	290	16.8
2161.0	316	15.3	276	20.6	279	19.5	286	19.2	269	18.3	288	15.6
2311.0	288	18.6	289	16.8	281	21.0	284	18.7	284	17.9	285	16.5
2461.0	287	20.4	288	18.2	288	17.8	284	17.4	282	17.6	290	17.9
2611.0	286	19.7	285	18.6	285	18.2	282	18.2	281	18.4	292	19.0
2761.0	279	20.0	278	20.5	283	20.9	285	19.9	285	19.8	291	19.6
2911.0	274	20.8	273	20.4	282	21.3	283	20.5	283	21.4	284	21.9
3061.0	278	20.5	270	20.5	271	21.1	275	21.2	276	22.7	289	21.9
3211.0	277	20.9	270	20.7	270	21.7	274	21.5	277	21.6	284	23.0
3361.0	276	21.7	275	21.2	277	22.7	278	21.8	277	22.1	281	23.1
3511.0	277	23.1	278	22.4	281	23.8	278	23.5	278	23.1	277	23.7
3661.0	280	24.3	283	25.1	282	26.7	278	25.2	276	24.8	276	25.1
3811.0	281	25.4	284	26.7	283	27.1	279	26.0	275	25.7	275	25.7
3961.0	276	26.0	280	26.7	282	26.7	276	26.1	272	27.1	271	26.5
4111.0	268	25.9	270	26.2	272	27.3	268	26.7	267	27.6	268	28.3
4261.0	266	26.0	264	26.5	266	28.5	266	27.8	264	28.2	262	28.1
4411.0	267	25.9	263	27.1	263	27.6	262	27.1	263	28.6	260	28.4
4561.0	263	24.9	259	25.3	260	26.8	259	26.6	260	28.1	259	29.0
4711.0	261	24.7	258	25.7	259	27.0	258	27.2	256	28.9	262	29.7
4861.0	260	25.6	257	26.4	258	28.5	256	27.9	260	30.5	264	30.6
5011.0	262	27.4	263	28.7	261	29.7	261	29.8	264	30.2	263	32.7

3.1.2. Visual observations

The Delta II explosion was captured on videotape by numerous Air Force and amateur video cameras. Most of the Air Force video focused very closely on the exploding rocket since these pictures were used for the investigation to determine the cause of the explosion. The amateur video provided a better look at the clouds resulting from the explosion since they were taken from a distance and showed a full panorama of the upper and lower clouds. Pictures extracted from on amateur video are presented in Figures 8 - 10. The person who shot the video and the exact location are unknown. However, the video was taken from the beach in Cocoa Beach. Bionetics was responsible for archiving all amateur and Air Force video of the Delta II explosion.

The video shows the huge lower cloud that was produced when the nine solid propellant motors and first stage exploded at approximately 13 seconds. The video also shows the upward movement and subsequent destruction/explosion of the Delta II's stage 2 and 3. The pictures show the upper plume to be darker and much smaller than the lower plume. The captured frames in Figures 8 to 10 show the two distinct clouds very well along with some other notable features. The inversion that existed at 900 meters was clearly evident as it capped the lower cloud and allowed very little of the buoyant smoke and gas to rise past the inversion.

One very key feature shown in the video and in the captured figures was the small dark orange cloud at the top of the lower cloud (Figure 10). This dark orange cloud indicates the presence of nitrogen tetroxide (N_2O_4) that was emitted when the second stage was destructed. Ha and Deane (1998) indicated that Stage 2 contained 8759 lbm of N_2O_4. Since this cloud was at the top of the lower cloud, the video indicates that this cloud was not completely trapped below the inversion, as was most of the lower cloud. This observation is important in the determination of the transport of the N_2O_4 because of its toxic nature (Sittig 1985). The following sections describe in detail the transport of the lower cloud as tracked by satellite and radar but the fate of the small orange cloud at the top of the lower cloud cannot be directly tied to the large lower cloud. The bulk of the N_2O_4 was likely contained in the upper cloud and was transported toward the east-southeast.

Figure 8. The two clouds produced from the explosion of the vehicle a few seconds after the explosion on 17 January 1997. This picture was captured from amateur video taken along Cocoa Beach.

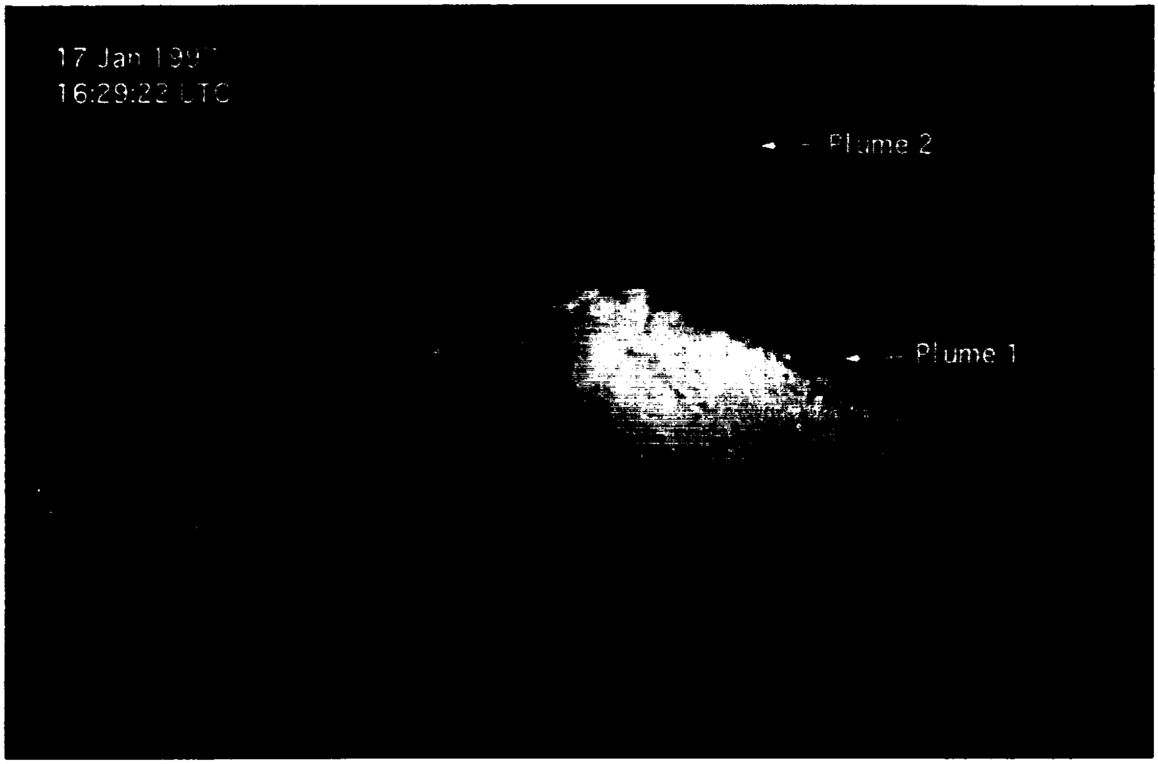

Figure 9. The two explosion clouds at approximately 16 seconds after the explosion. Note the orange area located at the top of Plume 1.

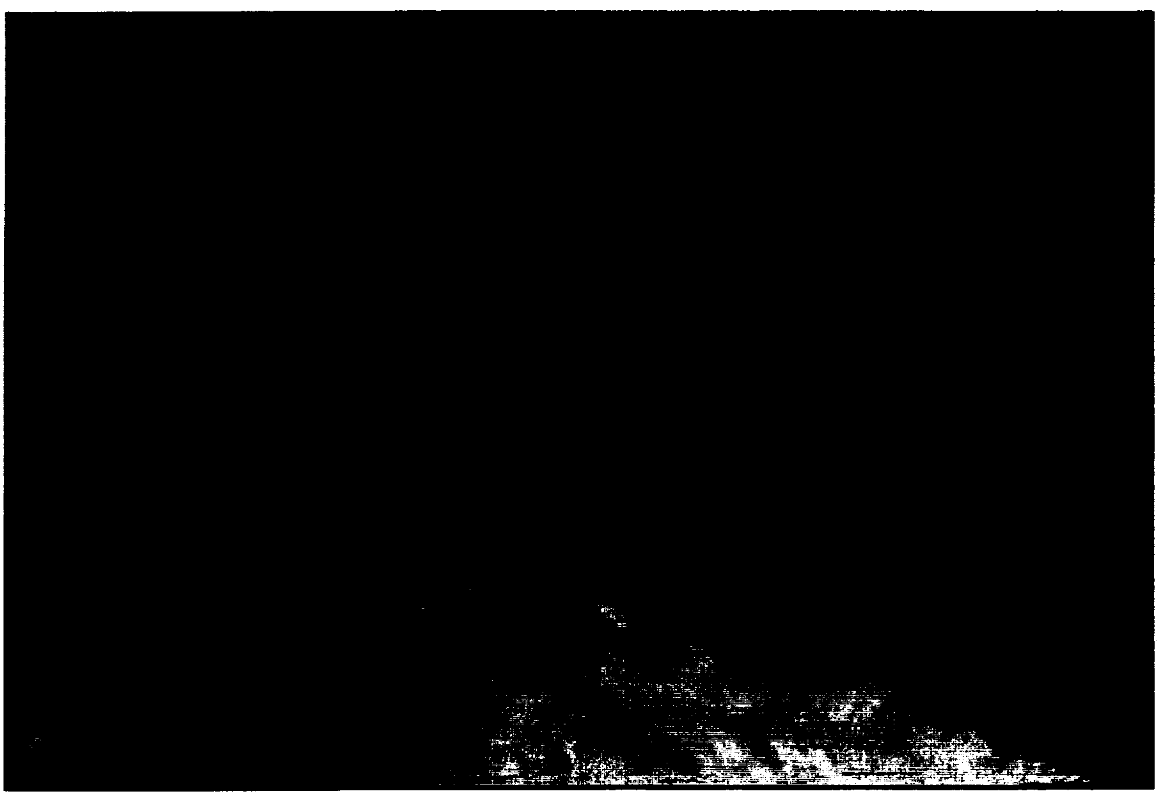

Figure 10. Zoomed in view of explosion clouds at approximately 12 seconds after the explosion. The small orange cloud at the top of the lower cloud most likely contains nitrogen tetroxide.

3.1.3. Satellite data

GOES satellite data for two times following the explosion is shown in Figures 11 and 12 (Brandli 1997). These satellite pictures show the lower explosion cloud as it moved south over the Melbourne area. Figure 11 shows the cloud as it reaches the coastline in Cocoa Beach at 1645 UTC while Figure 12 shows the cloud as it reaches the Melbourne area at 1715 UTC.

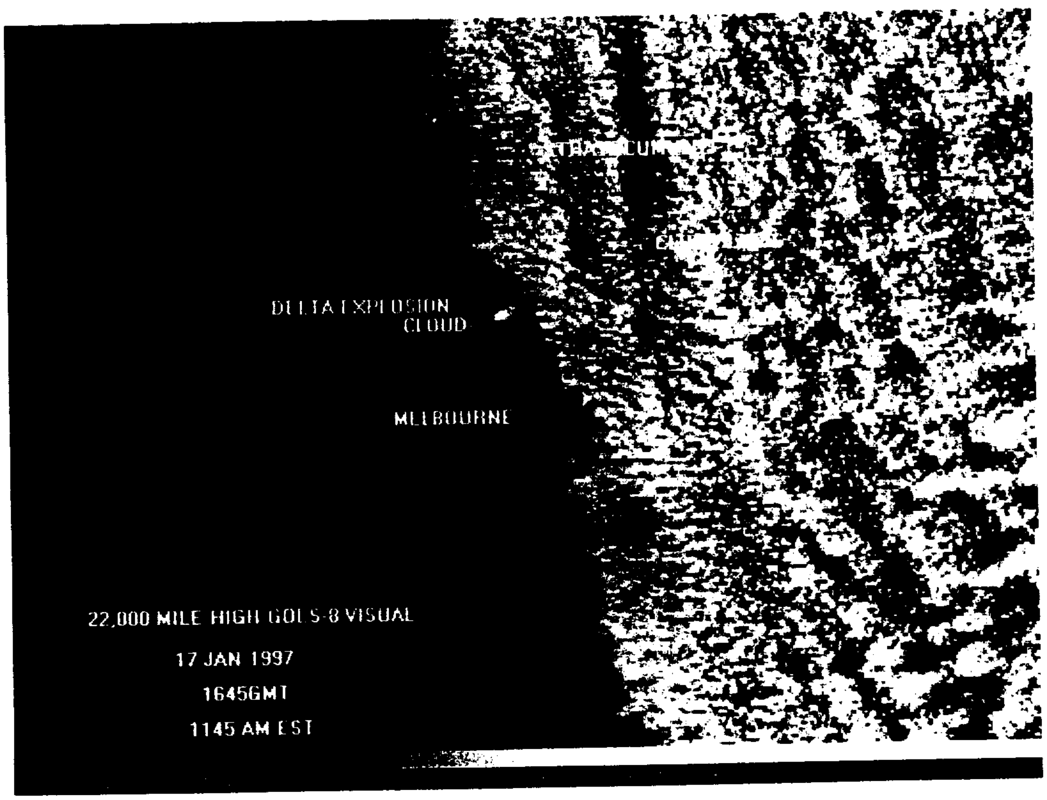

Figure 11. GOES satellite image of Delta II explosion cloud at 1645 UTC 17 January 1997. (from Brandli 1997).

Figure 12. GOES satellite image of Delta II explosion cloud at 1715 UTC 17 January 1997. (from Brandli 1997).

3.1.4. Radar data

For the 17 January case, the WSR-88D clearly displayed the echoes resulting from the rocket explosion. As discussed earlier, the display showed two distinctly separate plumes. Information on the two plumes was obtained for each 10-minute scan by using the 88Display information query function. This information is presented in Tables 2 and 3. Much of the data contained in the table was obtained by manually analyzing each time and elevation scan using the information query function. The scan start time, stop time, and elevation angle were displayed for each scan. We zoomed in on the area of interest to show the explosion clouds and found the location of the maximum reflectivity using the color contouring. By selecting this point with the mouse, we obtained the vital information such as location and height for that time and elevation. The actual maximum reflectivity value was estimated from the color contours. The plume dimensions such as downwind distance and alongwind and crosswind length were estimated using the cross-section tool of 88Display.

The plume top and bottom were found using the information query function for each elevation scan and finding the highest and lowest point of the cloud of interest. It should be noted that the heights of the clouds determined from this technique have a large uncertainty for reasons discussed earlier.

The Delta II abort cloud was first detected by the WSR-88D during the scan at 1635-1646 UTC. Figures 13 and 14 show the composite reflectivity and cross section of the radar image at that time. The cross section shows how the plume split into two distinct clouds with an upper cloud to the east and a lower cloud to the south of LC-17. Figures 15 and 16 show the clouds two hours later at the scan ending at 1834 UTC. The upper and lower clouds were still clearly detected by the radar. The lower cloud was more distinguishable, located south of the Melbourne area.

The composite reflectivity figures for each of the scans are shown in Figures 17 to 42.

Table 2. Data obtained from WSR-88D Level II archive for 17 January 1997 using the 88Display software. Data in this table show Plume 1 (lower cloud) information.

Scan Time Start (hhmmss)	Scan Time Start (hrs)	Scan Time Stop (hhmmss)	Lat. of Peak (deg N)	Lon.of Peak (deg W)	Height of Peak (km)	Max Reflect. (dBZ)	Plume 1 Center Lat. (deg N)	Plume 1 Center Lon. (deg W)	Plume 1 Down-wind Dist. (km)	Plume 1 Direction from LC-17 (deg)	Plume 1 Along wind length (km)	Plume 1 Cross-wind Dist. (km)	Plume 1 Top (km)	Plume 1 Bottom (km)
162552	16.4456	163639	28.4355	80.5641	0.444	45	28.4319	80.5641	1	180	2	3	2.7	0.97
163541	16.5947	164628	28.3839	80.5692	0.37	53	28.3863	80.5678	7	185	3	5.5	2.1	0.35
164531	16.7586	165616	28.3212	80.5733	0.29	47	28.3212	80.5802	13	190	5	11	1.9	0.27
165519	16.9219	170604	28.2667	80.5763	0.22	45	28.2477	80.6076	21	190	8	9	1.2	0.2
170538	17.0939	171519	28.2109	80.5748	0.17	39	28.1708	80.6300	30	190	11	13	1.1	0.08
171527	17.2575	172507	28.1554	80.5708	0.16	33	28.1589	80.5788	33	190	10	11	1.1	0.04
172515	17.4208	173455	28.0677	80.6284	0.15	33	28.0849	80.5927	42	200	10	25	1.1	0.04
173503	17.5842	174443	28.0356	80.6126	0.29	31	28.0303	80.5707	48	200	12	28	0.91	0.06
174451	17.7475	175431	27.9897	80.5288	0.18	28	27.9844	80.5528	51	180	11	35	0.99	0.09
175440	17.9111	180419	27.9726	80.5509	0.21	34	27.9612	80.5249	59	180	11	35	1.13	0.13
180428	18.0744	181407	27.8970	80.4882	0.33	38	27.8970	80.4882	62	175	15	38	1.09	0.17
181416	18.2378	182356	27.8581	80.5012	0.34	30	27.8581	80.5012	66	170	15	37	1	0.2
182404	18.4011	183344	27.7985	80.4780	0.46	28	27.7985	80.4780	72	170	15	47	1.08	0.24
183352	18.5644	184332	27.8166	80.5704	0.39	28	27.7707	80.4855	75	180	14	45	1.22	0.3
184341	18.7281	185320	27.7805	80.5778	0.44	27	27.7380	80.5003	77	180	14	52	1.35	0.31
185329	18.8914	190309	27.7454	80.5797	0.49	25	27.6865	80.4763	84	180	12	40	1.57	0.37
190317	19.0547	191258	27.7159	80.5945	0.532	23	27.6472	80.4838	90	180	15	55	1.52	0.41
191306	19.2183	192246	27.6865	80.5871	0.579	21	27.6177	80.4802	95	180	16	60	1.51	0.45
192254	19.3817	193234	27.6505	80.6056	1.45	18	27.5981	80.5134	95	180	14	65	1.35	0.45
193242	19.5450	194222	27.6014	80.5872	1.71	18	27.5948	80.5282	97	180	15	47	1.13	0.56
194231	19.7086	195316	27.5785	80.5798	0.76	17	27.5785	80.5798	97	180	16	45	1.15	0.54
195219	19.8719	200305	27.5457	80.5872	0.81	17	27.5457	80.5872	101	180	20	45	1.18	0.59
200207	20.0353	201253	27.5359	80.6242	0.83	17	27.5359	80.6242	102	185	18	50	1.34	0.59
201156	20.1989	202241	27.5065	80.6057	0.88	16	27.5065	80.6057	105	190	22	52	1.38	0.69
202144	20.3622	203230	27.4901	80.6352	0.91	14	27.4901	80.6352	110	190	20	45	1.31	0.69

Table 3. Data obtained from WSR-88D Level II archive for 17 January 1997 using the 88Display software. Data in this table show Plume 2 (upper cloud) information.

Scan Time Start (hhmmss)	Scan Time Start (hrs)	Scan Time Stop (hhmmss)	Plume 2 Center Lat. (deg N)	Plume 2 Center Lon. (deg W)	Plume 2 Down-wind Distance (km)	Plume 2 Direction – from LC-17 (deg)	Plume 2 Along wind length (km)	Plume 2 Cross-wind Distance (km)	Plume 2 Top (km)	Plume 2 Bottom (km)
162552	16.4456	163639	28.421	80.5011	6	110	4	4	3.2	1.7
163541	16.5947	164628	28.3971	80.4089	15	110	4	2	3.7	1.4
164531	16.7586	165616	28.3754	80.3391	24	110	8	3	3.7	1.5
165519	16.9219	170604	28.3569	80.2657	28	115	11	4	3.7	1.3
170538	17.0939	171519	28.3210	80.1466	42	115	16	5	3.6	1.4
171527	17.2575	172507	28.3067	80.0690	58	120	20	7	3.7	1.5
172515	17.4208	173455	28.3228	80.0824	60	120	55	10	3.8	0.66
173503	17.5842	174443	28.3087	80.0044	65	115	60	10	3.7	0.63
174451	17.7475	175431	28.2875	79.9306	70	110	55	11	3.8	0.45
175440	17.9111	180419	28.2500	79.8300	80	110	67	10	3.6	0.49
180428	18.0744	181407	28.2406	79.7757	82	110	87	11	3.7	0.45
181416	18.2378	182356	28.2429	79.6951	87	110	85	15	3.9	0.55
182404	18.4011	183344	28.2338	79.6354	110	115	87	15	3.8	0.62
183352	18.5644	184332	28.1962	79.4792	140	120	112	18	4.4	0.64
184341	18.7281	185320	28.1969	79.4477	145	120	115	18	4.2	0.73
185329	18.8914	190309	28.1577	79.3665	150	120	110	16	2.6	0.79
190317	19.0547	191258	28.1479	79.2517	147	120	115	18	2.65	0.93
191306	19.2183	192246	28.1119	79.1706	145	120	120	17	2.67	0.96
192254	19.3817	193234	28.0187	79.1867	145	120	110	10	2.66	1.02
193242	19.5450	194222	27.9646	79.2281	140	125	90	13	2.62	1.15
194231	19.7086	195316	27.7271	79.7336	120	135	30	4	1.69	1.23
195219	19.8719	200305	27.7126	79.6710	130	135	50	6	2.02	1.31
200207	20.0353	201253	27.6472	79.6310	135	135	35	5	2.10	1.34
201156	20.1989	202241	27.5981	79.6315	140	135	45	15	2.18	1.47

202144	20.3622	203230	27.5883	79.6721	130	140	10	3	1.86	1.59

Figure 13. Composite radar image from Melbourne WSR-88D for 10-minute scan beginning at 1635 UTC. A-B line indicates cross section shown in Figure 14.

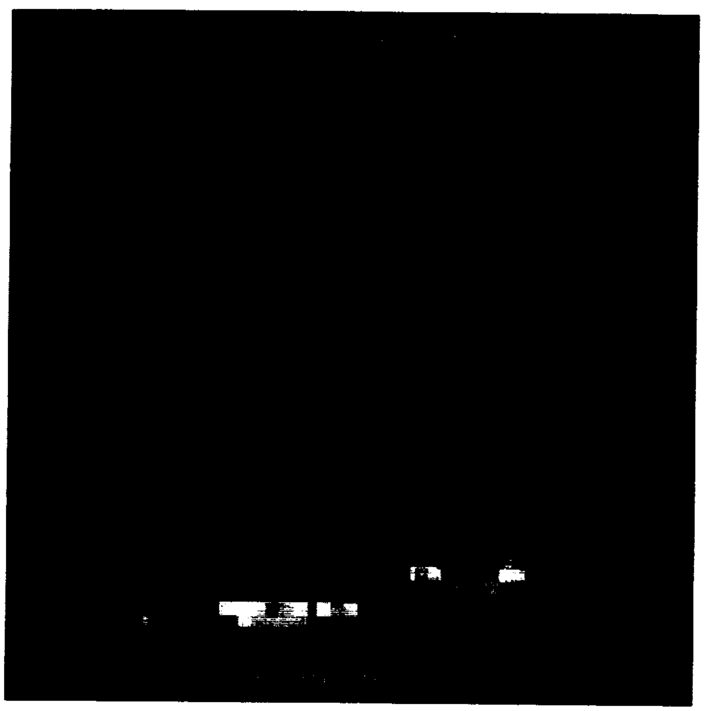

Figure 14. Cross section of composite radar image for 1635 UTC. East-west cross section location shown in Figure 13.

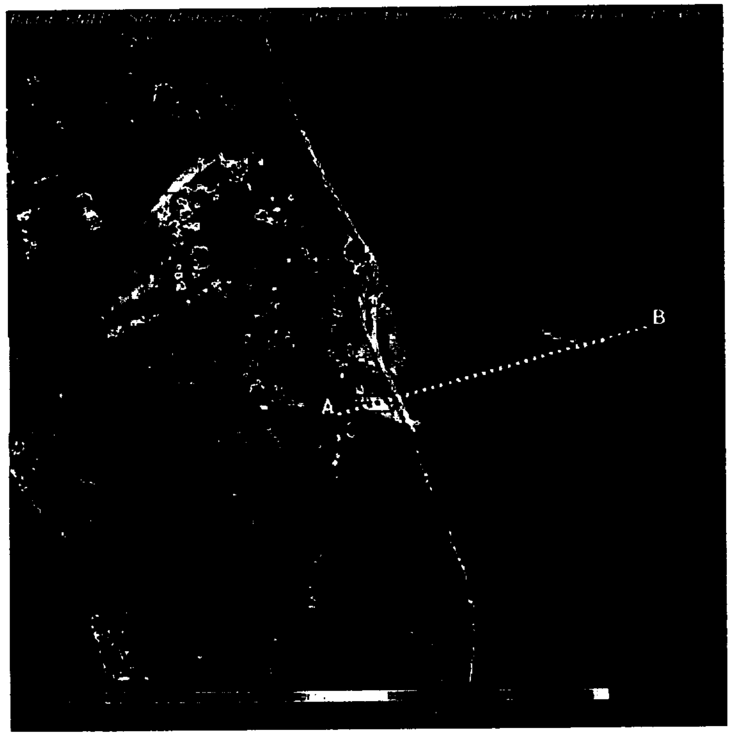

Figure 15. Composite radar image from Melbourne WSR-88D for 10-minute scan beginning at 1833 UTC. A-B line indicates cross section shown in Figure 16.

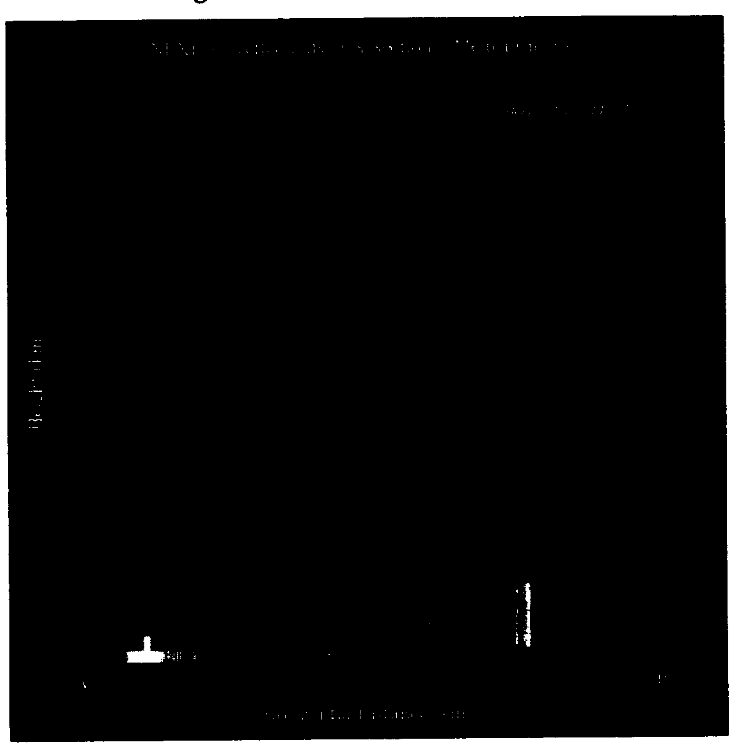

Figure 16. Cross section of composite radar image for 1833 UTC. East-west cross section location shown in Figure 15.

3.1.4.1. Cloud 1

The lower cloud, designated Cloud 1, moved to the south over the next four hours after the explosion as the WSR-88D radar clearly tracked the smoke and particles contained in the cloud. The reflectivity reached a maximum of 53 dBZ in the 1635-1646 UTC scan (Figures 13 and 19) but then gradually decreased to approximately 14 dBZ four hours later in the 2021-2032 UTC scan (Figure 42). The shape of the cloud as shown by radar appeared rounded initially but then became oval-shaped in the crosswind direction at approximately one hour after the explosion. The cloud maintained this oval shape for the next three hours as it became elongated in a northwest-southeast orientation. The analysis of the 1635 UTC scan (Figures 13 and 19) indicated the low-level cloud was approximately 3-km long, 2-km wide, at least 2-km thick and was located 1 km from LC-17. The cloud thickness is likely greatly exaggerated because of radar beam width and superrefraction effects. The direction the cloud moved was initially south and it maintained this southerly movement throughout the four hours. The cloud moved to intersect the coastline at approximately 1650 UTC (Figure 20) as it moved over the beaches between Cocoa Beach and Patrick AFB. It continued to move south over the Melbourne area and was centered over the Melbourne airport at approximately 1735 UTC (Figure 25). The cloud moved from Brevard County into Indian River County at approximately 1830 UTC (Figures 15 and 30).

Ground fires produced smoke plumes which were detected by the WSR-88D on 17 January. These fires as observed on the radar displays give a good indication of the surface level winds. The display at 1804 UTC (Figure 28) shows the smoke plume produced by the fires over Cape Canaveral that were started from the falling solid rocket fuel. The low level winds affecting this plume were from the north-northwest. It is important to note that this low-level smoke plume stays offshore and does not move westward as did the Delta II explosion cloud which was aloft. The plume from another fire (unrelated to the Delta II explosion) located in western Indian River County (southwest of the lower Delta II cloud) moves south and south-southwest. The low-level winds in this area were from the north and north-northeast.

The height of the cloud top and bottom as determined by the 88Display program on the Level II data is shown in Table 2. As discussed earlier these values are not very accurate because of errors caused by refraction of the radar beam through a strong temperature inversion and because the cloud passed directly over the Melbourne radar site. However, the cloud height data does provide some useful information. The plume top was initially determined to be 2700 meters which is obviously too high as determined by the capping inversion characteristics. The estimated plume top dropped to 1200 meters at 1655 UTC which more closely matches the other observations. The reason for the large initial discrepancy is probably due to the beam width and the beam inversion problem. The cloud bottom was initially measured at 970 meters and dropped to a low of 40 meters at 1725 UTC as the cloud passed over the radar site and then rose to 690 meters at 2011 UTC. The change over time of the height of the plume top and bottom most likely reflects the radar beam angle since the heights are directly proportional to the distance from the radar. A graph showing the plume height measurements is presented in Figure 43.

3.1.4.2. Cloud 2

The Delta II stages 2 and 3 along with the payload survived the initial explosion and drifted upward to just over 750 meters where destruct signals were sent at 22.4 seconds. This formed a second cloud which broke through the inversion. The upper cloud moved to the east and southeast over the four hours after the explosion at an average speed of approximately 13 m s^{-1}. This cloud was detached from the lower cloud and moved at a different speed and direction. The radar detected peak reflectivities of approximately 34 dBZ at 1645 UTC (Figure 20). The reflectivities slowly decreased over time, then dropped below 30 dBZ at 1715 UTC (Figure 23) and then below 20 dBZ at 1754 UTC (Figure 27). The cloud was moved by the strong westerly winds in the layer above the inversion between 1200 and 2000 meters. The radar showed that the cloud had a somewhat undulating shape as it was stretched from west to east.

The height of the cloud top and bottom as determined by the 88Display program on the Level II data is shown in Table 3. The initial scan of the upper level cloud at 1625 UTC indicated the cloud was approximately 4-km long, 4-km wide, 1.5-km thick and was located 6 km east of LC-17. The errors associated with the refraction of the radar beam through the strong inversion that caused estimation errors for the height of the lower cloud were more prominent in determining the height of the upper cloud. The radar indicated that the initial vertical plume dimensions ranged from a cloud bottom of 1700 meters up to a cloud top of 3200 meters (Figure 14). During the next three hours the radar detected that the cloud top rose to a height of 4400 meters at 1833 UTC while the cloud bottom lowered to a height of 450 meters at 1804 UTC (Table 3). The measurements indicate a maximum depth of the upper cloud of over 3700 meters at 1833 UTC. Visual observations discussed in Section 3.1.2 did not support these radar depth determinations. Therefore, we seriously question this cloud's radar height measurements which are shown in a graph in Figure 44.

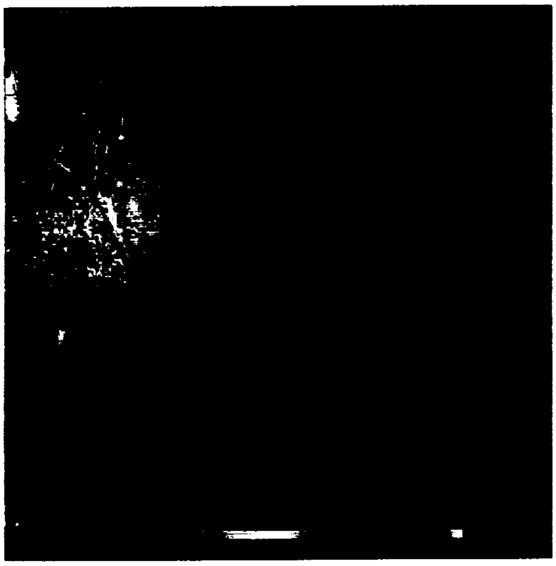

Figure 17. WSR-88D composite scan beginning at 1616 UTC.

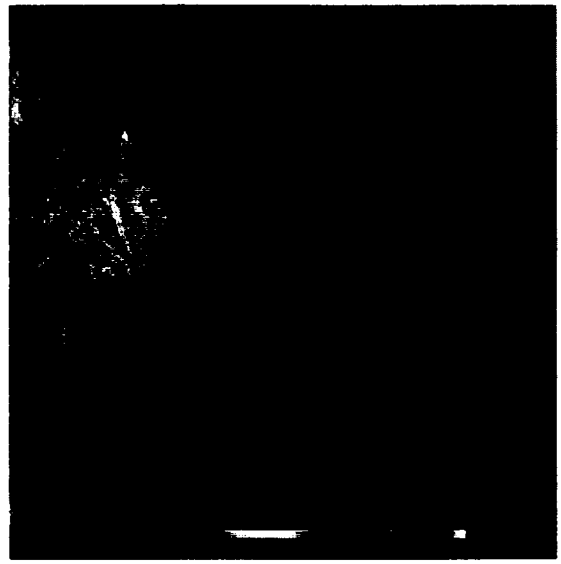

Figure 18. WSR-88D composite scan beginning at 1625 UTC.

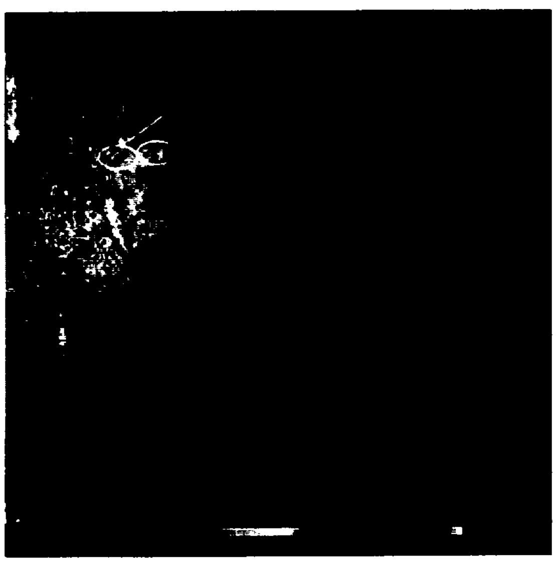

Figure 19. WSR-88D composite scan beginning at 1635 UTC.

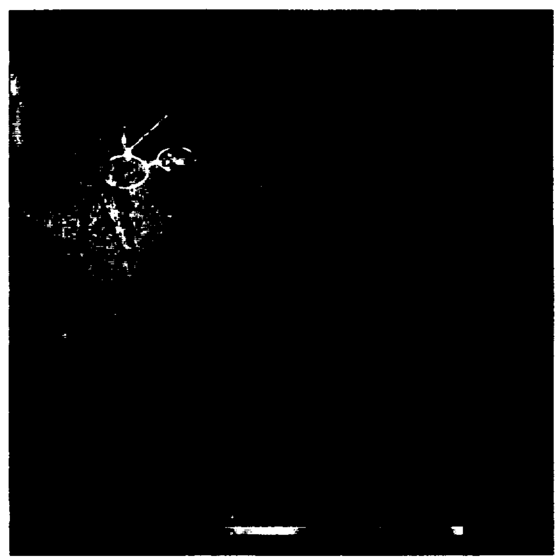

Figure 20. WSR-88D composite scan beginning at 1645 UTC.

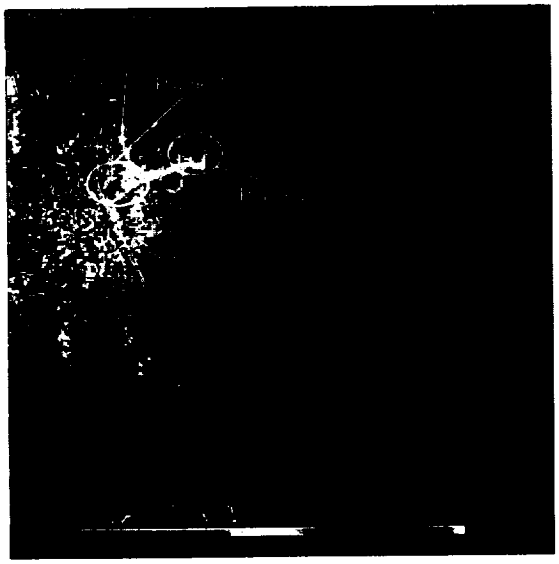

Figure 21. WSR-88D composite scan beginning at 1655 UTC.

Figure 22. WSR-88D composite scan beginning at 1705 UTC.

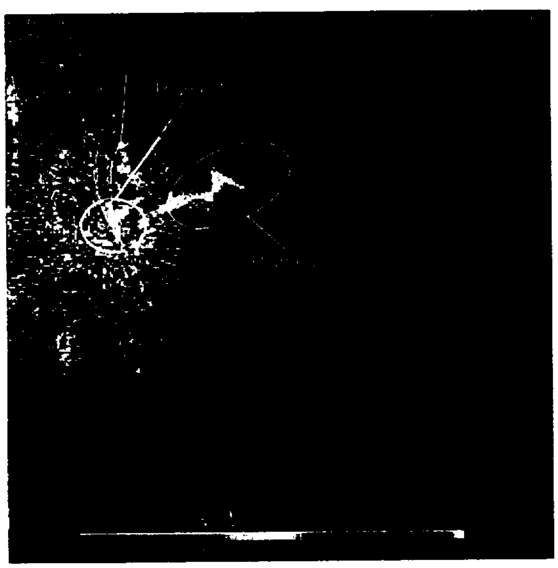

Figure 23. WSR-88D composite scan beginning at 1715 UTC.

Figure 24. WSR-88D composite scan beginning at 1725 UTC.

Figure 25. WSR-88D composite scan beginning at 1735 UTC.

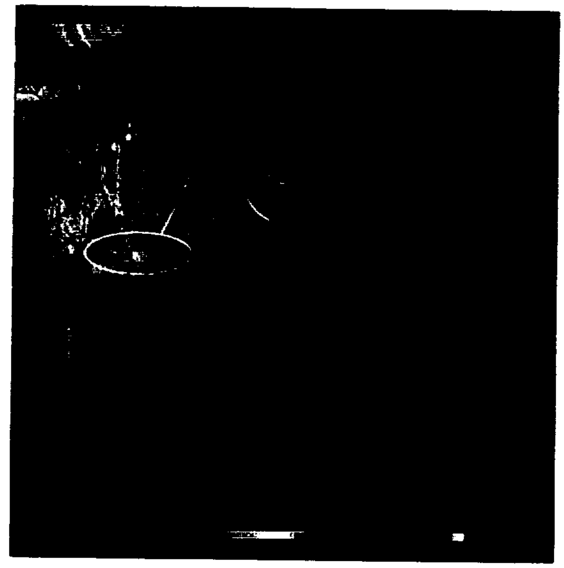

Figure 26. WSR-88D composite scan beginning at 1745 UTC.

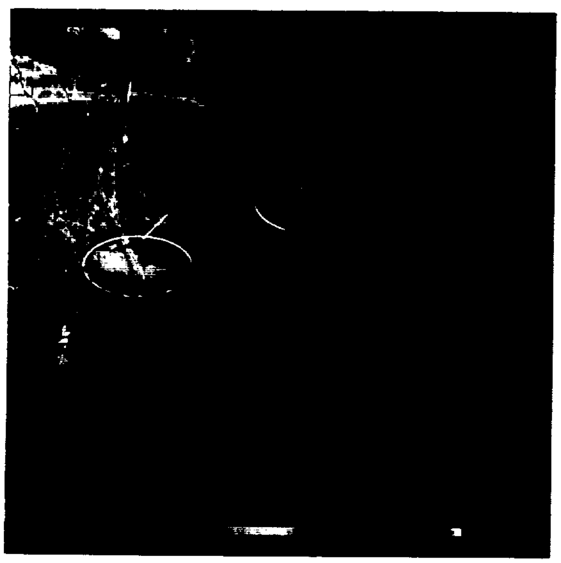

Figure 27. WSR-88D composite scan beginning at 1754 UTC.

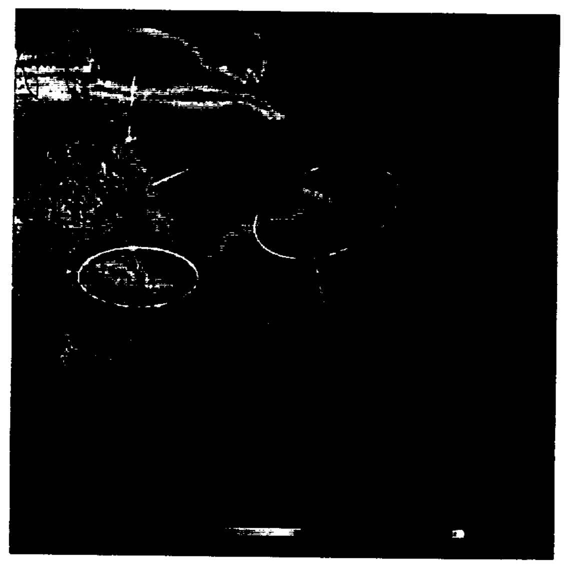

Figure 28. WSR-88D composite scan beginning at 1804 UTC.

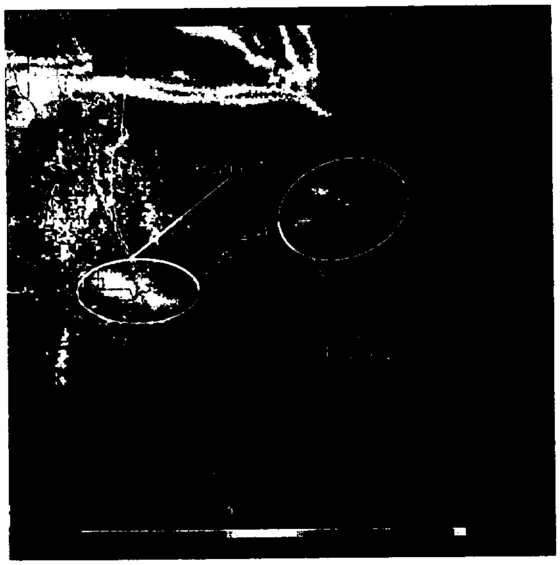

Figure 29. WSR-88D composite scan beginning at 1814 UTC.

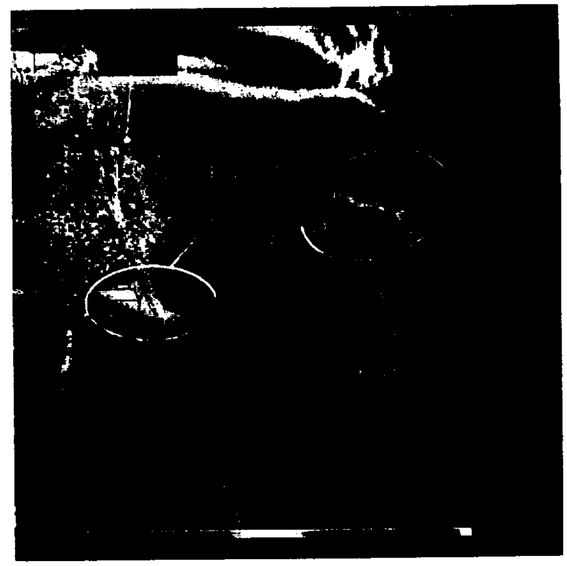

Figure 30. WSR-88D composite scan beginning at 1824 UTC.

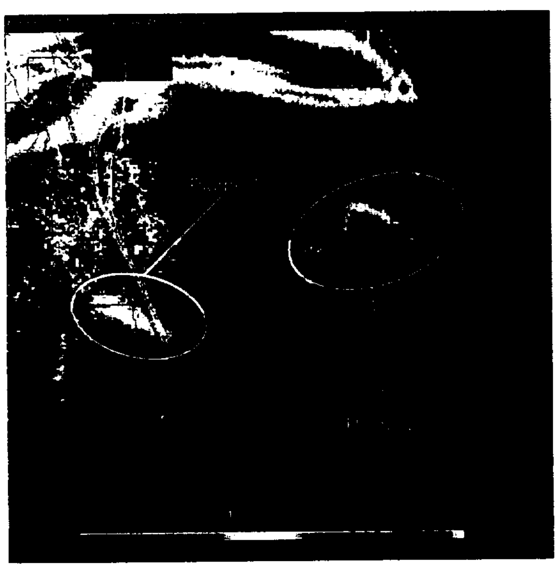

Figure 31. WSR-88D composite scan beginning at 1833 UTC.

Figure 32. WSR-88D composite scan beginning at 1843 UTC.

Figure 33. WSR-88D composite scan beginning at 1853 UTC.

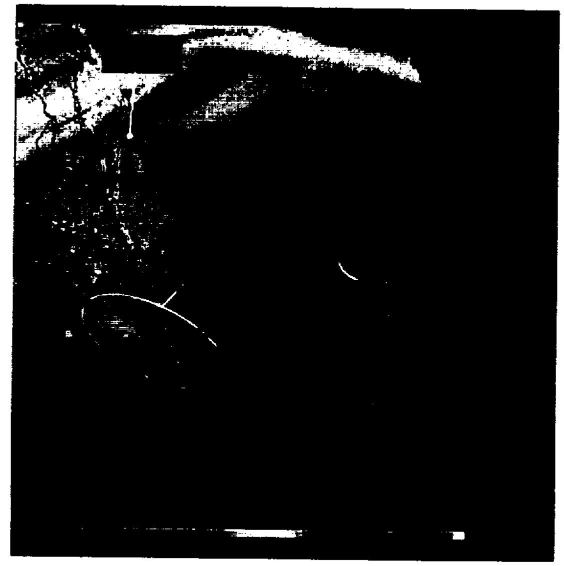

Figure 34. WSR-88D composite scan beginning at 1903 UTC.

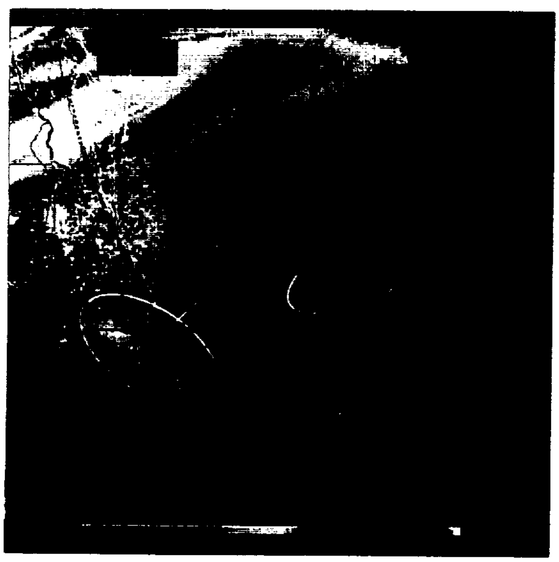

Figure 35. WSR-88D composite scan beginning at 1913 UTC.

Figure 36. WSR-88D composite scan beginning at 1922 UTC.

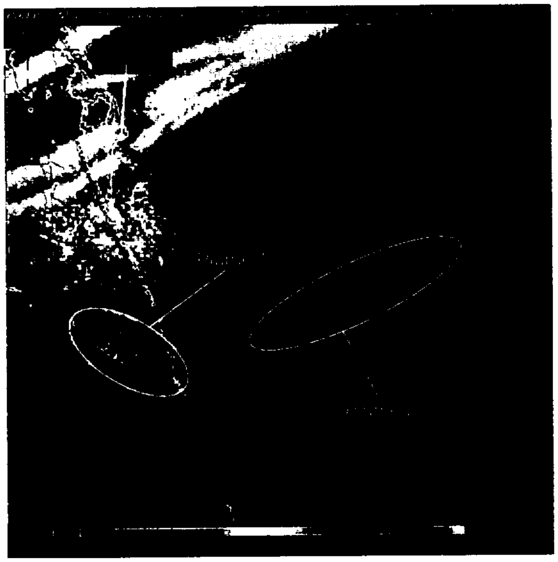

Figure 37. WSR-88D composite scan beginning at 1932 UTC.

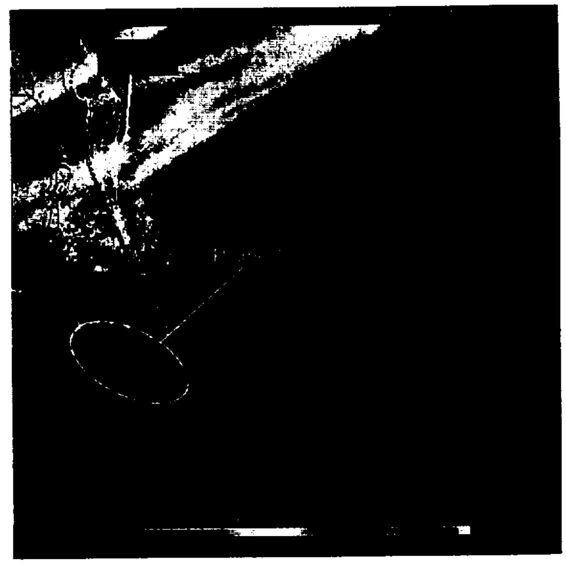

Figure 38. WSR-88D composite scan beginning at 1942 UTC.

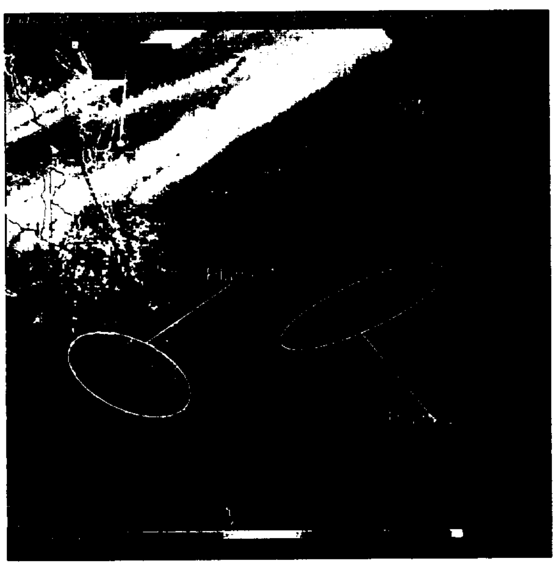

Figure 39. WSR-88D composite scan beginning at 1952 UTC.

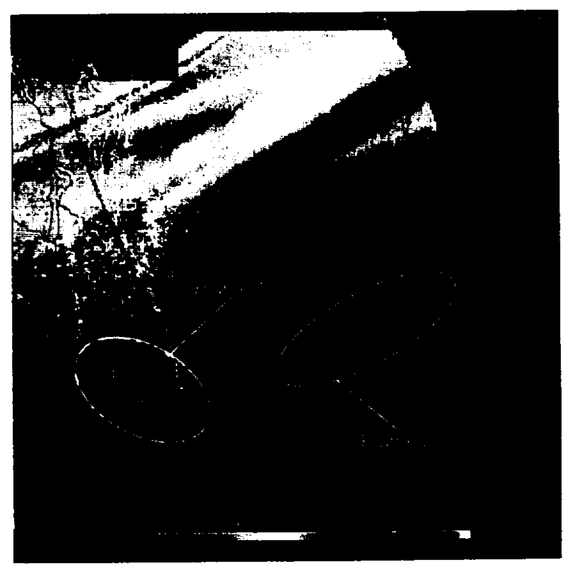

Figure 40. WSR-88D composite scan beginning at 2002 UTC.

Figure 41. WSR-88D composite scan beginning at 2011 UTC.

Figure 42. WSR-88D composite scan beginning at 2021 UTC.

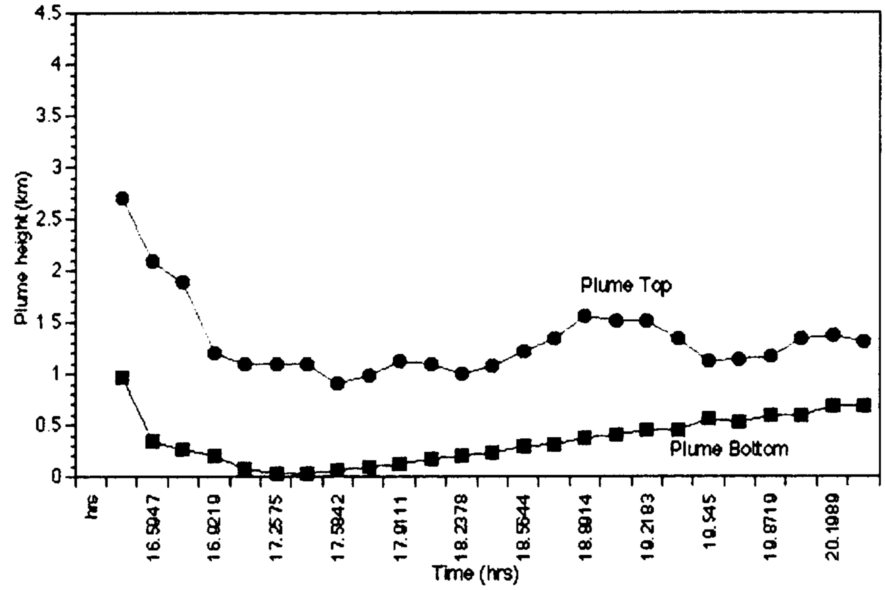

Figure 43. The plume height of the lower cloud (Plume 1) over the 4-h period. Heights were determined using the 88Display software tool. Note that the inaccuracies of these height determinations is high due to radar beam width spread and radar beam path through the strong inversion. However, the determination of error bars was not possible using the 88Display tool.

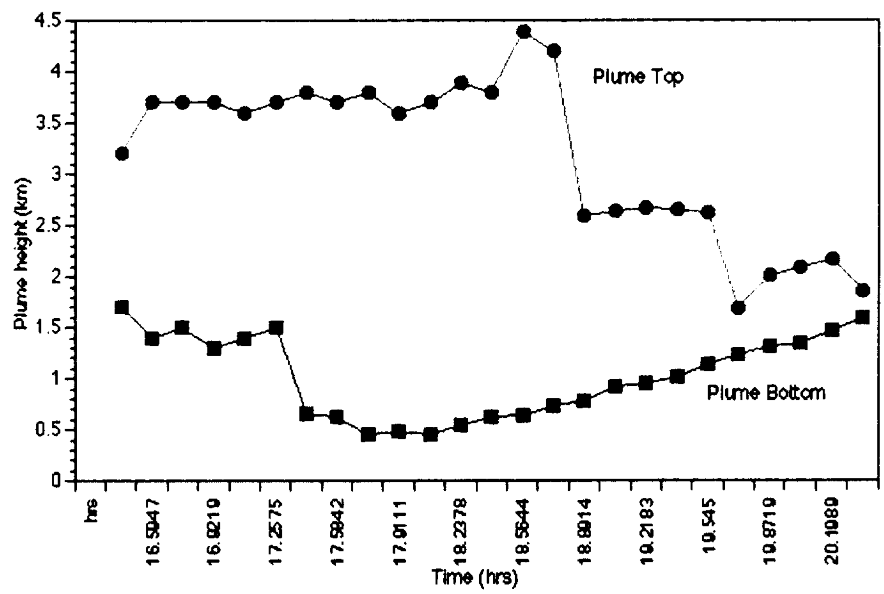

Figure 44. The plume height of the upper cloud (Plume 2) over the 4-h period. Heights were determined using the 88Display software tool. Note that the inaccuracies of these height determinations is high due to radar beam width spread and radar beam path through the strong inversion. However, the determination of error bars was not possible using the 88Display tool.

3.2. Model data

One of the primary goals of this study was to compare the model results with observations for 17 January 1997. This section presents the model data from RAMS, HYPACT, and REEDM for this day. Comparison with observational data discussed previously is provided.

3.2.1. REEDM results

These REEDM results were obtained from ACTA (Figures 45 and 46). A rawinsonde released at 1613 UTC provided data for input to REEDM. The REEDM vertical profiles of temperature, wind speed, wind direction, and potential temperature are shown in Figure 46. Winds were northerly with wind speeds near 11 m s^{-1} below the inversion, becoming northwesterly then westerly and stronger above the inversion.

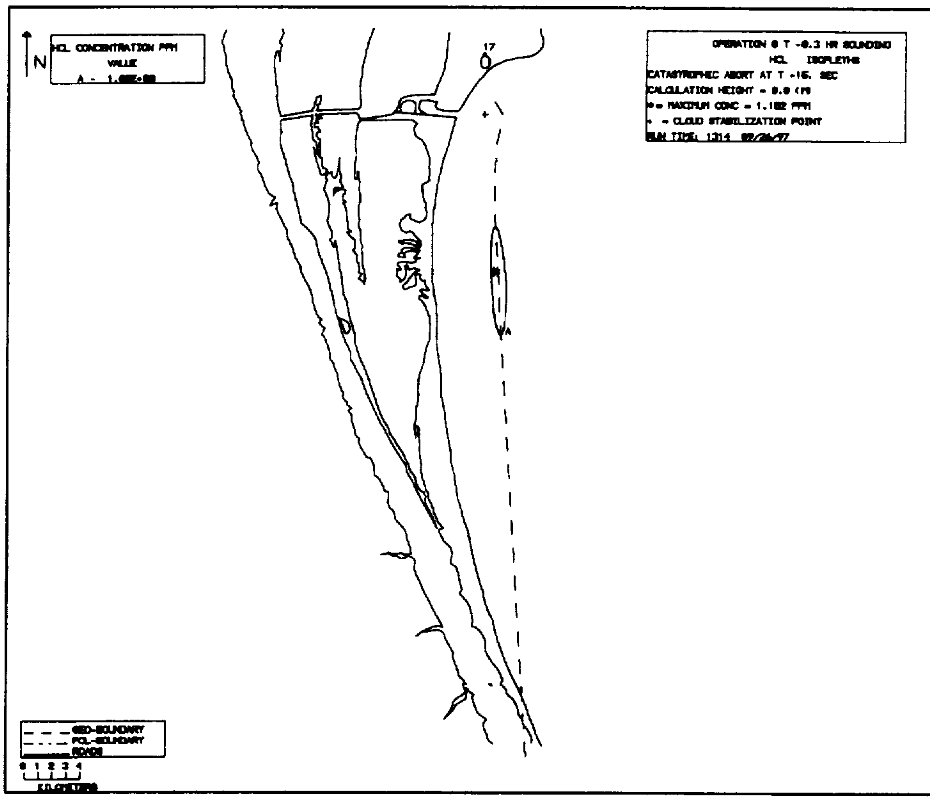

Figure 45. REEDM plots from the 1613 UTC rawinsonde just prior to the Delta II rocket failure on 17 January 1997. The REEDM run was for a conflagration at T+15 seconds simulating transport and ground-level concentration of HCl gas from burning solid rocket motors.

Following the Delta II accident, REEDM modeled only the lower toxic cloud, which was a potential health threat at the surface. The sounding detected northerly or northwesterly winds below the inversion, so the REEDM calculation drove the cloud southward, with landfall south of Melbourne. The peak HCl concentration predicted by REEDM as the plume moved southward was on the order of 1.0 ppm for the first 30 min; the highest peak (1.27 ppm) was predicted to occur 1.5 km downwind from the pad.

At the right of the Figure 46 is the predicted profile of the solid rocket propellant cloud as viewed from a position west of LC-17. Winds above and below the inversion sheared the cloud, moving the portion below the inversion toward the south, and the portion above the inversion toward the southeast. The REEDM predicted plume track and 1-ppm contour of ground-level HCl concentrations are shown in Figure 45. Not surprisingly, given the meteorological conditions shown in Figure 46, the plume was predicted to move almost due south over the ocean and not make landfall until south of the Melbourne area.

The results presented here were from REEDM 7.07 which was the version in use at the time of the Delta II explosion. Newer versions of REEDM (e.g. REEDM 7.08 and REEDM 7.09) produce different results and different ground level concentrations. Range Safety has continued to upgrade REEDM as the result of new scientific findings and uses the latest version available to evaluate launch cloud dispersion (Nyman 1999).

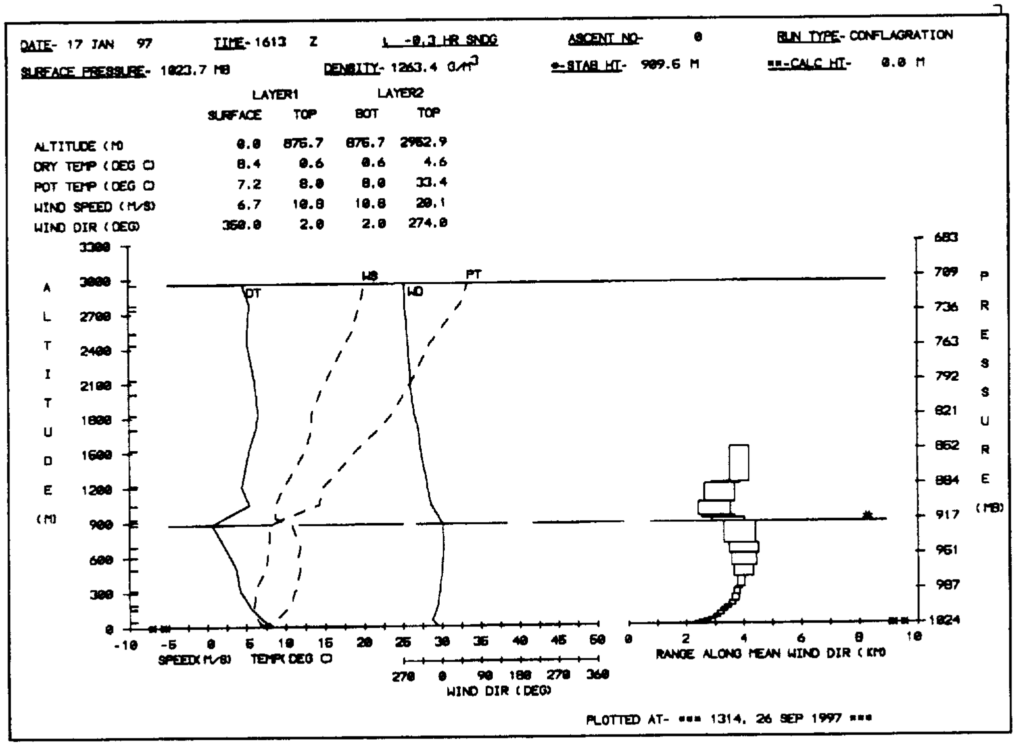

Figure 46. REEDM cross-section plot showing rawinsonde data from 1613 UTC on the left and REEDM source term predictions on the right.

3.2.2. RAMS results from ERDAS and PROWESS

The description and configuration of the two versions of RAMS used in this study were provided in Section 2.3. Discussion and figures showing the results of those RAMS runs are presented here.

The RAMS runs were initialized at 1200 UTC, approximately 4.5 hours before the Delta II explosion. The meteorology during this day did not change significantly because of the presence of the post-frontal regime with the continued cold air advection. There were no sea breezes, river breezes, thunderstorms, or other significant local-scale phenomena for RAMS to forecast for the Cape Canaveral area.

Graphs comparing ERDAS RAMS wind data with observed data are presented in Figures 47 and 48. These figures show the observed vertical wind profiles at 1613 UTC and the predicted vertical wind profiles at 1600 UTC. RAMS predicted the wind speed profile accurately through the mixing layer to the inversion at 900 meters and then accurately predicted the gradual increase to 25 m s^{-1} at 4500 meters. RAMS predicted the wind direction more westerly than northwesterly in the layer from the surface to approximately 500 meters but then accurately predicted the wind shear at the 900-meter inversion and the westerly winds aloft.

The potential temperature profile predicted by RAMS at 1600 UTC closely matched the observed profile at 1613 UTC (Figure 49). The base of the predicted inversion was only slightly lower than the base of the observed inversion.

Maps showing RAMS forecast data from ERDAS and PROWESS for the period 1500 UTC to 2000 UTC are shown in Figures 50 - 56. Data are presented that represent wind flow in the different layers important in the plume analysis. The wind flow as shown by streamline analysis for different times and different levels are presented in Figures 50 to 53. The streamlines indicate the wind direction at a point in time and space.

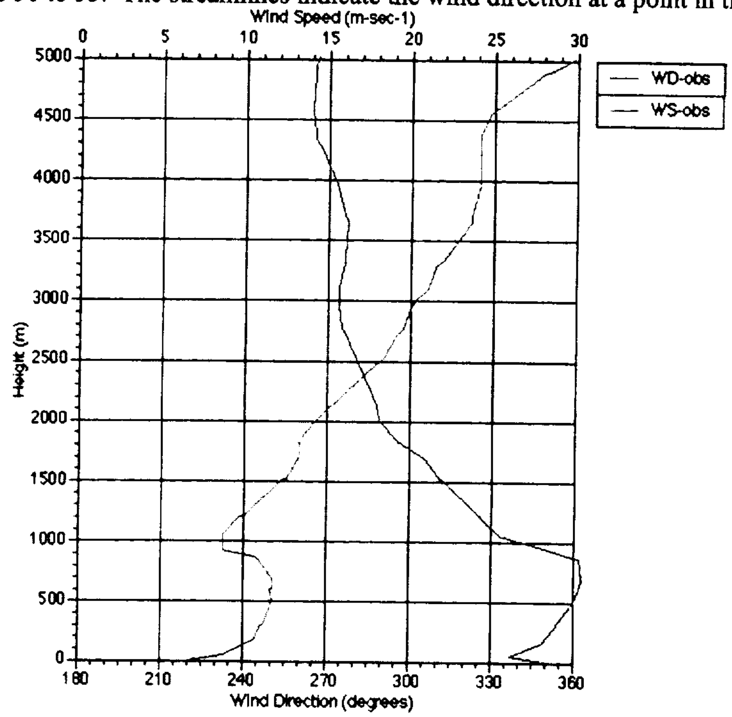

Figure 47. Observed wind speed and direction from rawinsonde at 1613 UTC. Note that the observed wind directions from 0 - 15° are shown on the graph as greater than 360°.

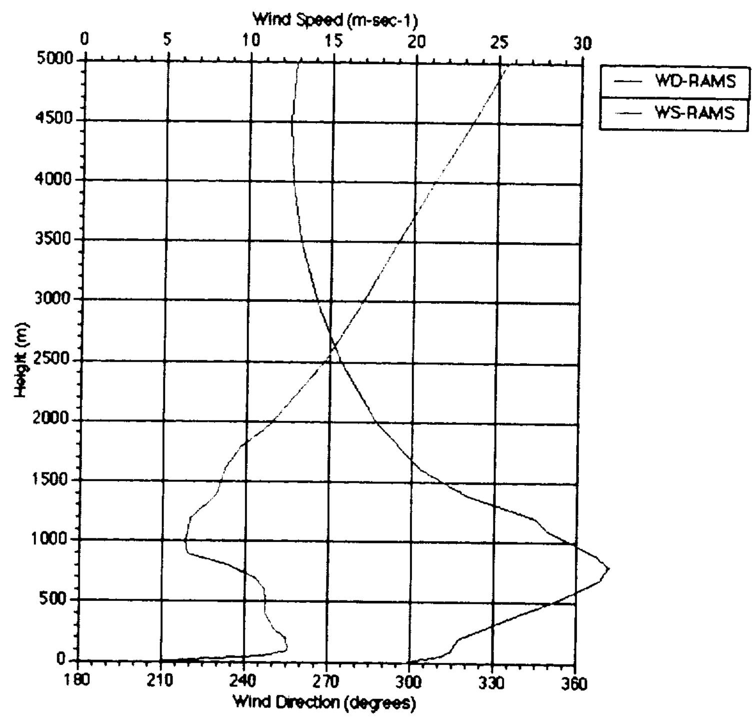

Figure 48. Predicted wind speed and direction from ERDAS RAMS at 1600 UTC. Note that the observed wind directions from 0 - 15° are shown on the graph as greater than 360°.

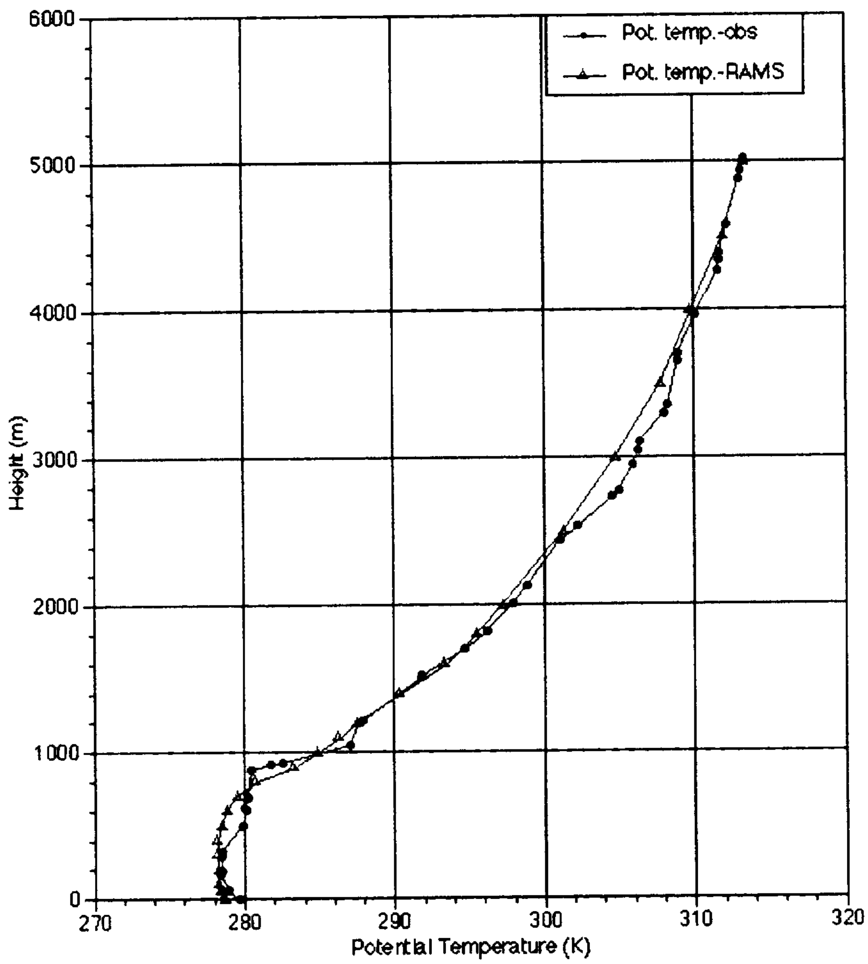

Figure 49. Rawinsonde-observed potential temperature at 1613 UTC compared to model-predicted potential temperature at 1600 UTC. The model predictions were from ERDAS RAMS.

The streamlines for the lowest RAMS level in both configurations indicate persistent northwesterly flow for the duration of the Delta II plume analysis over the Cape Canaveral region (Figs. 50, 51a and b). The models predicted a slight shift in flow from northwesterly to north-northwesterly from 1500 to 1900 UTC but the shift was not significant with respect to the plume transport in HYPACT.

The streamlines for the layers centered at 782 meters in ERDAS and 724 meters in PROWESS are shown in Figures 51c, 51d, and 52 for the Delta II analysis period. The 700-800 meter layer is important because this is the level just below the strong inversion that existed on 17 January. The winds in this level strongly influenced the transport of the lower plume. The analyses show that RAMS predicted northerly flow over Cape Canaveral at 1500 UTC. By 1700 UTC, RAMS predicted northeasterly wind flow in the region south of Cape Canaveral, over the ocean. The northeast flow became more pronounced at 1900 UTC. The ERDAS and PROWESS configurations generally agreed in predicting northeast winds south of Cape Canaveral but for the area north and west of Cape Canaveral, PROWESS RAMS predicted northerly flow while ERDAS RAMS predicted northeasterly flow across the entire Cape Canaveral region.

For the layers well above the inversion at 1580 meters for ERDAS RAMS and 1699 meters for PROWESS RAMS, the streamline analysis from both models showed persistent west-northwesterly flow through the Delta II analysis period (Fig. 53). Both models showed similar wind flow at 1500 and 2000 UTC. The winds at this level influenced the transport of the upper cloud.

The RAMS temperature predictions for the lowest levels in the ERDAS and PROWESS configurations are shown in Figure 54. The analyses are shown to compare the configuration differences and also to show the change over time of the predicted low-level temperature structure. At 1500 UTC, both configurations show an east-west temperature gradient with colder temperatures over the land and warmer temperatures to the east over the ocean. It is difficult to compare the actual temperatures since the lowest level in ERDAS is centered at 10 meters and the lowest level in PROWESS is centered at 35 meters. By 2000 UTC, the temperature gradient had shifted to north-south in both models and ERDAS RAMS, with its lowest level at 10 m, shows more influence of the land-water interfaces associated with rivers and islands.

The vertical potential temperature structure of the atmosphere as predicted by RAMS is shown in Figure 55. These figures show an east-west cross section of the potential temperature as predicted by the two configurations of RAMS at different times. The figures show that ERDAS RAMS predicted an elevated inversion at approximately 750 meters at 1500 UTC while PROWESS RAMS predicted the inversion at approximately 500 meters at 1500 UTC. By 2000 UTC the models lifted the inversion to approximately 1000 meters for ERDAS RAMS and 750 meters for PROWESS RAMS. Rawinsonde data from 1613 UTC indicated the base of the inversion was at approximately 900 meters (Figure 49).

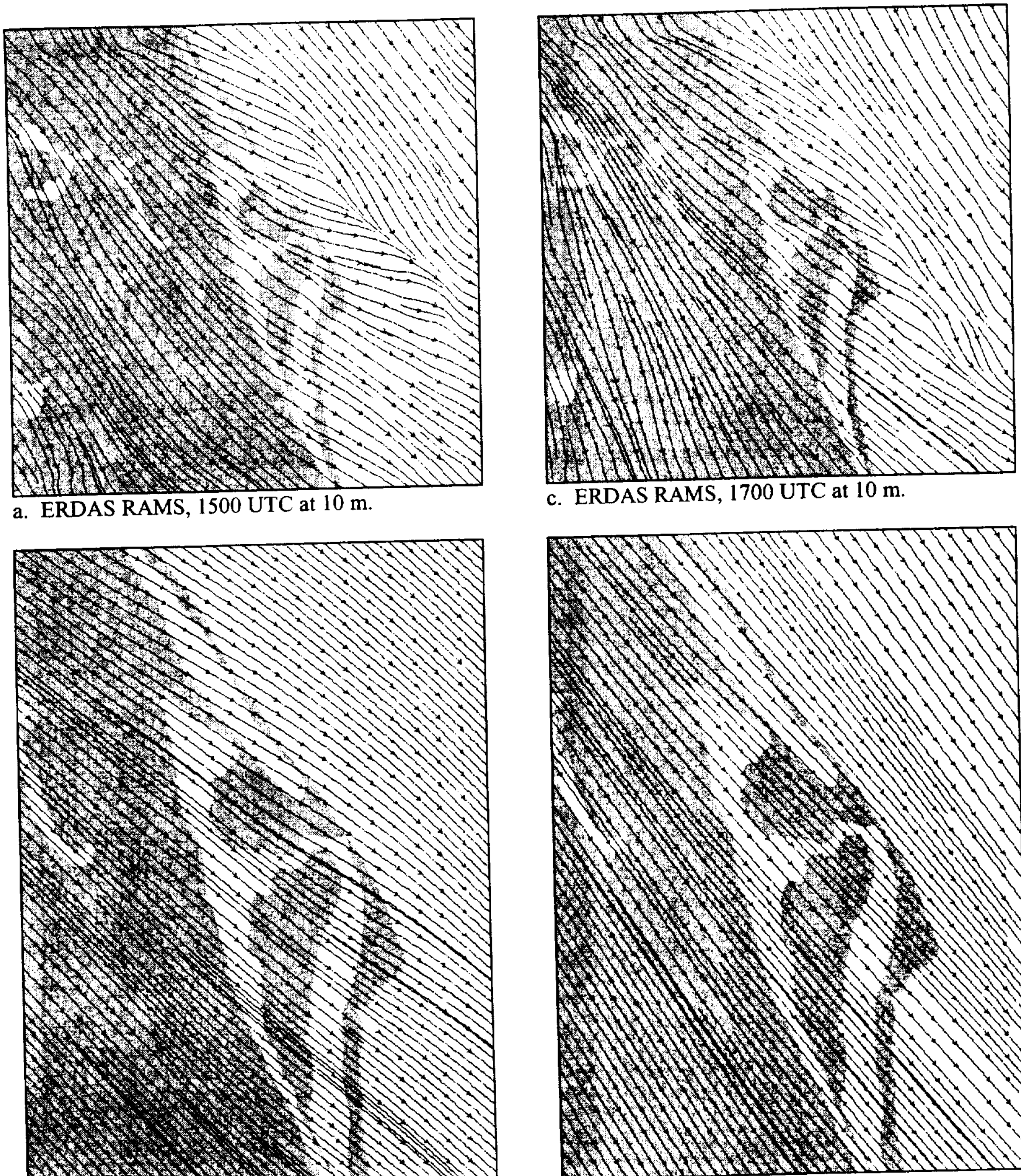

a. ERDAS RAMS, 1500 UTC at 10 m.

c. ERDAS RAMS, 1700 UTC at 10 m.

b. PROWESS RAMS, 1500 UTC at 35 m.

d. PROWESS RAMS, 1700 UTC at 35 m.

Figure 50. Streamline forecasts comparing output from ERDAS and PROWESS on 17 January 1997. Each figure is marked with its model configuration, time, and height.

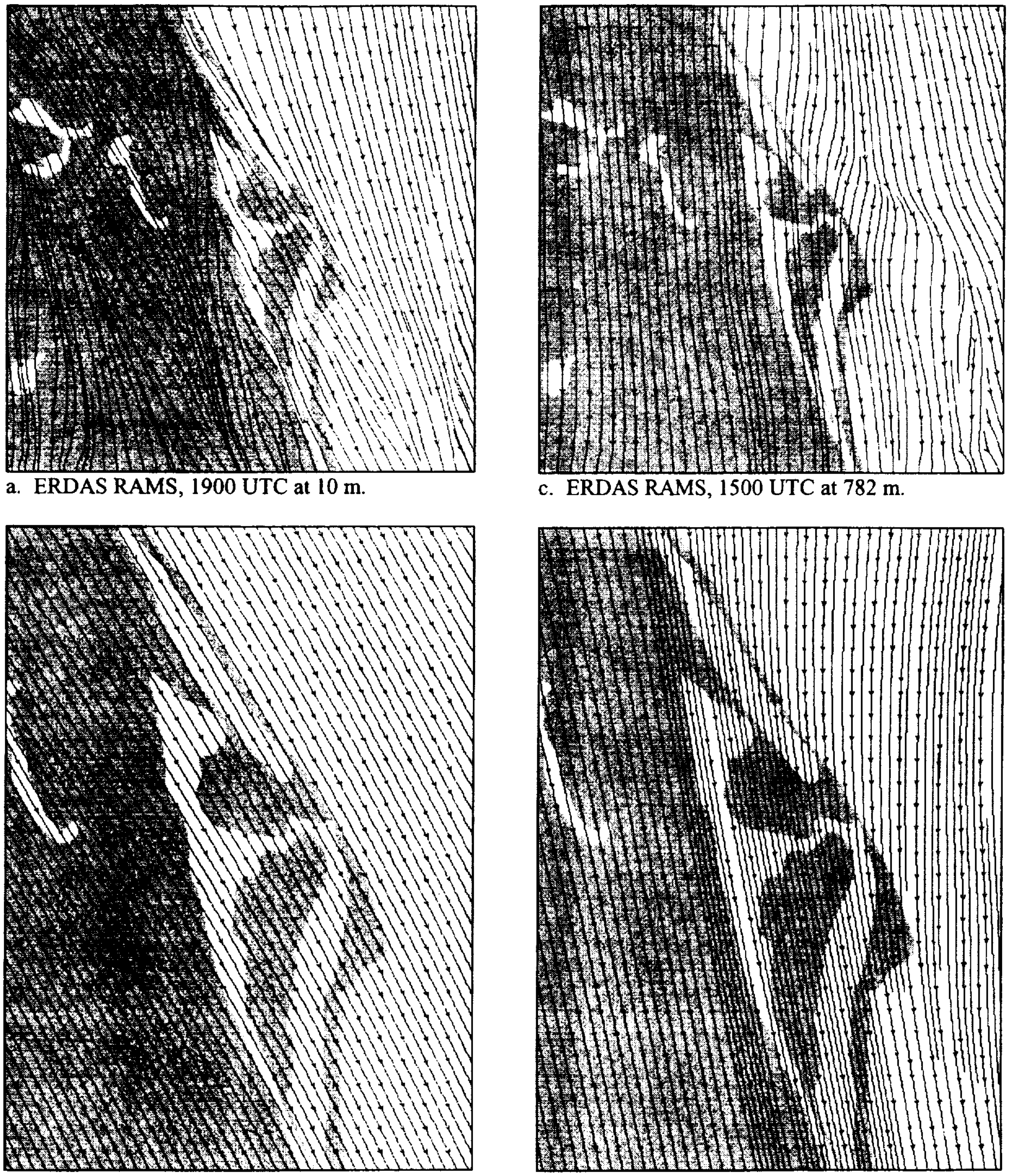

a. ERDAS RAMS, 1900 UTC at 10 m.

c. ERDAS RAMS, 1500 UTC at 782 m.

b. PROWESS RAMS, 1900 UTC at 35 m.

d. PROWESS RAMS, 1500 UTC at 724 m.

Figure 51. Streamline forecasts comparing output from ERDAS and PROWESS on 17 January 1997. Each figure is marked with its model configuration, time, and height.

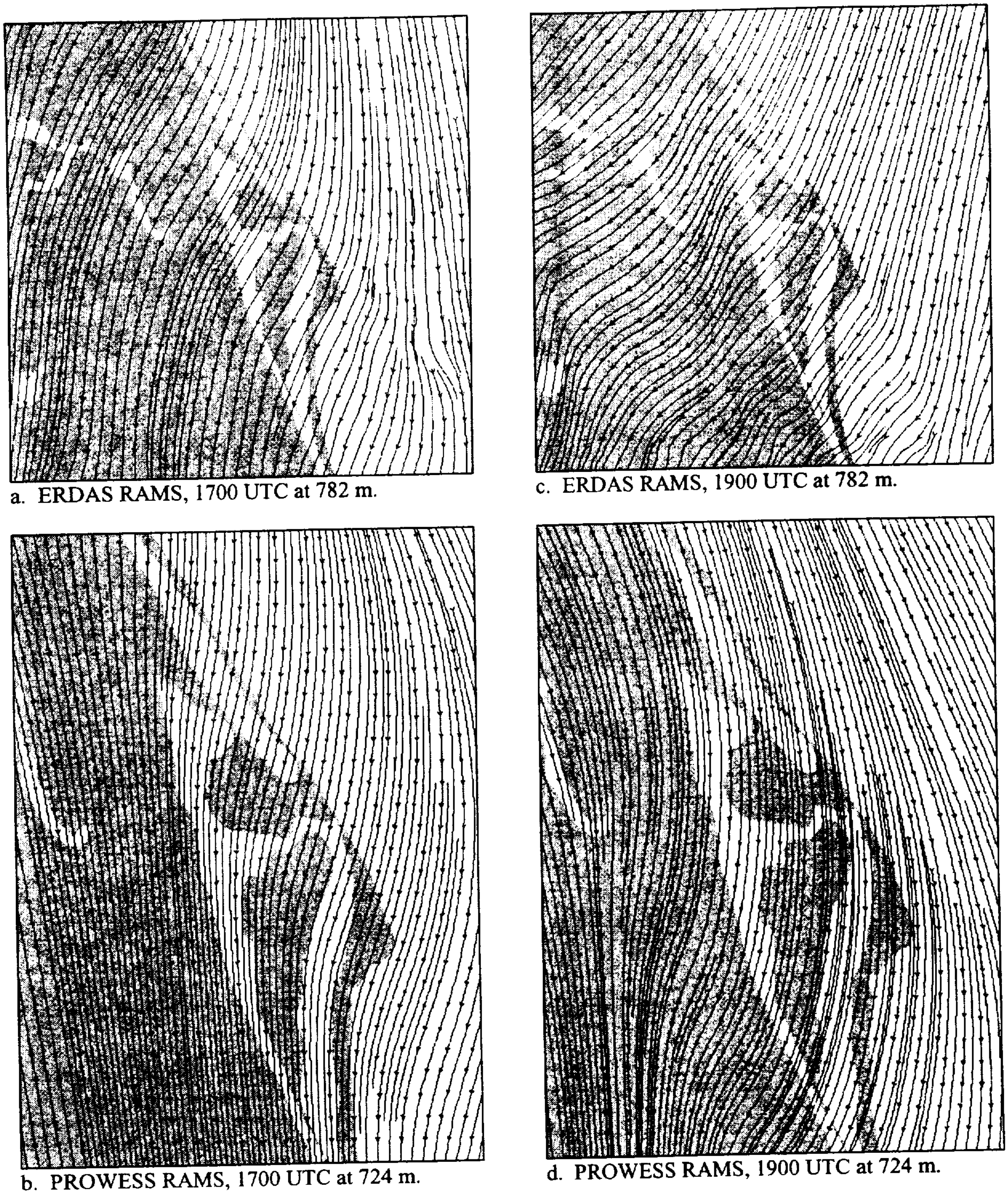

a. ERDAS RAMS, 1700 UTC at 782 m.

c. ERDAS RAMS, 1900 UTC at 782 m.

b. PROWESS RAMS, 1700 UTC at 724 m.

d. PROWESS RAMS, 1900 UTC at 724 m.

Figure 52. Streamline forecasts comparing output from ERDAS and PROWESS on 17 January 1997. Each figure is marked with its model configuration, time, and height

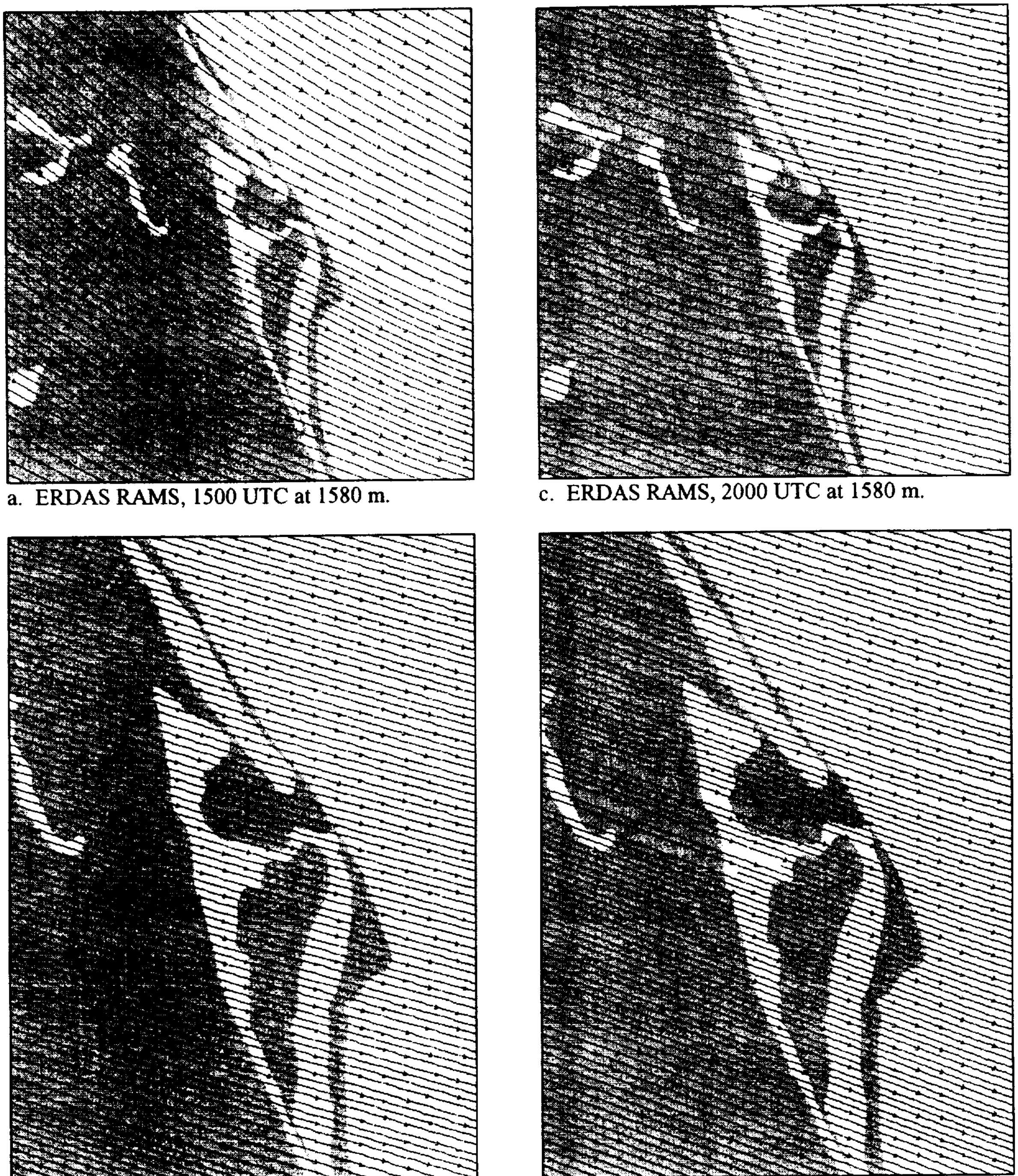

a. ERDAS RAMS, 1500 UTC at 1580 m.

c. ERDAS RAMS, 2000 UTC at 1580 m.

b. PROWESS RAMS, 1500 UTC at 1699 m.

d. PROWESS RAMS, 2000 UTC at 1699 m.

Figure 53. Streamline forecasts comparing output from ERDAS and PROWESS on 17 January 1997. Each figure is marked with its model configuration, time, and height.

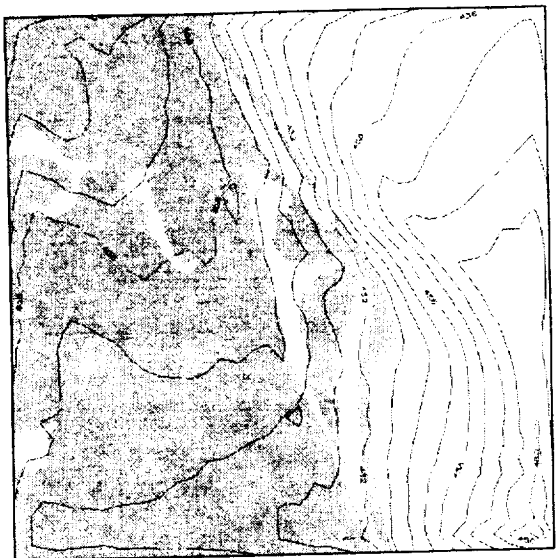

a. ERDAS RAMS, 1500 UTC at 10 m.

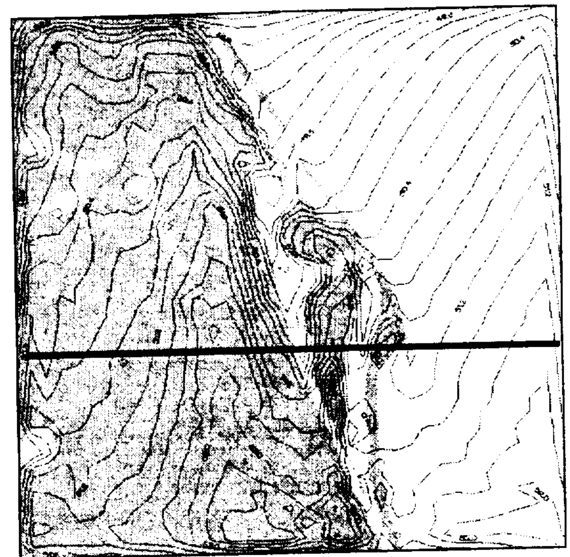

c. ERDAS RAMS, 2000 UTC at 10 m.

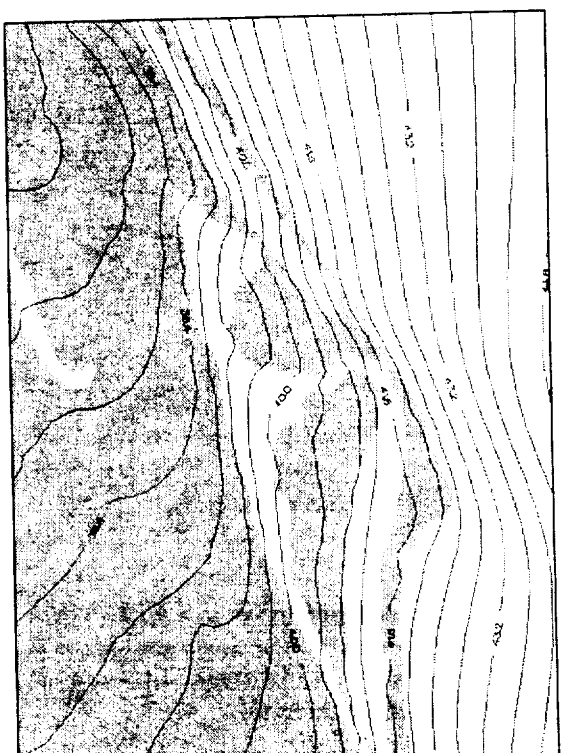

b. PROWESS RAMS, 1500 UTC at 35 m.

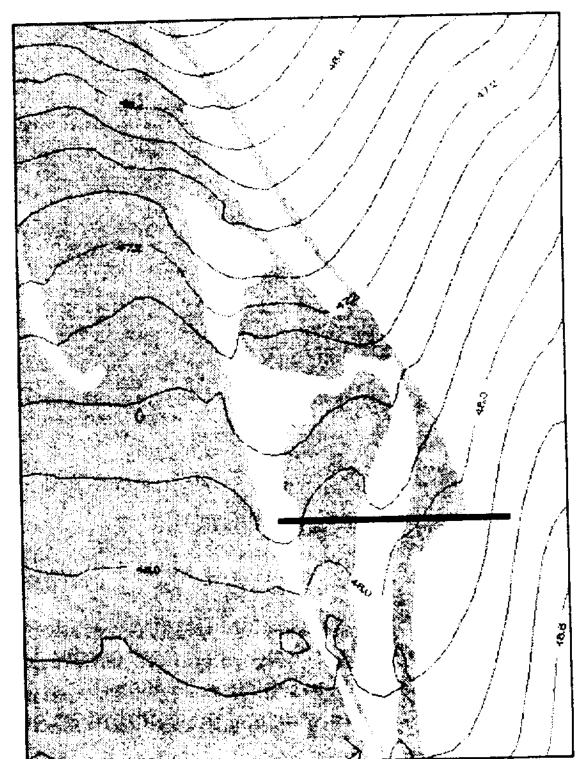

d. PROWESS RAMS, 2000 UTC at 35 m.

Figure 54. Surface temperature (F) forecasts comparing output from the lowest levels of ERDAS (10 m) and PROWESS (35 m) on 17 January 1997. Each figure is marked with its model configuration, time, and height. The dark bold line in panels c and d shows the approximate location of the potential temperature cross sections shown in Figure 55.

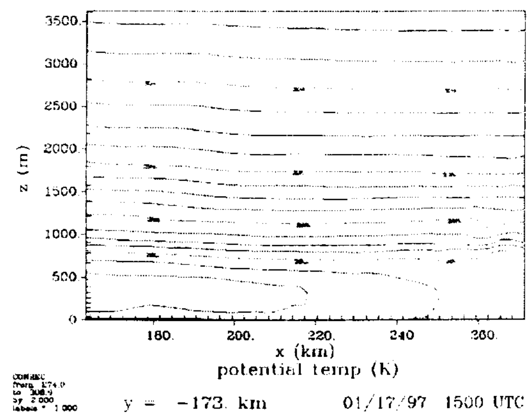

a. ERDAS RAMS, 1500 UTC.

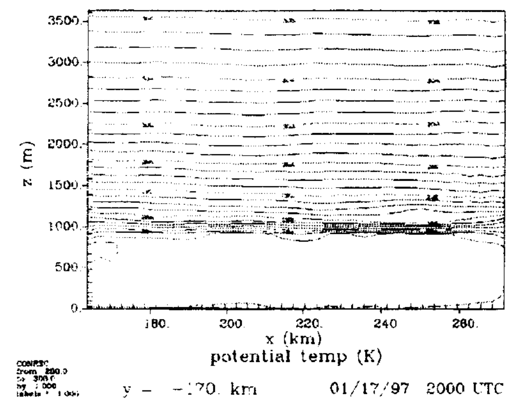

b ERDAS RAMS, 2000 UTC.

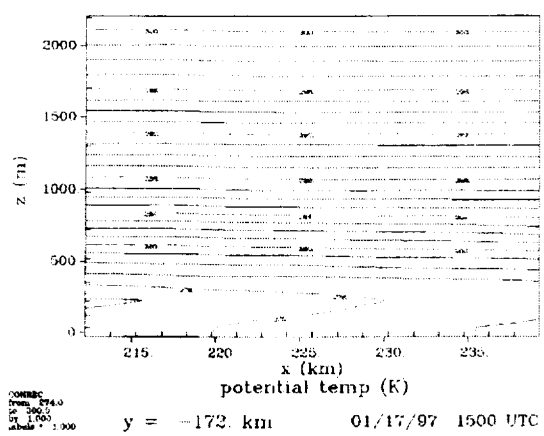

c. PROWESS RAMS, 1500 UTC.

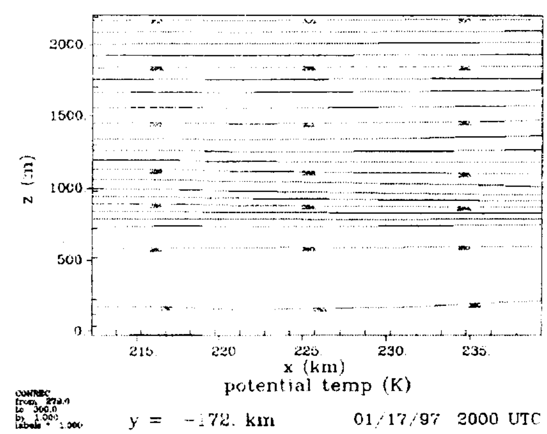

d. PROWESS RAMS, 2000 UTC.

Figure 55. Potential temperature (K) cross section forecasts comparing output from ERDAS and PROWESS on 17 January 1997. Each figure is marked with its model configuration and time. The cross-sections intersect the Cape Canaveral Air Force Station along an east-west line as shown in Figure 54. The ERDAS cross-section is approximately 110 km wide and the PROWESS cross section is approximately 25 km wide.

3.2.3. HYPACT results from ERDAS and PROWESS

3.2.3.1. HYPACT Configuration

As discussed in Section 2.3.4, we modified the HYPACT input data configuration file to simulate the Delta II explosion plume. When we first ran REEDM within ERDAS for the Delta II explosion, the source term was characterized as 21 different sources extending from 300 to 2100 m above the ground. Table 4 presents the source term data produced by REEDM for the 21 sources.

Table 4. Location and dimensions of plume determined by REEDM and modeled by HYPACT. These plume dimensions were used in the ERDAS HYPACT simulation.

Source no.	latitude	longitude	height (m)	x-size (m)	y-size (m)	z-size (m)	shape
1	28.42615	-80.55101	349.9	470.4	470.4	100.0	ellipse
2	28.42622	-80.55413	449.9	705.8	705.8	100.0	ellipse
3	28.42408	-80.55320	508.3	789.0	789.0	16.7	ellipse
4	28.42531	-80.55086	524.9	808.2	808.2	16.7	ellipse
5	28.42695	-80.54810	550.0	833.8	833.8	33.4	ellipse
6	28.42695	-80.54810	583.5	862.0	862.0	33.5	ellipse
7	28.42695	-80.54810	614.5	883.0	883.0	28.5	ellipse
8	28.42695	-80.54810	643.0	898.0	898.0	28.6	ellipse
9	28.42695	-80.54810	671.5	909.2	909.2	28.5	ellipse
10	28.42695	-80.54810	742.9	921.2	921.2	114.3	ellipse
11	28.42695	-80.54810	856.3	894.6	894.6	112.5	ellipse
12	28.42695	-80.54810	925.1	848.8	848.8	25.0	ellipse
13	28.42695	-80.54810	950.1	826.0	826.0	25.0	ellipse
14	28.42695	-80.54810	975.1	799.4	799.4	25.0	ellipse
15	28.42695	-80.54810	1000.9	767.4	767.4	26.7	ellipse
16	28.42695	-80.54810	1028.6	727.6	727.6	28.6	ellipse
17	28.42695	-80.54810	1057.2	679.4	679.4	28.6	ellipse
18	28.42695	-80.54810	1085.8	622.2	622.2	28.5	ellipse
19	28.42695	-80.54810	1200.0	399.8	399.8	200.0	ellipse
20	28.42695	-80.54810	1450.1	399.8	399.8	300.2	ellipse
21	28.42695	-80.54810	2050.1	399.8	399.8	899.8	ellipse

The visual and radar observations of the plume indicated that the plume had obviously split into two distinct clouds. To initialize more accurately HYPACT, we modified the source size and shape to more closely represent the observed size and shape of the actual plume. Therefore, the plume was represented as two sources. The plume's location and dimensions are presented in Table 5. A complete listing of the HYPACT configuration used to model the Delta II explosion is presented in Appendices C and D.

Table 5. Location and dimensions of plume determined from visual and radar observations and modeled by HYPACT. These plume dimensions were used in the PROWESS HYPACT simulation.

Source no.	latitude	longitude	height (m)	x-size (m)	y-size (m)	z-size (m)	shape
1	28.448	-80.566	600.	600.	600.	400.	ellipse
2	28.448	-80.566	1800.	600.	600.	400.	ellipse

3.2.3.2. HYPACT runs

The HYPACT model was run for two scenarios. There were two reasons for the modeling exercise of comparing the observed and predicted plumes. The principal of the two reasons was to determine how well the modeled plume trajectories compared with the observed plume trajectories. The secondary reason for the exercise was to determine how the REEDM-predicted source term compared with the actual source term. To reduce the number of runs and the number of figures we displayed, we combined the trajectory and source term analysis in the ERDAS-HYPACT runs and we did not perform a source term analysis for the PROWESS-HYPACT runs. Combining the runs did not hinder the results since we adequately assessed the trajectories of both runs and we were able to assess how the REEDM-predicted source term compared with the actual source term.

The figures presented in this report compare the predicted plume locations from ERDAS-HYPACT and PROWESS-HYPACT with the observed plume locations from the WSR-88D radar. The comparisons presented are for each 10-minute HYPACT model time during the four hours that the plume was tracked. The HYPACT source terms were generated from the REEDM model using the REEDM function of ERDAS. REEDM generates the HYPACT source term for a rocket launch by creating a column that contains mass of the chemical species of interest. The column is composed of separate sources (volumes) of mass, which are 75 meters in thickness. We assessed the REEDM-predicted source term by observing how the modeled initial plume changed during the simulation and comparing its shape with observed plume. The ERDAS-HYPACT run was made leaving the mass in the entire column from the surface up to 2500 meters. We assessed the ERDAS-HYPACT trajectories by tracking only the lower and upper part of the plume and comparing those with the trajectory of the observed plume.

The source term for the PROWESS configuration was modified slightly to simulate the observed source term since in our analysis we knew the initial shape of the plume. The plume was modified by removing the initial mass in the layers between 925 and 1550 meters. We assessed the PROWESS-HYPACT trajectories by tracking the two plumes and comparing those with the observed plume.

For the explosion time, both ERDAS-HYPACT and PROWESS-HYPACT transported the upper and lower explosion clouds in different directions. The split transport occurred because the upper cloud was at a height where the winds were strong and from the west while the lower cloud was trapped below a strong inversion with winds were from the north.

The primary purpose of analyzing the trajectory of the ERDAS-HYPACT and PROWESS-HYPACT plumes was to determine how the model predictions compared with observations. Therefore, the part of the HYPACT plumes which were compared and which are the focus of the discussion below are the lower plume below 925 meters and the upper plume above 1550 meters. Even though, the ERDAS-HYPACT simulation was run with the entire plume, we were not concerned with the transport of the center of the plume between 925 and 1550 meters.

3.2.3.3. HYPACT results

The HYPACT predictions of the ERDAS and PROWESS plumes are shown in Figures 56 to 115. The figures show two-dimensional views of the plume from a horizontal map perspective and from a northward-facing vertical cross section. HYPACT output was produced every ten minutes.

HYPACT moved the lower cloud to the south where it reached the coast in the vicinity of Cocoa Beach at approximately 30 minutes after the explosion. Figures 56 - 63 show the lowest part of the ERDAS cloud out over the ocean and extending upward and westward to the coastline where it curves north and then east as it extends upward. The cross-section shows the slight shift to the east of the particles in the lowest part of the plume. HYPACT begins spreading the lower cloud as shown by the diffusion of the lower plume particles (Figures 62 and 63).

Figures 86 - 93 show the two PROWESS clouds (due to the initial source split) with the lower cloud to the southwest of the upper cloud. The lower cloud extends upward and westward from over the ocean to the coastline. The upper cloud extends eastward and upward from approximately 10 km offshore out to approximately 20 km offshore. HYPACT begins to also diffuse the lower PROWESS plume similar to the ERDAS plume.

The observed radar plume between 1616 and 1705 UTC (Figures 17 - 23) show that the low-level cloud had reached the coast north of Cocoa Beach and had moved slightly more westward than the model runs had predicted. The orientation of the cloud was east-west in a shape similar to the model predictions. The upper cloud was also oriented in an east-west direction as it was transported eastward by the westerlies.

Between 1710 and 1730 UTC, HYPACT continued to diffuse both the ERDAS (Figures 64 - 69) and PROWESS (Figures 94 - 99) lower clouds as shown by the cross-sections which show considerable particle spread in the layers from the surface up to approximately 500 meters. HYPACT continued to carry the lower cloud southward keeping most of the plume over the ocean extending barely on to the land. HYPACT moved the ERDAS and PROWESS upper clouds rapidly to the east and causes very little spreading or diffusion within them.

Figures 23 - 25, presenting the observed radar cloud from 1715 to 1735 UTC, show the lower cloud moved over the land further west than predicted by HYPACT but kept the shape and orientation similar to that predicted by HYPACT. The upper cloud exhibited an undulating shape as it moved south and east.

During the period from 1740 to 1820 UTC, the ERDAS HYPACT runs (Figures 70 - 75) and the PROWESS HYPACT runs (Figures 100 to 105) moved the low level cloud to the south and spread it wider to the east and west. This trend continued for the remaining period of the simulation (Figures 76 - 85 and Figures 110 - 115). The ERDAS low-level cloud extended slightly further west than the PROWESS low-level cloud. The upper cloud continued to move quickly to the east in both runs.

From 1745 to 1833 UTC, the observed radar maps showed the movement of the two distinct clouds (Figures 26 - 31). The low-level cloud moved over Melbourne with part of the cloud extending eastward over the ocean. The bulk of the cloud was located over the land, to the west of where the model runs had predicted. The observed upper cloud matched the model predictions closely in its orientation from east-northeast to west-southwest and in its movement toward the east-southeast. Another interesting feature which was similar in the ERDAS HYPACT upper plume (Figures 78 - 105) and the observed radar upper plume (Figures 24 - 36) was the wavelike, undulating shape. The wavelike structure formed in the direction of the strong westerly flow in the 1000- to 1500-m layer.

Over the final two hours of the simulation, from 1840 to 2030 UTC, the ERDAS (Figures 76 - 85) and PROWESS (Figures 106 - 115) HYPACT runs continued moving the lower cloud south. Both runs diffused the lower clouds considerably with ERDAS HYPACT causing more spread especially in the north-south direction.

3.2.3.4. HYPACT results summary

One very interesting occurrence in the ERDAS HYPACT simulation was the split that took place beginning at 1840 UTC between the upper and lower parts of the plume. The split occurred at height of approximately 1100 meters. During the final hour of the simulation from 1940 to 2030, the cross-section showed that the upper and lower part of the plumes looked distinctly different. The lower part was very diffuse and individual particles were visible. The upper part of the cloud was ribbon-like and showed little diffusion except for its elongation to the east as it was moved with the westerly flow. The importance of the decoupling of the plume was that the break occurred at the height of the inversion and it matched the two-cloud scenario which was observed visually and by radar. Both observed and modeled plumes had an undulating shape as discussed earlier.

The discussion, provided in this section, indicates that the RAMS/HYPACT predictions of the lower cloud's direction of movement, speed, and dispersion matched closely with observations. However, the onshore component of the winds affecting the observed plume appeared stronger than the RAMS modeled winds. As a result, the observed plume moved more to the west than the modeled plume indicated. The model's prediction of the upper cloud's direction and shape showed good agreement with the observed plume's direction and shape.

Comparing the PROWESS-HYPACT plume to the ERDAS-HYPACT plume indicated that each model showed strengths and weaknesses when compared to the observations.

The source term used for the PROWESS-HYPACT (split column source term) run was a better fit than the source term used for ERDAS-HYPACT (continuous column source term). This result is not surprising since we decided to use the split column after viewing video and photography of the explosion cloud. The continuous column source term, however, showed a separation of the upper and lower clouds which began to take place at approximately 1840 UTC at a height of about 1100 meters. The separation was due to the strong shear above and below the strong inversion that existed and that was predicted by RAMS.

The upper plume as predicted by ERDAS-HYPACT matched the observed upper plume slightly better than the upper plume predicted by PROWESS-HYPACT. PROWESS-HYPACT moved the plume faster to the east than ERDAS-HYPACT and did not show the undulations that ERDAS-HYPACT predicted. The RAMS-predicted winds, which control the plume movement in HYPACT, were predicted to be slightly stronger in PROWESS compared to ERDAS.

At the surface, ERDAS-HYPACT and PROWESS-HYPACT both predicted approximately the same amount of spread of the lower plume in the east-west direction (Figures 79 and 107). The upper part of the lower ERDAS-HYPACT plume extended a little further west than the PROWESS-HYPACT plume. The observed lower plume at 1853 UTC (Figure 33) was shifted slightly to the west of the modeled plumes and did not extend as far to the east over the water as predicted by the models.

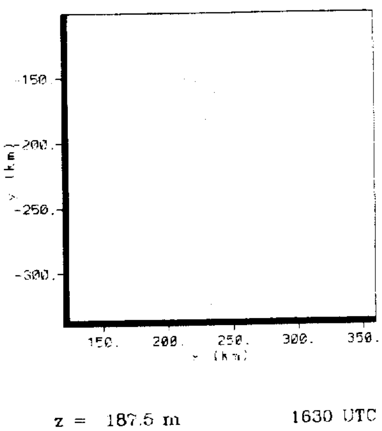

Figure 56. ERDAS HYPACT, 1630 UTC, 17 Jan 1997.

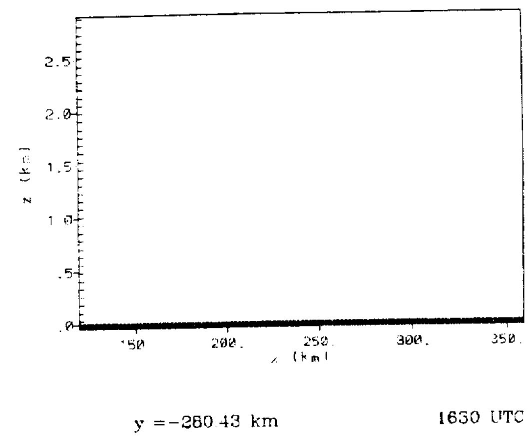

Figure 57. Same as Figure 56, vertical view from south.

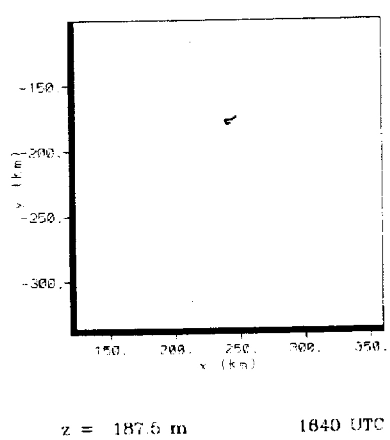

Figure 58. ERDAS HYPACT, 1640 UTC, 17 Jan 1997.

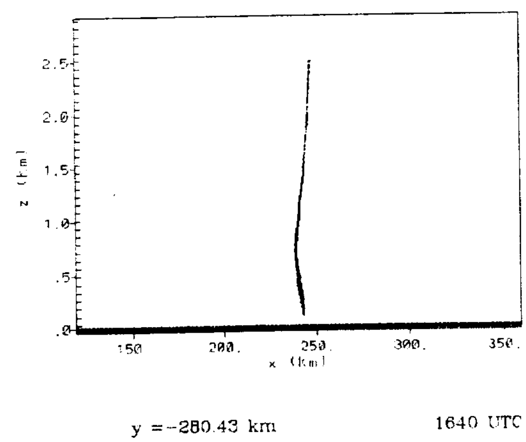

Figure 59. Same as Figure 58, vertical view from south.

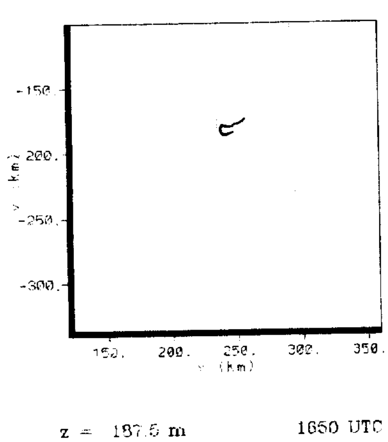

Figure 60. ERDAS HYPACT, 1650 UTC, 17 Jan 1997.

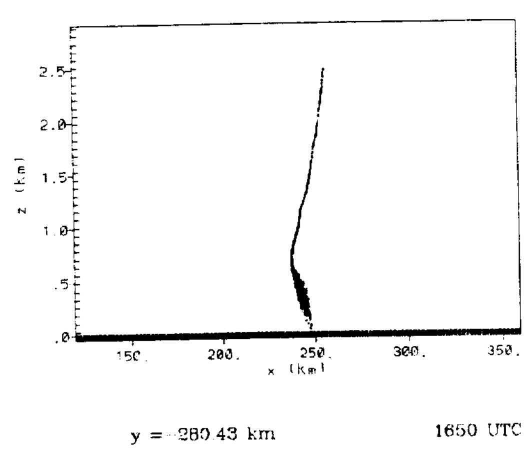

Figure 61. Same as Figure 60, vertical view from south.

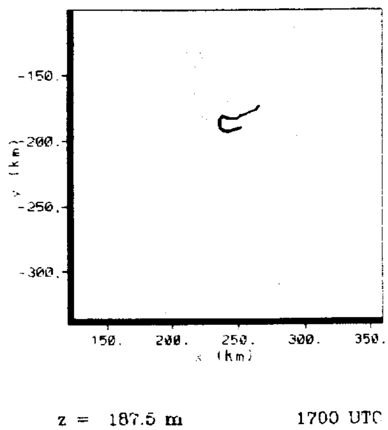

Figure 62. ERDAS HYPACT, 1700 UTC, 17 Jan 1997.

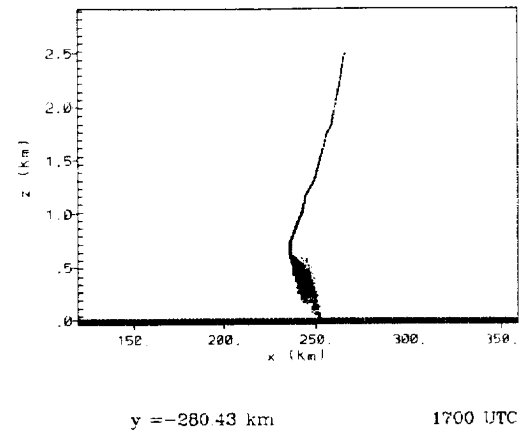

Figure 63. Same as Figure 62, vertical view from south.

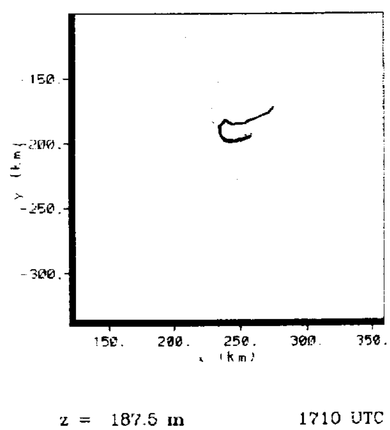

Figure 64. ERDAS HYPACT, 1710 UTC, 17 Jan 1997.

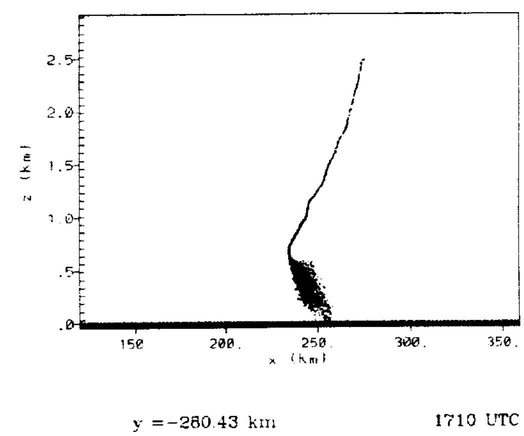

Figure 65. Same as Figure 64, vertical view from south.

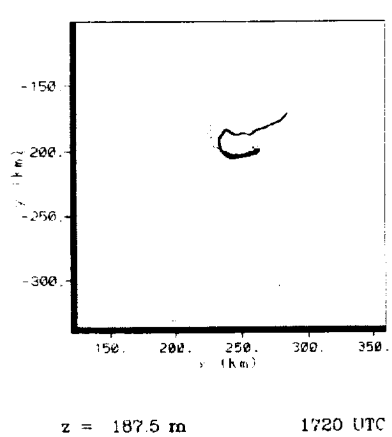

Figure 66. ERDAS HYPACT, 1720 UTC, 17 Jan 1997.

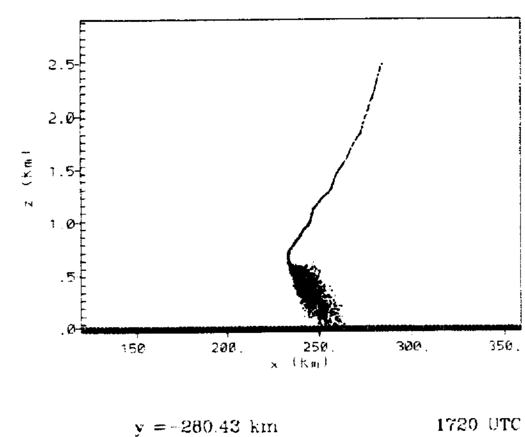

Figure 67. Same as Figure 66, vertical view from south.

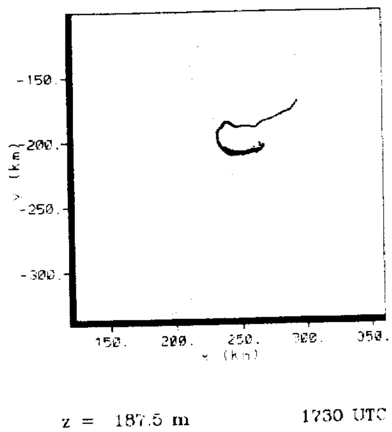

Figure 68. ERDAS HYPACT, 1730 UTC, 17 Jan 1997.

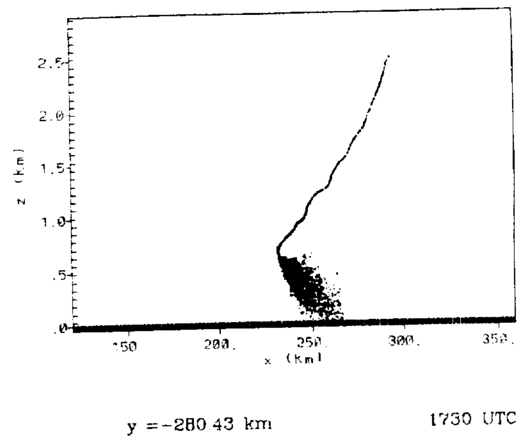

Figure 69. Same as Figure 68, vertical view from south.

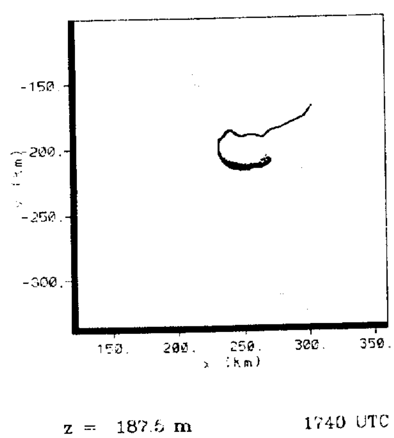

Figure 70. ERDAS HYPACT, 1740 UTC, 17 Jan 1997.

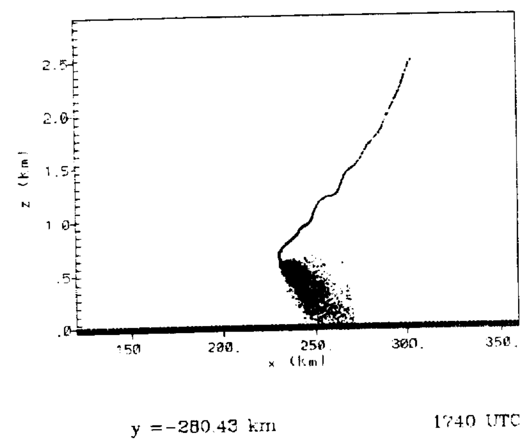

Figure 71. Same as Figure 70, vertical view from south.

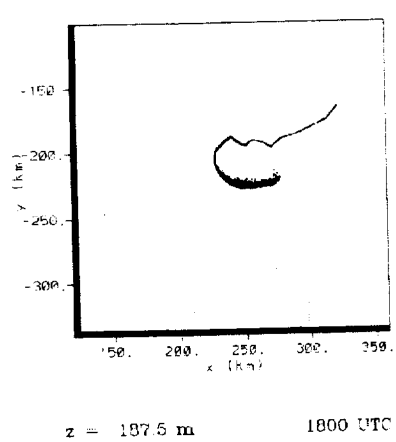

Figure 72. ERDAS HYPACT, 1800 UTC, 17 Jan 1997.

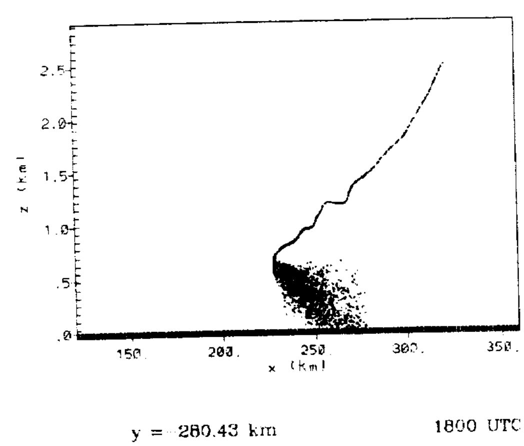

Figure 73. Same as Figure 72, vertical view from south.

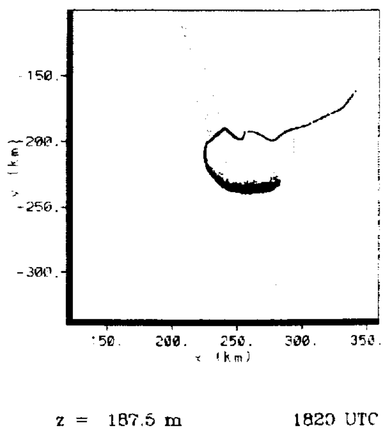

Figure 74. ERDAS HYPACT, 1820 UTC, 17 Jan 1997.

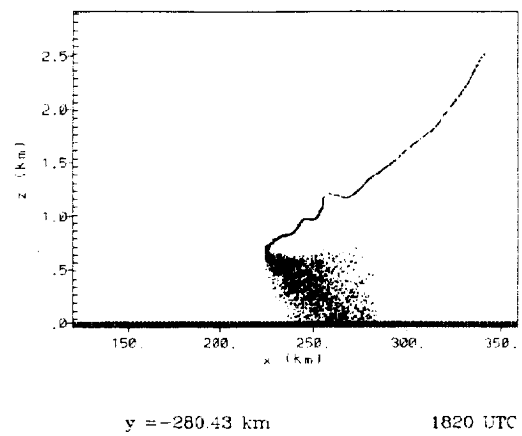

Figure 75. Same as Figure 74, vertical view from south.

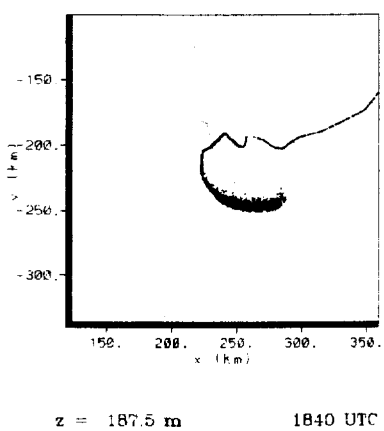

Figure 76. ERDAS HYPACT, 1840 UTC, 17 Jan 1997.

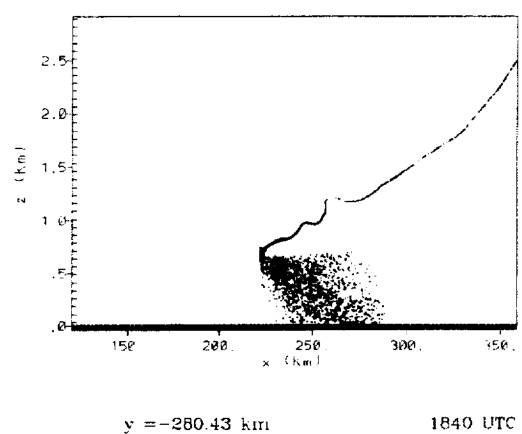

Figure 77. Same as Figure 76, vertical view from south.

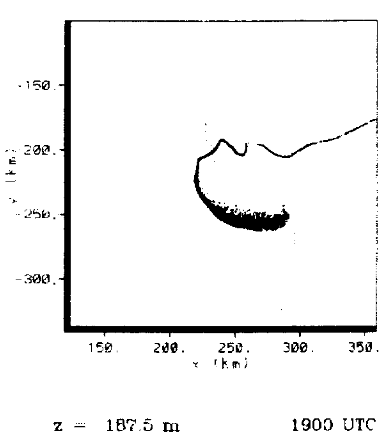

Figure 78. ERDAS HYPACT, 1900 UTC, 17 Jan 1997.

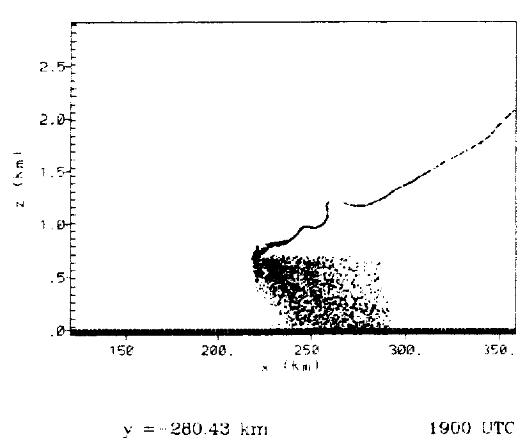

Figure 79. Same as Figure 78, vertical view from south.

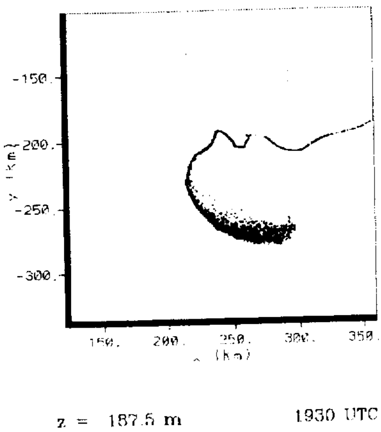

Figure 80. ERDAS HYPACT, 1930 UTC, 17 Jan 1997.

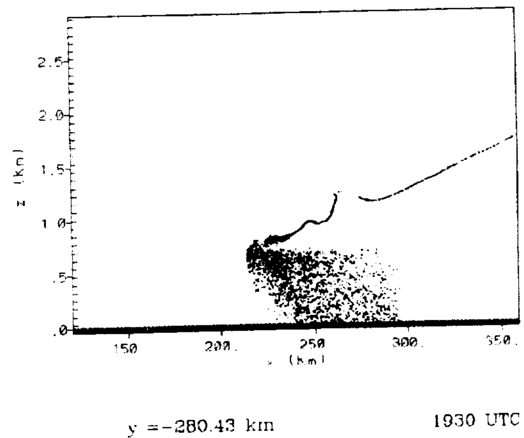

Figure 81. Same as Figure 80, vertical view from south.

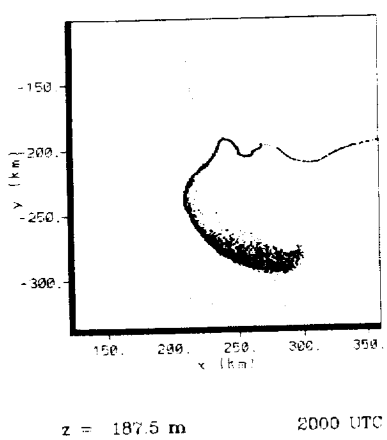

Figure 82. ERDAS HYPACT, 2000 UTC, 17 Jan 1997.

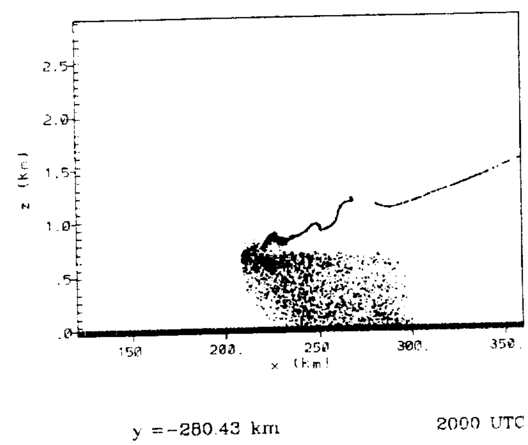

Figure 83. Same as Figure 82, vertical view from south.

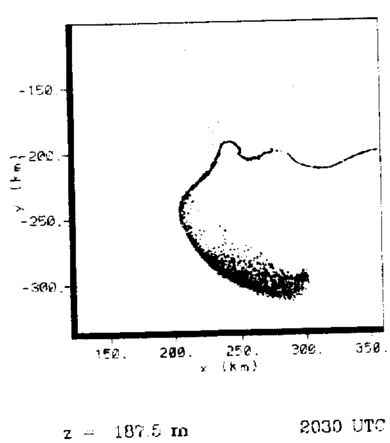

Figure 84. ERDAS HYPACT, 2030 UTC, 17 Jan 1997.

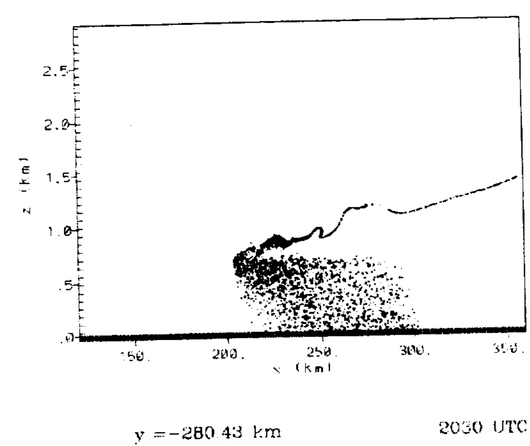

Figure 85. Same as Figure 84, vertical view from south.

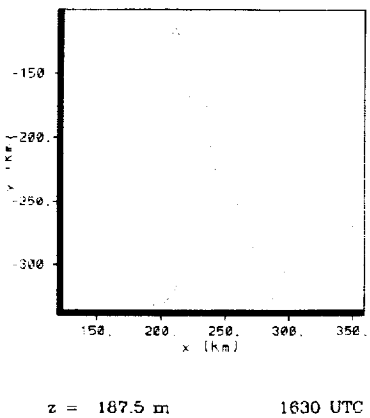

Figure 86. PROWESS HYPACT, 1630 UTC, 17 Jan 1997.

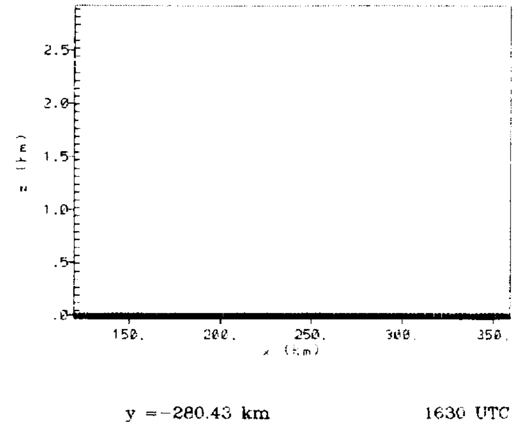

Figure 87. Same as Figure 86, vertical view from south.

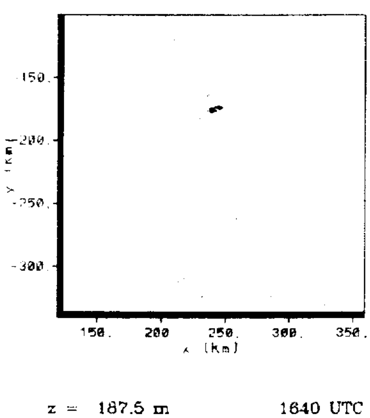

Figure 88. PROWESS HYPACT, 1640 UTC, 17 Jan 1997.

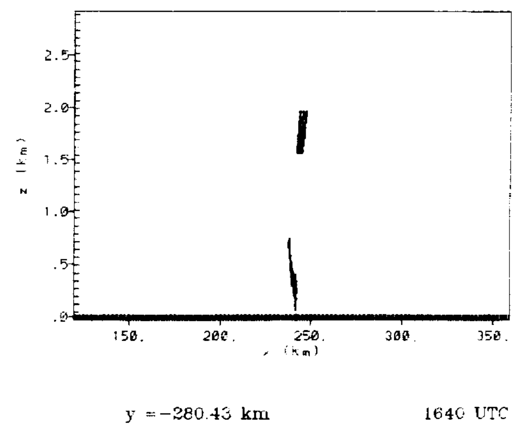

Figure 89. Same as Figure 88, vertical view from south.

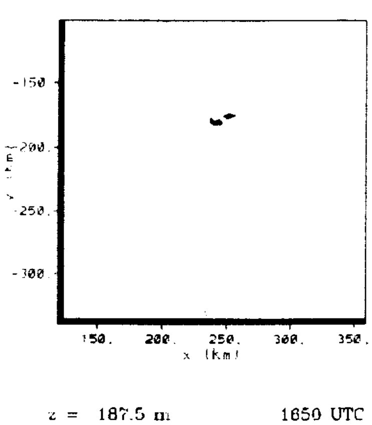

Figure 90. PROWESS HYPACT, 1650 UTC, 17 Jan 1997.

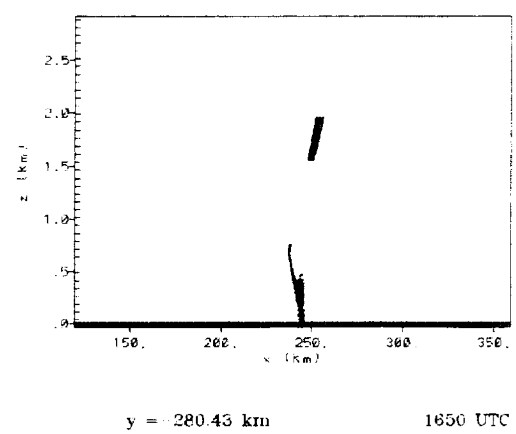

Figure 91. Same as Figure 90, vertical view from south.

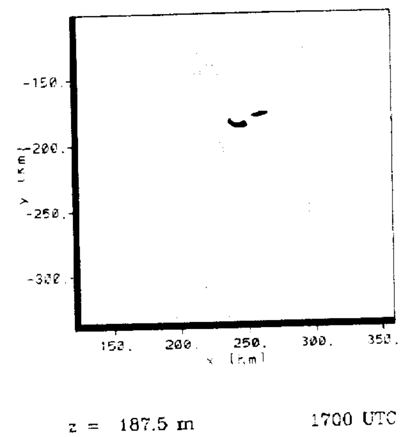

Figure 92. PROWESS HYPACT, 1700 UTC, 17 Jan 1997.

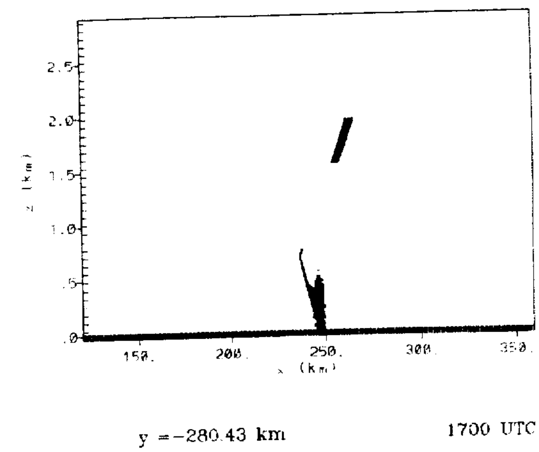

Figure 93. Same as Figure 92, vertical view from south.

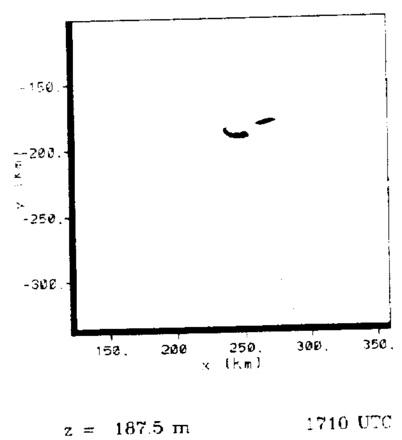

Figure 94. PROWESS HYPACT, 1710 UTC, 17 Jan 1997.

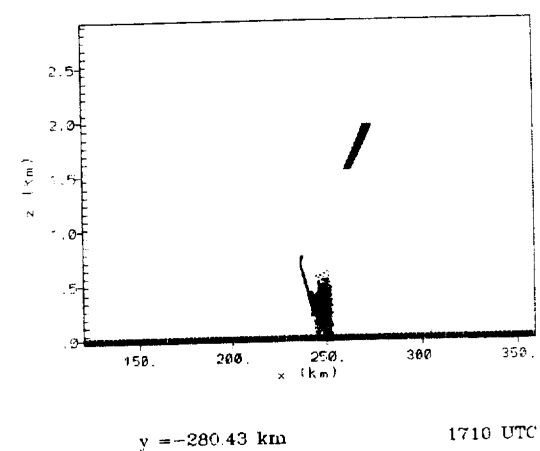

Figure 95. Same as Figure 94, vertical view from south.

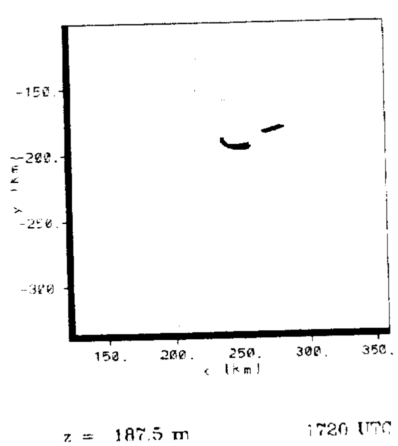

Figure 96. PROWESS HYPACT, 1720 UTC, 17 Jan 1997.

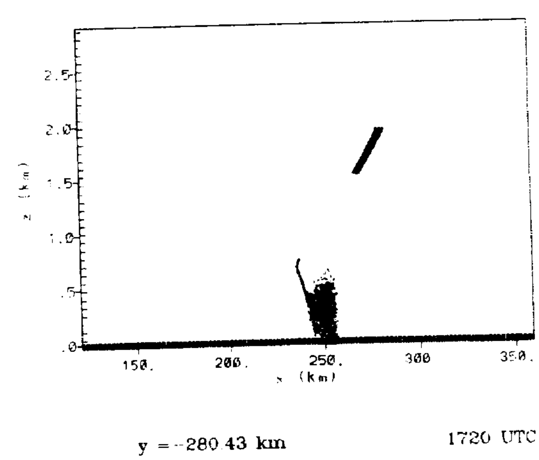

Figure 97. Same as Figure 96, vertical view from south.

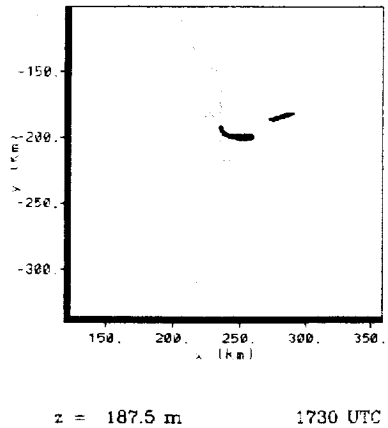

Figure 98. PROWESS HYPACT, 1730 UTC, 17 Jan 1997.

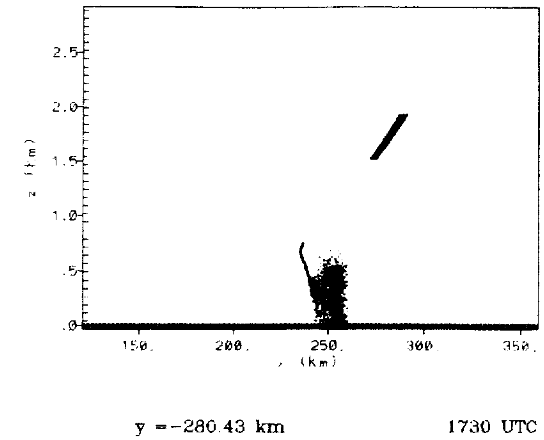

Figure 99. Same as Figure 98, vertical view from south.

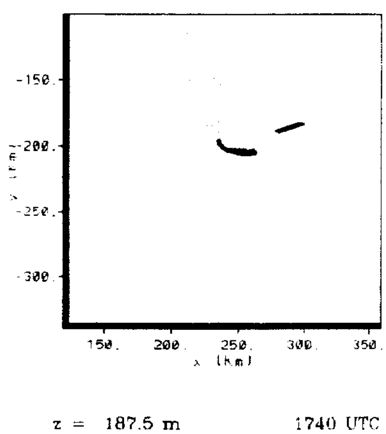

Figure 100. PROWESS HYPACT, 1740 UTC, 17 Jan 1997.

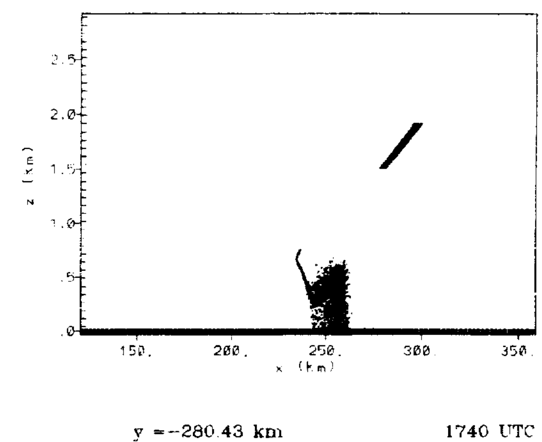

Figure 101. Same as Figure 100, vertical view from south.

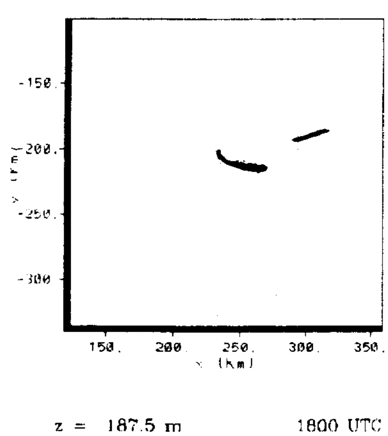

Figure 102. PROWESS HYPACT, 1800 UTC, 17 Jan 1997.

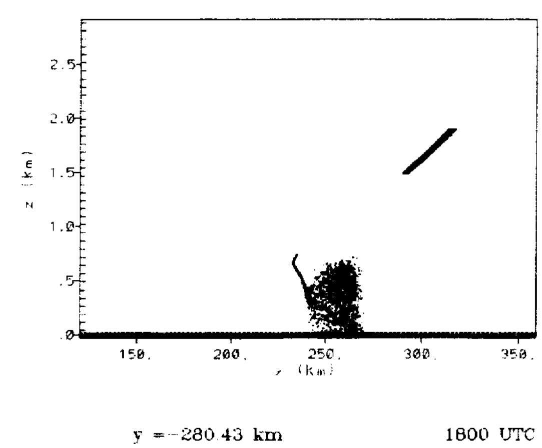

Figure 103. Same as Figure 102, vertical view from south.

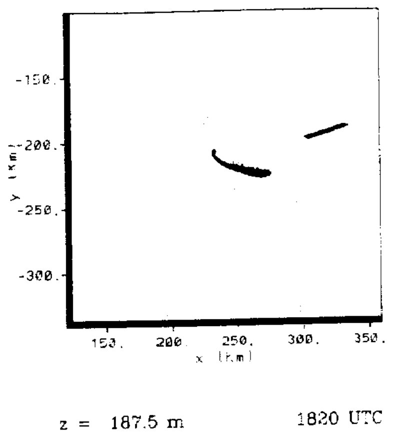

Figure 104. PROWESS HYPACT, 1820 UTC, 17 Jan 1997.

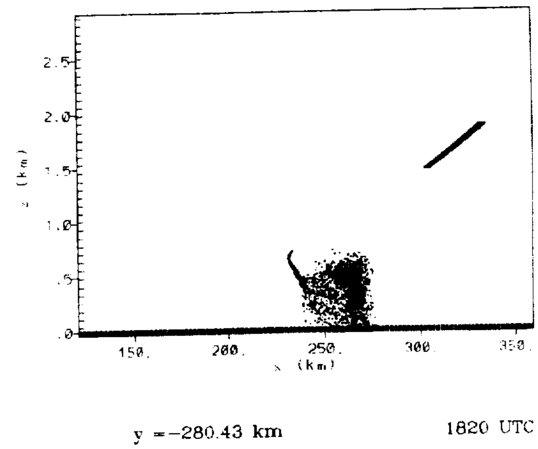

Figure 105. Same as Figure 104, vertical view from south.

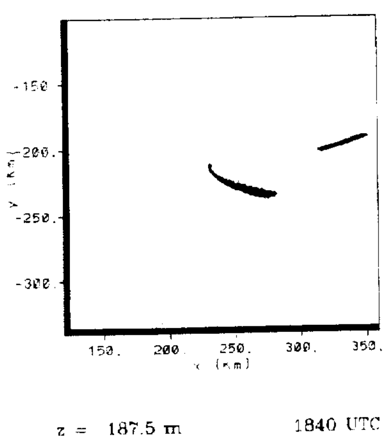

Figure 106. PROWESS HYPACT, 1840 UTC, 17 Jan 1997.

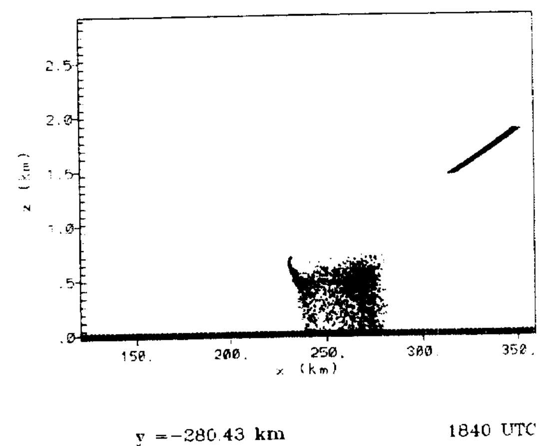

Figure 107. Same as Figure 106, vertical view from south.

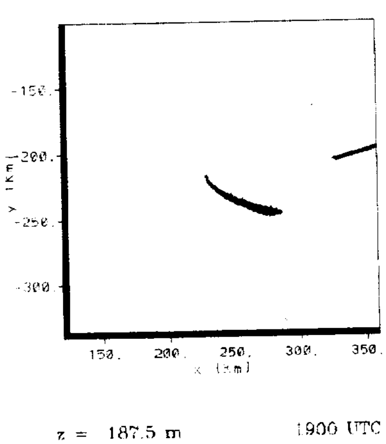

Figure 108. PROWESS HYPACT, 1900 UTC, 17 Jan 1997.

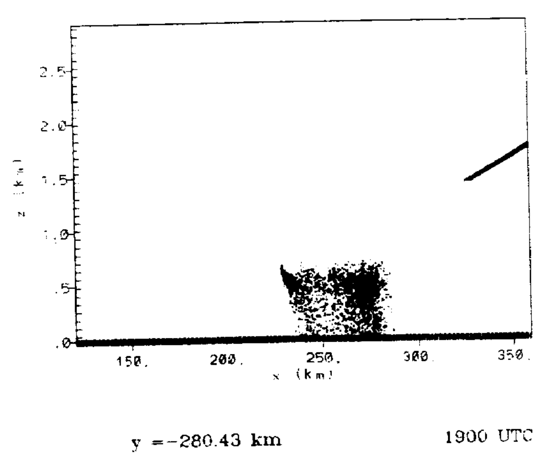

Figure 109. Same as Figure 108, vertical view from south.

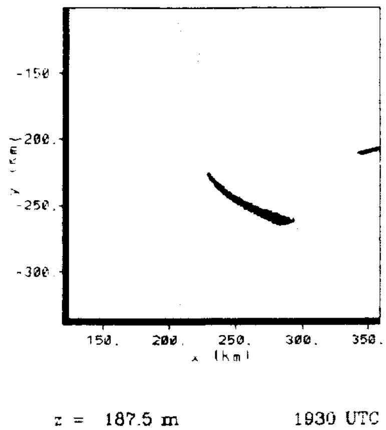

Figure 110. PROWESS HYPACT, 1930, UTC, 17 Jan 1997.

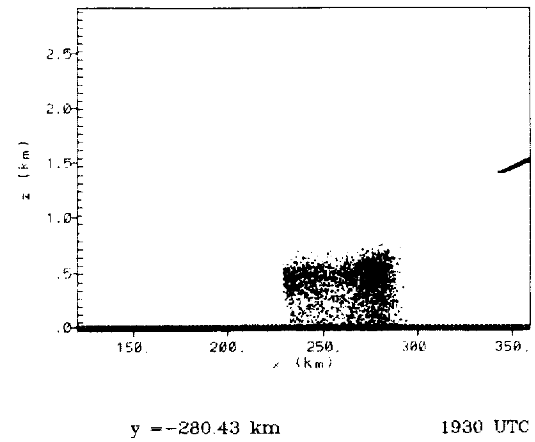

Figure 111. Same as Figure 110, vertical view from south.

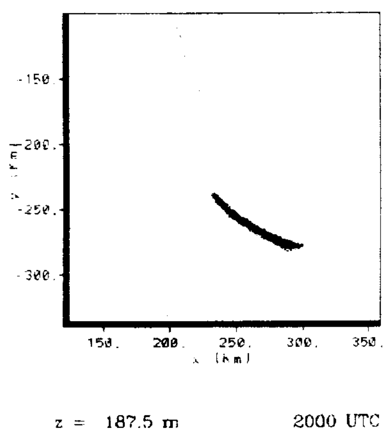

Figure 112. PROWESS HYPACT, 2000 UTC, 17 Jan 97.

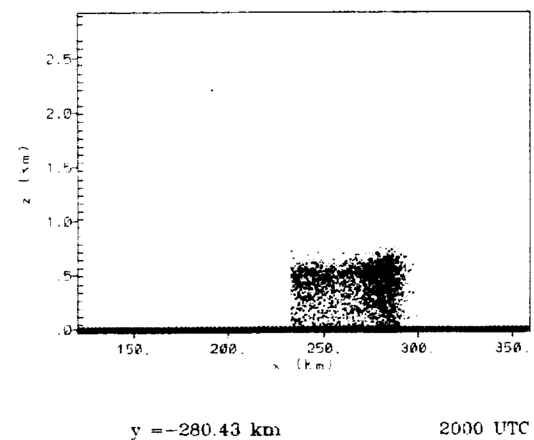

Figure 113. Same as Figure 112, vertical view from south.

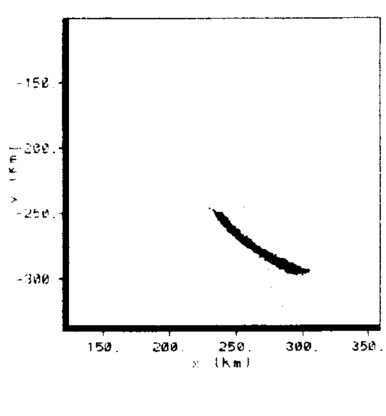

Figure 114. PROWESS HYPACT, 2030 UTC, 17 Jan 97.

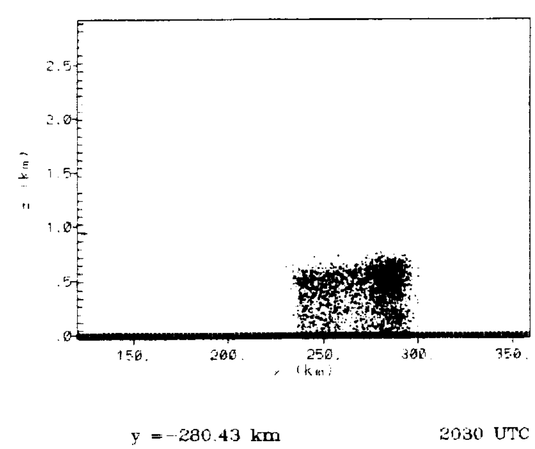

Figure 115. Same as Figure 114, vertical view from south.

3.2.4. ERDAS HYPACT trajectory analysis

We conducted an analysis to determine how well the model predicted the track of the plume when compared to observations. We did not compare observed versus predicted concentrations because no concentration measurements were available for this case. However, we used concentration predictions from ERDAS HYPACT to help identify the model's prediction of plume location. HYPACT was configured to output concentrations every 10 minutes and in layers with a thickness of 75 meters. HYPACT produced concentrations on a 3-dimensional grid at 10-minute intervals from 1630 UTC until 2030 UTC. The location of the observed plume was determined from the WSR-88D analysis. The location of the predicted plume was determined by finding the maximum concentrations predicted by the ERDAS HYPACT model for each 10-minute period in each vertical layer of interest. The latitude, longitude, and height of this maximum concentration were then noted. By tracking this maximum at the 10-minute intervals we were able to determine the trajectory of the HYPACT-predicted plume.

We had determined from the visual and radar observations of the initial explosion plume that its dimensions were not precisely defined. However, the plume extended vertically from the ground up to a height of approximately 900 meters. Because we did not know the height of maximum concentrations, we chose a layer that was representative of the lower plume. We chose a layer centered at 412.5 meters since this layer was near the midpoint of the lower plume.

The graph in Figure 116 shows the location of the maximum concentration of the layer centered on 412.5 m. This layer is near the center of the ground-based layer which contained the lower plume resulting from the explosion. The plume originated at Launch Complex 17 and then moved south over the following 4 hours. The observed and predicted plume locations closely agreed for the first two hours except that the observed plume was slightly west of the predicted plume. During the last two hours of the model simulation, the graph gives the appearance of a widely spreading plume. This spread was not due to the plume shifting from the east to the west but due to the shift in the location of the predicted maximum concentration within the plume from one 10-minute period to the next.

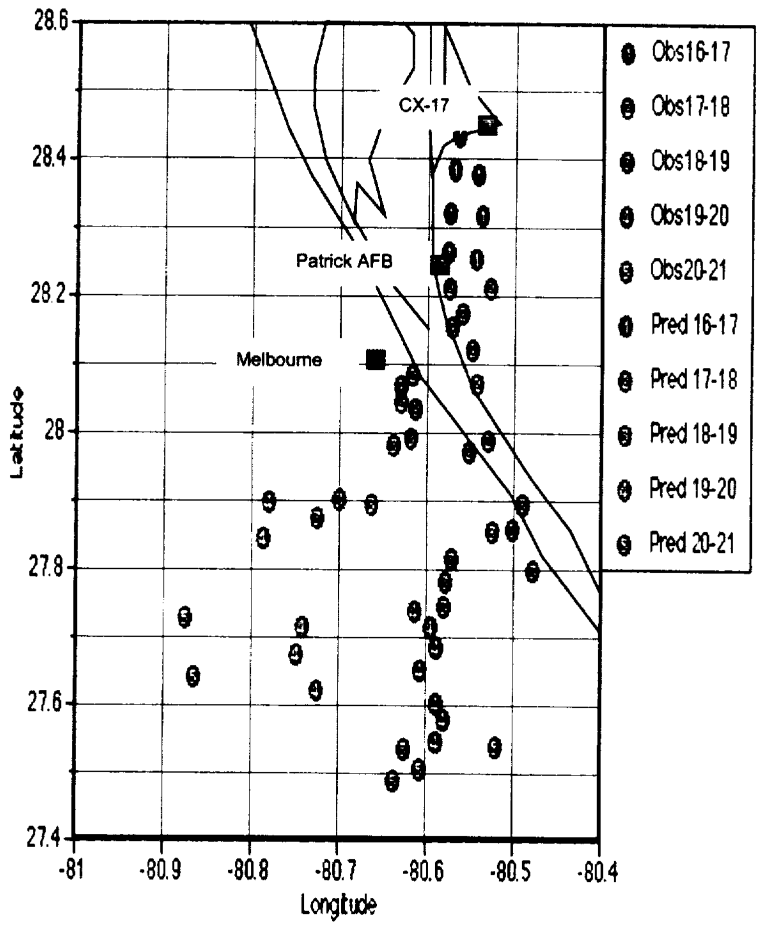

Figure 116. Data of observed vs. predicted plume location for lower plume resulting from Delta II explosion at 1628 UTC on 17 January 1997. The observed plume location was determined by WSR-88D radar. The predicted plume location was determined by finding the maximum predicted ERDAS HYPACT concentration in the 75-m layer centered at a height of 412 m. The numbered circles represent the time of the observed and predicted plumes with the following time tags: 1: 1600-1700 UTC, 2: 1700-1800 UTC, 3: 1800-1900 UTC, 4: 1900-2000 UTC, 5: 2000-2100 UTC.

4. Conclusions and Recommendations

The primary goal of this study was to conduct a case study of the dispersing cloud and the models used to predict the dispersion resulting from the explosion of the Delta II on 17 January 1997 at Cape Canaveral Air Force Station (CCAFS). The case study was conducted by comparing mesoscale and dispersion model results with available meteorological and plume observations. The meteorological conditions on this day were strongly influenced by synoptic rather than local forcing.

The conclusions of this study can be categorized according to the plume observation technique and according to the models used in the analysis. The findings of this study are:

WSR-88D radar as a plume observation tool

- The WSR-88D is a good tool for providing plume tracks from rocket explosion plumes. The radar provided excellent data on the location and track of the resulting potentially toxic cloud. The data was extremely useful for model verification since no ongoing program is in place to measure plume track or concentrations. Bud Parks of ACTA, Inc. is conducting a study to capture data from nominal and abort launch clouds and has captured radar data from three Eastern Range abort clouds and 36 of 46 (78%) nominal launch clouds (Parks and Evans 1998).

- The WSR-88D does not provide concentration data. The only data obtained by the radar is the reflectivity value measured in dBZ. While this measurement gives an estimate on the relative density of material (smoke particles, water, dust, or other particulate matter), a methodology is needed to convert dBZ to concentrations of hydrochloric acid (HCl), nitrogen tetroxide (N_2O_4), or other materials of interest. One of Range Safety's main concerns is determining the exposure limit (concentration over a specified time) of certain toxic materials.

  A dark orange cloud at the very top of the large lower cloud was initially visible. The dark orange cloud most likely contained some amount of nitrogen tetroxide. Because it was located near the top of the cloud, it is unsure how much, if any, of the N_2O_4 mixed within the cloud and made it to the surface. Our analysis was not able to determine the concentration of N_2O_4 in the explosion cloud.

- Vertical plume height data for this case was not very accurate. The radar appeared to accurately track the clouds' trajectories in the x-y dimension. However, the vertical measurements appeared to be inaccurate for two reasons. The first reason was that for long distances from the radar, such as the 35+ kilometers distance from Melbourne to Cape Canaveral, the radar beam widened enough to introduce inaccuracies in the vertical plume height measurements. The second reason for inaccurate vertical measurements was because of the strong inversion causing the radar beam to bend and bring about measurement inaccuracies.

RAMS model

- The vertical wind profile predictions in this case show agreement with observations. Both ERDAS and PROWESS configurations of RAMS produced wind flow measurements that matched closely with rawinsonde and profiler measurements and seemed to provide adequate input to HYPACT.

- RAMS under-predicted onshore flow at the level of the Delta II cloud. Both versions of RAMS predicted onshore flow in the 600- to 900-meter layer in the area south of Cape Canaveral. However, the observed winds had more of a northeast, onshore component than the RAMS-predicted winds. The movement of the actual explosion cloud tracked onshore north of the model-predicted cloud. The prototype ERDAS RAMS predicted winds with more of an onshore component than PROWESS RAMS.

- RAMS accurately predicted the strength and height of inversion for this case. The well-defined inversion that was measured by rawinsonde and based at approximately 800 meters above the ground was predicted by RAMS to be based at approximately 750 meters above the ground. The inversion, as determined by the vertical temperature profile, had a significant influence on the explosion cloud.

REEDM source term

- Characterizing the source term of unique explosions is difficult. If a rocket explosion occurs, the circumstances will be different each time it happens. For example: What was the flight time? How much fuel was consumed? What were the height, location and distribution of the explosion products? Were the hazardous and toxic materials separated or mixed within the cloud? Did the second stage ascend and then explode as with the Delta II? Did the solid rocket motors explode immediately or did they follow an errant path before they exploded? All of these questions make it difficult to develop a model that will accurately assess and characterize the source term. We were able to use information obtained after-the-fact from radar and video to characterize the source term but in a real-time scenario only estimates of the source term characterization can be made.

- Splitting the source into two sources for HYPACT model was a reasonable approximation. In the post-explosion mode of this analysis, we split the source into two sources for the HYPACT model based on observations. This methodology proved better for this case as opposed to using the single column source term that was generated by REEDM. In real-time, REEDM currently does not split the source term.

HYPACT model

- Plume came onshore further to the north and earlier than predicted. HYPACT moved the large lower cloud resulting from the Delta II explosion onshore at a point that was approximately 12 kilometers south of where it actually came onshore. HYPACT predicted the plume would come across the coastline in the Satellite Beach/Indian Harbor Beach area when it actually crossed the coastline in the Cocoa Beach area. The observed winds at the level moving the cloud at 600-900 m were northerly prior to the explosion but then shifted to northeasterly during the 1-2 hours following the explosion. RAMS predicted the shift of these winds from northerly to northeasterly but did not predict the shift as quickly as observed. RAMS supplies wind and meteorological data to HYPACT. Because of RAMS' gradual response to shift the winds, HYPACT missed the location and timing of the plume impact on the coastline.

- Trajectory, diffusion and timing of HYPACT plumes showed similarities to observed plume. Except for the problem mentioned above, the trajectory, diffusion, and the timing of the HYPACT plumes were similar to the plumes observed by radar. One favorable result was noted in the spread and diffusion of the lower cloud as it moved south. The cloud spread in the crosswind direction at a rate and in distance similar to observed.

- Range Safety's REEDM predicted the movement of plume to the south (176 degrees). REEDM using the 1613 UTC rawinsonde from Cape Canaveral moved the plume to the south and kept it offshore until it reached the Melbourne Beach area. REEDM did not account for the winds with an easterly component that existed at a height of 700-800 meters in the area over the ocean to the south of Cape Canaveral.

Recommendations

- Develop methodology to correlate concentrations with radar reflectivity measurements. The WSR-88D proved to be a valuable tool in tracking nominal and abort rocket plumes. However, the radar provides no information on the concentrations within the clouds. What is needed is measurement of concentrations within the plumes using a sample collection method or another remote sensing technique such as lidar. This data could then be correlated with radar measurements of reflectivity in dBZ.

- Improvements are needed in HYPACT plume dynamics algorithms. HYPACT currently treats plumes as non-buoyant, non-depositing entities. We recommend that future enhancements should be made to HYPACT to improve its ability to handle buoyant plumes and particle deposition. These improvements would allow HYPACT to model rocket exhaust plumes better than the current version of HYPACT.

- Conduct other studies of rocket explosion plumes. Since the explosion of the Delta II, two other rockets have exploded after launch from Cape Canaveral-Titan IV on 12 August 1998 and Delta III on 26 August 1998. In both cases the explosion clouds were tracked by WSR-88D radar. Detailed studies should be conducted to verify mesoscale models, diffusion models, and radar tracking techniques.

5. References

Banta, R.M., L.D. Oliver, E.T. Holloway, R.A. Kropfli, B.W. Bartram, R.E. Cupp, and M.J. Post, 1992: Smoke-column observations from two forest fires using Doppler lidar and Doppler radar. *J. Appl. Meteor.*, **31**, 1328-1349.

Bionetics Corp. film/video: Delta-II/GPS-II-R-1 Composite Tape of File#'s 102-979, 102-980, 102-981, and 102-982.

Brandli, H., 1997: GOES satellite photographs for 17 January 1997. Electronic mail received (hbrandli@winnie.fit.edu), Feb. 1997.

Doviak, R.J. and D.S. Zrnic, 1993: Doppler Radar and Weather Observations. Academic Press, Inc., 562 pp.

Evans R. J. and C.J. Tremback, 1998: Operational implementation and continued evaluation of a mesoscale and dispersion modeling system at Cape Canaveral Air Force Station/Kennedy Space Center, FL. Preprints, 10th Joint Conf. of Air Pollution Meteorology with AWMA, Phoenix, AZ, Amer. Meteor. Soc., Boston, 6 pp. [Available from ENSCO, Inc, 445 Pineda Court, Melbourne, FL 32940]

Evans R. J., C.J. Tremback, and W.A. Lyons, 1996: The implementation and evaluation Emergency Response Dose Assessment System (ERDAS) at Cape Canaveral Air Force Station/Kennedy Space Center, FL. Preprints, 9th Joint Conf. of Air Pollution Meteorology with AWMA, Atlanta, GA, Amer. Meteor. Soc., Boston, 193-197.

Evans, R.J., 1996: Final report on the evaluation of the emergency response dose assessment system (ERDAS). NASA CR-201353. Prepared by Applied Meteorology Unit, 184 pp.

Evans, R.J., A.V. Dianic, and L.N. Moore, 1994. The meteorological monitoring system (MMS). Preprints, 5th Conf. on IIPS. Nashville, TN, Amer. Meteor. Soc., Boston, 362-367.

Ha, C.T. and N.A. Deane, 1998: Validation Analysis of the PUFF and SATRAP Codes and Cassini Methods Against the 17Jan97 Delta II Accident Data. Lockheed Martin Astronautics Interoffice Memo, Cassini Memo No. 579, 17 July 1998, 35 pp.

Herring, H., 1999: Electronic message, RE: 74-C data, 17Jan97. Electronic mail received (HAROLD.HERRING@pafb.af.mil), May, 1999.

Hoffert, S. and M. Pearce, 1996: 88Display software package, obtained by Applied Meteorology Unit from Pennsylvania State University.

Lane, R.E. and R.J. Evans 1989: The meteorological and range safety support system (MARSS). Preprints, 5th Conf. on IIPS, Anaheim, CA, Amer. Meteor. Soc., Boston, 226-231.

Lyons, W.A., and C.J. Tremback, 1994: Predicting 3-D wind flows at Cape Canaveral Air Force Station using a mesoscale model. Contract No. F04701-91-C-0058. Prepared by ASTER/MRC for US Air Force Space and Missile Systems Center, SMC/CLNE, 30 June 1994.

National Weather Service, 1997: Delta rocket explosion 2.5 degree reflectivity loop. (http://sunmlb.nws.fit.edu/17jan97b.gif).

Nyman, Randolph L., REEDM Version 7.09 Technical Description Manual, Technical Report No. 99-400/11.3-02, ACTA Inc., Torrance, CA, 30 September 1999.

Overbeck K., 1997: Memorandum for Record to Safety Investigation Board: Delta GPS 2R-1 Toxic Support Review, undated, 19 pp.

Pace, J.C., J.R. Albritton, R.L. Baskett, X.J. Zhang, M.C. Masonjones, N.A. Moussa, K. Overbeck, C.R. Parks, R.J. Evans, 1998: Modeling the 17 January 1997 Delta-II Explosion by ARAC, ADORA, and REEDM. Preprints, 10th Joint Conf. of Air Pollution Meteorology with AWMA, Phoenix, AZ, Amer. Meteor. Soc., Boston, 294-301.

Parks, C.R. and R.J. Evans, 1998, Tracking nominal launch and abort rocket plumes using WSR-88D Doppler radar. Presented at JANNAF SEP Subcommittee meeting, Houston TX, May 1998, 10 pp.

Rogers, R.R. and W.O.J. Brown, 1997: Radar observations of major industrial fire. Bull. Amer. Meteor.Soc., 78, 803-814.

Sittig, Marshall, 1985: Handbook of Toxic and Hazardous Chemicals and Carcinogens 2nd ed., Noyes Pub. Park Ridge, NJ, 659-660.

Tremback, C.J., W.A. Lyons, W.P. Thorson, and R.L. Walko, 1994: An emergency response and local weather forecasting software system. Preprints, 8th Joint Conf. of Air Pollution Meteorology with AWMA, Nashville, TN, Amer. Meteor. Soc., Boston, 219-223.

Tremback, C.J., W.A. Lyons, I.T. Baker, M.J. Weissbluth, 1996: Enhanced Mesoscale Modeling for Kennedy Space Center: Parallelized RAMS Operational Weather Simulation System: Final Report. Mission Research Corp./ASTER Division, 184 pp. [Available from ENSCO, Inc, 1980 N. Atlantic Ave., Suite 230, Cocoa Beach, FL 32931]

APPENDIX A

ERDAS RAMSIN file

```
$MODEL_GRIDS

! Simulation title (64 chars)
 EXPNME  =    'CCAFS/KSC-Version 3a' ,
                                               ! -1=diagnostic, 0=normal run
  IOTYPE   = 0,

  RUNTYPE = 'INITIAL',     ! type of run: INITIAL, HISTORY, or MAKEVFILE

  TIMEUNIT = 'h',                          ! 'h','m','s' - Time units of
                                           !   TIMMAX, TIMSTR, VTIME

  TIMMAX=    12.,                          ! Final time of simulation


  NGRIDS   =    3,                             ! Number of grids to run
                                               !
  NNXP     =  38,   34, 37,                    ! Number of x gridpoints
  NNYP     =  36,   38, 37,                    ! Number of y gridpoints
  NNZP     =  25,   25, 25,                    ! Number of z gridpoints
  NNZG     =  11,   11, 11,                    ! Number of soil gridpoints

  NXTNEST =    1,    1,  2,                    ! Grid number which is the next
                                               !   coarser grid


     ! Coarse grid specifications

  IHTRAN  =       1,                       ! 0-Cartesian, 1-Polar stereo
  DELTAX  =   60000.,                      ! X and Y grid spacing
  DELTAY  =   60000.,

  DELTAZ  =     75.,                       ! Z grid spacing (set to 0. to use ZZ)
  DZRAT   =     1.25,                      ! vertical grid stretch ratio
  DZMAX   =     1000.,                     ! maximum delta Z for vertical stretch

  ZZ=0., 25., 75., 150., 250., 500., 750., 1000., 1500., 2000., 2500.,
     3250., 4000., 5000., 6000.,
                                           ! Vertical levels if DELTAZ = 0

  DTLONG   =       90.,                    ! Coarse grid long timestep
  NRATIO   =        3,                     ! Small timestep ratio

  IMONTH1 =   01,         ! Month
  IDATE1  =   17,         ! Day
  IYEAR1  =   97,         ! Year
  STRTIM  =   12.0,       ! GMT of model TIME = 0.
                                            ! Nest ratios between this grid
                                            !  and the next coarser grid.
  NSTRATX =   1, 4, 5,                   ! x-direction
  NSTRATY =   1, 4, 5,                   ! y-direction
  NNDTRAT =   1, 2, 2,                   ! time

  NESTZ = 3,                                ! contort coarser grids if negative
  NSTRATZ=3,3,2,2,2,2,2,2,2,2,1,    !


  POLELAT   =  30.0,                        ! Latitude of pole point
  POLELON   =   -83.0,                      ! Longitude of pole point

  CENTLAT=    30.0,
  CENTLON=   -83.0,

                                            ! Grid point on the next coarser
                                            ! nest where the lower southwest
                                            ! corner of this nest will start.
                                            ! IF NINEST or NJNEST = 0, use CENTLAT/LON
                                               !    coarser grid
  NINEST   =   1, 17,  20,                  ! i-point
  NJNEST   =   1, 10,  19,                  ! j-point
  NKNEST   =   1,   1,  1,                  ! k-point

  NNSTTOP =    1,    1,   0,              ! Flag (0-no or 1-yes) if this
  NNSTBOT =    1,    1,   1,              ! nest goes the top or bottom of the
                                             ! coarsest nest.

  GRIDU    =  0.,   0.,   0.,             ! u-component for moving grids
  GRIDV    =  0.,   0.,   0.,             ! v-component for moving grids
                                               !   (still not working!)
```

```
$END


$MODEL_FILE_INFO

               ! History file input

TIMSTR=    0.,        ! time of history start (see TIMEUNIT)
HFILIN = 'ci.h0h',    ! input history file name

               ! History/analysis file output

IOUTPUT=       1,                  ! 0-no files, 1-save/dispose
HFILOUT='hist/f.h',                    ! history file prefix
AFILOUT='f.a',                    ! analysis file prefix
HFUNITS='h',      AFUNITS='d',      ! history/anal file units (M,m,H,h,S,s)
FRQHIS  =43200.,   FRQANL  =3600.,   ! history/anal file frequency

               ! Variable initialization input

INITIAL =   2,             ! Initial fields - 1=horiz.homogeneous, 2=variable
VTIME   =  0., 6., 12., 18., 24.,    ! model times for varfiles (See TIMEUNIT)

VARFIL(1)='isan/iv17-jan-97-12',  VTIME(1)=0.,
VARFIL(2)='isan/iv17-jan-97-18',  VTIME(2)=6.,
VARFIL(3)='isan/iv17-jan-97-24',  VTIME(3)=12.,
VARFIL(4)='isan/iv17-jan-97-30',  VTIME(4)=18.,
VARFIL(5)='isan/iv17-jan-97-36',  VTIME(5)=24.,

IVWIND =       0,            ! initial winds ( only 0 works)

NUDLAT    =     5,            ! number of points in the lateral bnd region
TNUDLAT   =     900.,         ! nudging time scale (s) at lateral boundary
TNUDCENT =     00.,        ! nudging time scale (s) in center of domain
TNUDTOP   =     00.,        ! nudging time scale (s) at top of domain
ZNUDTOP   =     15000.,       ! nudging at top of domain above this height (m)

               ! Printed output controls

 FRQPRT   =   21600.,     ! Printout frequency
 FRQIPR   =   99930.,     ! Integral print frequency
 FRQIST   =   99900.,     ! Integral store frequency

 ISTPFL   =        1,     ! Timestep message frequency flag
 INITFLD =        1,     ! Initial field print flag 0=no print, 1=print
 INPRTFL =        1,     ! Namelist print flag 0=no print, 1=print

                ! Input topography variables

  SFCFILES = '/ul/met/sfc/sfcb_jan',            ! File path and prefix for surface
characteristic

  ITOPTFLG = 1,1,1,            ! 2 - Fill data in "ruser"
  IPCTLFLG = 1,1,1,            ! 1 - Interp data from latlon dataset
  ISSTFLG  = 1,0,0,            ! 0 - Interpolate from coarser grid
  IVEGTFLG = 1,1,1,


                                !
                                ! The following only apply for IxxxxFLG=1
                                !
  ITOPTFN = '/usr/geode/data/rams/topo10m/H',
            '/usr/geode/data/rams/topo30s/U',          ! Input topography file name
            '/usr/geode/data/rams/topo30s/U',          ! Input topography file name

  IPCTLFN = '/usr/geode/data/rams/pctl10m/L',
            '/usr/geode/data/rams/pctl10m/L',
            '/usr/geode/data/rams/pctl10m/L',

  ISSTFN  = '/usr/geode/data/rams/sst/SJUL',

  IVEGTFN  = '/usr/geode/data/rams/ndvi/V',
             '/usr/geode/data/rams/ndvi/V',
             '/usr/geode/data/rams/ndvi/V',


  SILAVWT  = 0.0, 0., 0.,              ! Weighting of topo silhouette averaging
```

```
 TOPTWVL   = 4.0, 4., 4.,                 ! Topo wavelength cutoff in filter
 PCTLWVL   = 2.0, 2., 2.,                 ! Land pct wavelength cutoff in filter
 SSTWVL    = 2.0, 2., 2.,                 ! Land pct wavelength cutoff in filter

$END

$MODEL_OPTIONS

 NADDSC    =     0,0,0,

 NTOPSMTH  =        0,   ! Number of passes for topography smoother
 IZFLAT    =        0,   ! Width of flat margin around domain (in grid points)

    ! Numerical schemes

 ITMDIFF =        3,    ! 1=forward, 2=leapfrog, 3=hybrid
 NONHYD  =        1,    ! nonhydrostatic=1, hydrostatic=0
 SSPCT   =       0.,    ! Sound speed fraction for the nonhydrostatic model
 IMPL    =        1,    ! Implicit flag for acoustic model  -  0=off, 1=on
 ICNTEQ  =        2,    ! Hyd - continuity equation - 1 -incomp, 2 -anelastic
 WTKD    =       0.,    ! Klemp/Durran - current timestep weighting

 ICORFLG =        1,    ! Coriolis flag/2D v-component  -  0=off, 1=on

 IBCTOP =         0,    ! top boundary condition
                        ! 0-wall on top(nonhyd)        2-prognostic sfc prs(hyd)
                        ! 1-Klemp-Durran(nonhyd/hyd) 3-material surface(hyd)

 IBND    =        1,    ! Lateral boundary condition flags
 JBND    =        1,    ! 1-Klemp/Wilhelmson, 2-Klemp/Lilly, 3-Orlanski
                        ! 4-cyclic
 CPHAS   =      20.,    ! Phase speed if IBND or JBND = 1
 LSFLG   =        0,    ! Large-scale gradient flag for variables other than
                        ! normal velocity:
                        ! 0 = zero gradient inflow and outflow
                        ! 1 = zero gradient inflow, radiative b.c. outflow
                        ! 2 = constant inflow, radiative b.c. outflow
                        ! 3 = constant inflow and outflow
 NFPT    =       0,    ! Rayleigh friction - number of points from the top
 DISTIM  =       0.,    !                     - dissipation time scale

 TIMSCL  =       0.,    ! Initial wind spin-up - time scale
 KSPIN   =      33,     !                        - below this level (velocity)
 KMSPIN  =      10,     !                        - below this level (momentum)

 IPRSPLT =        0,    ! precipitation time-split scheme - 0=off, 1=on
 IADVL   =        2,    ! Order of advection - Leapfrog - 2 or 4
 IADVF   =        2,    ! Order of advection - Forward - 2 or 6
 IPGRAD  =        1,    ! Pressure gradient scheme for topo.: 1-transform
                        !                                       2-interpolate
 FILT4   =     000.,    ! Fourth order filter coefficient (0 - off)
                        !    ( > 0  timestep at which 2 delta waves are
                        !    totally removed)
 FXLONG  =   0.0000,    ! Long filter coefficient 0=off
 FYLONG  =   0.0000,    ! Long filter coefficient 0=off

    ! Radiation parameters

 ISWRTYP =     2,     ! Shortwave radiation type 0-none, 2-Mahrer/Pielke, 1-Chen
 ILWRTYP =     2,     ! Longwave radiation type 0-none, 2-Mahrer/Pielke, 1-Chen
 RADFRQ  = 1200.,     ! Frequency of radiation tendency update in seconds
 LONRAD  =     1,     ! Longitudinal variation of shortwave  (0-no, 1-yes)

    ! Cumulus parameterization parameters

 NNQPARM =   0,   0,  0,                  ! convective parameterization flag
                                          !   0-off, 1-on
 CONFRQ  = 1200.,     ! Frequency of conv param. updates in seconds
 WCLDBS  =  .001,     ! vertical motion needed at cloud base for convection

    ! Surface layer and soil parameterization

 ISFCL   =      1,    ! surface layer/soil/veg model
                      ! 0-specified surface layer gradients
                      ! 1-soil/vegetation model

 NVGCON  =      1,      ! Vegetation type
                        ! 1 -- Crop/mixed farming          2 -- Short grass
```

```
                        ! 3 -- Evergreen needleleaf tree  4 -- Deciduous needleleaf tree
                        ! 5 -- Deciduous broadleaf tree   6 -- Evergreen broadleaf tree
                        ! 7 -- Tall grass                  8 -- Desert
                        ! 9 -- Tundra                     10 -- Irrigated crop
                        !11 -- Semi-desert                12 -- Ice cap/glacier
                        !13 -- Bog or marsh               14 -- Inland water
                        !15 -- Ocean                      16 -- Evergreen shrub
                        !17 -- Deciduous shrub            18 -- Mixed woodland
TSEASN  =    298.,      ! Average seasonal temp
TVGOFF  =      0.,      ! Initial veg temp offset
VWTRCON =      .000,    ! Initial veg water storage (not working)

UBMIN   =    0.25,      ! Minimum U value to use in computing U_*
PCTLCON =   1.0,        ! constant land percentage if for all domain
NSLCON  =     6,        ! constant soil type if for all domain
                      !  1=sand           2=loamy sand      3=sandy loam
                      !  4=silt loam      5=loam            6=sandy clay loam
                      !  7=silty clay loam 8=clay loam      9=sandy clay
                      ! 10=silty clay     11=clay          12=peat

ZROUGH  =  0.25,        ! constant roughness if for all domain
ALBEDO  =    0.2,       ! constant albedo when not running soil model
SEATMP  = 280.,         ! constant water surface temperature

DTHCON  =  -10.,        ! constant surface layer temp gradient for no soil
DRTCON  = .000,         ! constant surface layer moist gradient for no soil
SOILDZ  =    0.,        ! soil model grid spacing
SLZ   = -.50,-.40,-.30,-.25,-.20,-.16,-.12,-.09,-.06,-.03,  0.,! soil grid levels
SLMSTR  =  0.6, 0.6, 0.5, 0.5, 0.5,                ! initial soil moisture
           0.5, 0.5, 0.4, 0.4, 0.4, 0.4,
STGOFF=  5., 5., 5., 5., 3.5,  2.,  .5, -1.,-1.5,-1.8, -2.,
                        ! Initial soil temperature offset from lowest
                        ! atmospheric level


    ! Eddy diffusion coefficient parameters

IDIFFK = 1,1,1,              ! K flag:
                             !    1 - Horizontal deformation/ Vertical Mellor-Yamada
                             !    2 - Anisotropic deformation (horiz and vert differ)
                             !    3 - Isotropic deformation (horiz and vert same)
                             !    4 - Deardorff TKE (horiz and vert same)
CSX = .2,.2,.2,  ! momentum M-Y k
CSZ = 20.,20.,20., ! scalar M-Y K
XKHKM = 3.,3.,3.,            ! Ratio of horizontal K_h to K_m for TKE or deformation
ZKHKM = 3.,3.,3.,            ! Ratio of vertical K_h to K_m for TKE or deformation
AKMIN= .3,.3,.3,            ! Ratio of minimum horizontal eddy viscosity coefficient
                             !    to typical value from deformation K

    ! Microphysics

 NLEVEL  =   1,   1,  1,              ! moisture complexity level

 ICLOUD =   0,    0,  0,
 IRAIN  =   0,    0,  0,            ! Microphysics flags
 IPRIS  =   0,    0,  0,            !------------------
 ISNOW  =   0,    0,  0,            ! where x= R - rain
 IAGGR  =   0,    0,  0,            !          P - pristine crystals
 IGRAUP =   0,    0,  0,            !          S - snow
 IHAIL  =   0,    0,  0,             !          A - aggregates

 CPARM  =  0.,  0.,0.,
 RPARM  =  0.,  0.,0.,              !          G - graupel
 PPARM  =  0.,  0.,0.,              !          H - hail
 SPARM  =  0.,  0.,0.,              ! NIxCNFL = 0 - no species
 APARM  =  0.,  0.,0.,              !           1 - diagnostic concen.
 GPARM  =  0.,  0.,0.,              !           2 - specified mean diameter
 HPARM  =  0.,  0.,0.,              !           3 - specified y-intercept
                                    !           4 - specified concentration
                                    !           5 - prognostic concen.


AMI0    =  0.0000001, ! minimum crystal mass (gm)
CON     =   300.0 ,   ! CCN concentration (number/cc)
THOMO   =  233.0,     ! homogeneous nucleation temperature

$END

$MODEL_SOUND
      ! Sounding specification
```

```
          ! Flags for how sounding is specified

 IPSFLG=0,       ! specifies what is in PS array
                 ! 0 - pressure (mb), 1 - heights (m), PS(1)=sfc press(mb)

 ITSFLG=2,       ! specifies what is in TS array
                 ! 0 - temp(C), 1 - temp(K), 2 - pot. temp(K)

 IRTSFLG=3,      ! specifies what is in RTS array
                 ! 0 - dew pnt.(C), 1 - dew pnt.(K), 2 - mix rat(g/kg)
                 ! 3 - relative humidity on %, 4 - dew pnt depression(K)

 IUSFLG=0,       ! specifies what is in US and VS arrays
                 ! 0 - u,v component(m/s), 1 - umoms-direction, vmoms-speed

 IUSRC = 0,      !  source of wind profile:
                 !  0  - umoms, vmoms, valid at sounding levels (PS)
                 !  -1 - usndg, vsndg, valid at model levels    (Z)


 PS=1012.00, 1000.00 ,  977.00 ,  949.00 ,  936.00 ,  850.00 ,  848.00 ,
  797.00,   700.00 ,  662.00 ,  595.00 ,  579.00 ,  565.00 ,  560.00 ,
  500.00,   498.00 ,  461.00 ,  443.00 ,  406.00 ,  400.00 ,  387.00 ,
  383.00,   328.00 ,  325.00 ,  316.00 ,  309.00 ,  307.00 ,  300.00 ,
  285.00,   250.00 ,  200.00 ,  150.00 ,  100.00 ,   80.00 ,   10.0,


TS= 288.18,    288.36 ,   288.88 ,   293.11 ,   294.27 , 298.93 , 298.92 ,
    304.48,    309.35 ,   310.27 ,   313.50 ,   315.02 , 317.23 , 317.80 ,
    318.75,    318.88 ,   320.88 ,   322.03 ,   326.27 , 327.02 , 328.41 ,
    328.73,    330.56 ,   331.02 ,   333.69 ,   335.55 , 335.89 , 336.99 ,
    340.82,    343.42 ,   347.35 ,   364.39 ,   379.82 , 398.66 ,  480.,


RTS= 90.7,   95.5,  98.0,  96.8,   96.1,  100.0,  100.0,   94.1,   90.6,
    99.3,    94.1,  75.8,  49.3,   38.4,   55.8,   55.7,   85.1,   80.6,
    78.0,    71.1,  57.6,  52.3,   74.9,   74.0,   39.6,   22.7,   16.0,
    09.7,    02.5,  06.1,  15.8,   03.6,   02.1,   01.5,   01.5,


 US=4.,4.,4.,4.,4.,4.,4.,4.,4.,4.,4.,4.,4.,4.,4.,4.,4.,4.,4.,4.,
    4.,4.,4.,4.,4.,4.,4.,4.,4.,4.,4.,4.,4.,4.,4.,4.,4.,4.,4.,4.,

 VS=0.,0.,0.,0.,0.,0.,0.,0.,0.,0.,0.,0.,0.,0.,0.,0.,0.,0.,0.,0.,
    0.,0.,0.,0.,0.,0.,0.,0.,0.,0.,0.,0.,0.,0.,0.,0.,0.,0.,0.,0.,

! US= -10., -10., -11., -12., -12., -5., 5.,
!     6.5,  8.7,11.0,14.0,16.0,17.0,18.0,
!    21.9, 22.0,24.0,26.0,30.0,30.0,32.0,
!    33.0, 34.0,35.0,36.0,37.0,39.0,40.6,
!    42.0, 50.7,46.6,35.0,30.0,30.0,30.,

! VS= 2.1,  2.1, 2.5,3.0,3.5,4.0,4.0,
!     3.5,  3.1, 3.3,3.5,3.7,4.2,4.5,
!     6.0,  6.0, 7.0,8.0,9.0,10.0,11.0,
!    12.0, 13.0,14.0,14.1,14.5,15.0,15.0,
!    14.8, 8.0,8.0,8.0,8.0,8.0,8.0,

  USNDG = 0.,    ! Wind components if IUSRC= -1
  VSNDG = 0.,    !

  KMEAN1 = 0,    !  lower model level for calculation of (umean,vmean)
  KMEAN2 = 0,    !  upper model level for calculation of (umean,vmean)

  UMEAN = 0.0,   !  u-component for Galilean transformation
  VMEAN = 0.0,   !  v-component for Galilean transformation

 $END


 $MODEL_PRINT
          ! Specifies the fields to be printed during the simulation

  NPLT  =  6,               ! Number of fields to be printed at each time
                            !    for various cross-sections (limit of 50)
  IPLFLD = 'UP','VP','WP','THETA','TKE','TVEG',
                            ! Field names - see table below
!  PLFMT(6) = '0PF7.2',      ! Format specification if default is unacceptable
```

```
 IXSCTN = 3,3,3,3,3,3,3,3,3,3,3,3,
                                  ! Cross-section type (1=XZ, 2=YZ, 3=XY)
 ISBVAL = 2,2,2,2,2,2,2,2,2,2,2,2,

                                  ! Grid-point slab value for third direction

 ! The following variables can also be set in the $PRNT namelist:  IAA,
 ! IAB, JOA, JOB, NAAVG, NOAVG, PLTIT, PLCONLO, PLCONHI, and PLCONIN.

$END
C     'UP'    - UP(M/S)       'RC'    - RC(G/KG)      'PCPT' - TOTPRE
C     'VP'    - VP(M/S)       'RR'    - RR(G/KG)      'TKE'  - TKE
C     'WP'    - WP(CM/S)      'RP'    - RP(G/KG)      'HSCL' - HL(M)
C     'PP'    - PRS(MB)       'RA'    - RA(G/KG)      'VSCL' - VL(M)
C     'THP'   - THP(K)
C     'THETA' - THETA(K)      'RL'    - RL(G/KG)      'TG'    - TG (K)
C     'THVP'  - THV'(K)       'RI'    - RI(G/KG)      'SLM'   - SLM (PCT)
C     'TV'    - TV(K)         'RCOND' - RD(G/KG)      'CONPR' - CON RATE
C     'RT'    - RT(G/KG)      'CP'    - NPRIS         'CONP'  - CON PCP
C     'RV'    - RV(G/KG)      'RTP'   - RT'(G/KG)     'CONH'  - CON HEAT
C                                                     'CONM'  - CON MOIS
C     'THIL' - Theta-il (K)      'TEMP'  - temperature (K)
C     'TVP'  - Tv' (K)           'THV'   - Theta-v     (K)
C     'RELHUM'-relative humidity (%)          'SPEED'- wind speed (m/s)
C     'FTHRD'- radiative flux convergence ()
C     'MICRO'- GASPRC
C     'Z0'   - Z0 (M)         'ZI'   - ZI (M)         'ZMAT'  - ZMAT (M)
C     'USTARL'-USTARL(M/S)  'USTARW'-USTARW(M/S)  'TSTARL'-TSTARL (K)
C     'TSTARW'-TSTARW(K)    'RSTARL'-RSTARL(G/G)  'RSTARW'-RSTARW(G/G)
C     'UW'    - UW  (M*M/S*S)                     'VW'    - VW (M*M/S*S)
C     'WFZ'   - WFZ (M*M/S*S)                     'TFZ'   - TFZ (K*M/S)
C     'QFZ'   - QFZ (G*M/G*S)                     'RLONG'- RLONG
C     'RSHORT'-RSHORT


$ISAN_CONTROL
   MSTAGE  = 1,  1,  1,               ! Main switches for
                                      ! pressure, isentropic, "varfile" processing

   NATIMES = 1,                   ! Number of times on which to perform analysis

   IAHOUR  = 00, 06, 12, 18, 24,               ! Hours to analyze
   IADATE  = 18, 18, 19, 19, 20,                ! Dates
   IAMONTH = 7,   7,  7,  7,  7,   ! Months
   IAYEAR  = 91, 91, 91, 91, 91,   ! Years

                   !    NCAR archived data file names

   IAPR     = 'grid.0',         ! Input pressure level dataset

   IARAWI   = 'tempdb',         ! Archived rawindsonde file name

   IASRFCE = 'not-used',         ! Archived surface obs file name

                    ! File names and dispose flags

   IFNPRS = 'ip',  ! Pressure file name prefix
   IOFLGP= 1,                ! Dispose flag:  0 = no write, 1 = write

   IFNISN = 'ii',  ! Isentropic file name prefix
   IOFLGI= 1,                ! Dispose flag:  0 = no write, 1 = write

   IFNSIG = 'is',  ! Sigma-z file name prefix
   IOFLGS= 1,                ! Dispose flag:  0 = no write, 1 = write

   IFNVAR = 'iv',  ! "Variable initialization" file name prefix
   IOFLGV= 1,                ! Dispose flag:  0 = no write, 1 = write


$END

$ISAN_PRESSURE

                   !----------------------------------
                   !   Pressure grid information:
                   !----------------------------------
```

```
 NPRX=36,             ! number of grid points in x (lon) direction
 NPRY=33,             ! number of grid points in y (lat) direction
 NPRZ=10,             ! number of pressure levels

 PDATA= 'SPC',       ! 'NMC' or 'ECMWF' if from NCAR archives.

 WPLON =  -140.0,     ! West longitude bound of pressure data access
 SPLAT =   20.0,     ! South latitude bound
                      ! Latitude and longitude bounds are north and east
                      !   if positive, south and west if negative.


 SPCNPRX = 2.5,       ! East-west grid spacing of pressure data
 SPCNPRY = 1.25,       ! North-south spacing

                      ! Pressure levels (mb) in input dataset to access
 LEVPR  = 1000,850,700,500,400,300,250,200,150,100,

$END

----------------------------------------
    Isentropic and sigma-z processing
----------------------------------------

$ISAN_ISENTROPIC

                 !---------------------------------
                 !     Specify isentropic levels
                 !---------------------------------

 NISN    =    32,       ! number of isentropic levels
 LEVTH   =  280,282,284,286,288,290,292,294,296,298,300,303,306,309,312,
            315,318,321,324,327,330,335,340,345,350,355,360,380,400,420,
            440,460,

                 !---------------------------------
                 !   Analyzed grid information:
                 !---------------------------------

 NIGRIDS =  3,          ! number of RAMS grids to analyze

 TOPSIGZ =  20000.,     ! sigma-z coordinates to about this height

 HYBBOT  = 4000.,       ! Bottom (m) of blended sigma-z/isentropic layer in varfiles
 HYBTOP  = 6000.,       ! Top (m) of blended sigma-z/isentropic layer

 SFCINF  = 1000.,       ! Vertical influence of surface observation analysis

 SIGZWT  =    1.,       ! Weight for sigma-z data in varfile:
                        !     0.= no sigz data, 1.=full weight from surface to HYBBOT

 NFEEDVAR =    1,       ! 1 = feed back nested grid varfile info, 0 = don't

                 !---------------------------------
                 !   Observation number limits:
                 !---------------------------------

 MAXSTA=150,              ! maximum number of rawindsondes (archived + special)
 MAXSFC=1000,             ! maximum number of surface observations

 IARCSND =       0,       ! Input archived soundings ? (0-no, 1-yes)
 IARCSFC =       0,       ! Input archived surface obs ?
 ISPCSND =       1,       ! Input special soundings ?
 ISPCSFC =       1,       ! Input special surface obs ?

 NONLYS  =       0,       ! Number of stations only to be used
 IDONLYS ='76458',        ! Station ID's used

 NOTSTA  =       0,       ! Number of stations to be excluded
 NOTID   ='r76458',       ! Station ID's to be excluded
                          !   Prefix with 'r' for rawindsonde, 's' for surface


 STASEP  =     .0001,      ! Minimum surface station separation in degrees.
                          !   Any surface obs within this distance
                          !   of another obs will be thrown out unless it has
                          !   less missing data, in which case the other obs
                          !   will be thrown out.

 ISTAPLT =       0,       ! If ISTAPLT = 1, soundings are plotted;
```

```
 ISTAREP =       0,        ! If ISTAREP = 1, soundings are listed;
                           !    no objective analysis is done.
                           ! If ISTAREP/ISTAPLT = 0, normal processing is done


 IUPPER  =       1,        ! 1-Do upper air analysis, 0-Only do surface

 IGRIDFL =       1,        ! Grid flag = 0, if no grid point data, only obs
                           !             1, if all grid point data and obs
                           !             2, if partial grid point and obs
                           !             3, if only grid data


 GRIDWT  =       .01, .01,.01,
                           ! Relative weight for the gridded pressure data compared
                           !   to the observational data in the objective analysis


 GOBSEP  =     5.0,        ! Grid-observation separation (degrees)
 GOBRAD  =     5.0,        ! Grid-obs proximity radius (degrees)

 WVLNTH  =  1600., 1200., 400.,
                           ! Used in S. Barnes objective analysis.
                           !    Wavelength in km to be retained to the RESPON
                           !    percent from the data to the upper air grids.
 SWVLNTH =  1000., 400., 100.,
                           ! Wavelength for surface objective analysis

 RESPON  =     .90, .9, .9,
                           ! Percentage of amplitude to be retained.


$END

------------------------------------------
    Graphical processing
------------------------------------------

$ISAN_GRAPH

        ! Main switches for plotting

 IPLTPRS  =   0,      ! Pressure coordinate horizontal plots
 IPLTISN  =   1,      ! Isentropic coordinate horizontal plots
 IPLTSIG  =   1,      ! Sigma-z coordinate horizontal plots
 IPLTSTA  =   0,      ! Isentropic coordinate "station" plots
        !------------------------------------
        ! Pressure plotting information
        !------------------------------------
 ILFT1I  =   0,      ! Left boundary window
 IRGT1I  =  18,      ! Right boundary window
 IBOT1J  =  -3,      ! Bottom boundary window
 ITOP1J  =  13,      ! Top boundary window
                     !    Window defaults to entire domain if one equals 0.

 NPLEV   =   8,              ! Number of pressure levels to plot
 IPLEV   = 1000,850,700,500,400,300,200,100,
                             ! Levels to be plotted
 NFLDU1  =   4,              ! Number of fields to be plotted
 IFLDU1  =   'U','THETA','GEO','RELHUM',         ! Field names
 CONU1   = 0.,0.,0.,0.,      ! Field contour increment
 IVELU1  = 1,0,0,0,          ! Velocity vector flag


        !--------------------------------------
        ! Isentropic plotting information
        !--------------------------------------
 ILFT3I  =   0,      ! Left boundary window
 IRGT3I  =  18,      ! Right boundary window
 IBOT3J  =   3,      ! Bottom boundary window
 ITOP3J  =  13,      ! Top boundary window
                     !    Window defaults to entire domain if one equals 0.

                     ! Upper air plots:

 IUP3BEG = 340,      ! Starting isentropic level for plotting
 IUP3END = 400,      ! Ending isentropic level
 IUP3INC =  60,      ! Level increment

 NFLDU3  =   4,              ! Number of fields to be plotted
```

```
IFLDU3  =   'U','PRESS','MONTSTR','RELHUM',        ! Field names
CONU3   = 0.,0.,                 ! Field contour increment
IVELU3  = 1,0,                   ! Velocity vector flag


        !---------------------------------------
        ! Surface plotting information
        !---------------------------------------
! Uses isentropic plotting window info

NFLDS3  =   4,                   ! Number of surface fields to plot
IFLDS3  =   'U','TEMP','PRESS','RELHUM',        ! Field names
CONS3   = 0.,0.,0.,0.,0.,        ! Field contour increment
IVELS3  = 1,0,0,0,0,             ! Velocity vector flag


        !---------------------------------------
        ! Sigma-z plotting information
        !---------------------------------------
! Uses isentropic plotting window info

ISZBEG = 2,      ! Starting sigma-z level for plotting
ISZEND = 26,      ! Ending sigma-z level
ISZINC = 6,      ! Level increment

NFLDSZ  =   4,                   ! Number of fields to be plotted
IFLDSZ  =   'U','PRESS','THETA','RELHUM',        ! Field names
CONSZ   = 0.,0.,                 ! Field contour increment
IVELSZ  = 1,0,                   ! Velocity vector flag



        !---------------------------------------
        ! "Station" plotting information
        !---------------------------------------

NPLTRAW=0,

NSTIS3  =   4,             ! number of station surface plots
ISTIS3  =  'U','PRESS','RELHUM','TEMP',      ! field names


        !---------------------------------------
        ! Cross-section plotting information
        !---------------------------------------
NCROSS3 =    0,                  ! number of cross section slabs
ICRTYP3 =   2,1,                 ! type of slab: 1=E-W, 2=N-S
ICRA3   =   1,1,                 ! left window
ICRB3   =   35,43,               ! right window
ICRL3   =   22,25,               ! cross section location
NCRFLD3 =   3,                   ! number of plots on each cross section
ICRFLD3 =  'MIXRAT','RELHUM','THETAE',      ! field names
THCON3  =   5.,5.,5.,                       ! contour interval of isentropes
ACON3   =   0.,0.,0.,                       ! contour interval of other field

$END
!-----------------------------------
!   Field values for graphical stage
!-----------------------------------
!
!     Pressure        Isentropic    Station      Sigma-z
!--------------------------------------------------------------------------
!     U               U             U            U
!     V               V             V            V
!     TEMP            PRESS         PRESS        PRESS
!     GEO             GEO           TEMP         THETA
!     RELHUM          RELHUM        RELHUM       RELHUM
!     MIXRAT          MIXRAT        MIXRAT
!     THETA           THETA
!     SPEED           SPEED
!     ENERGY          ENERGY
!     THETAE          THETAE
!     SPRESS          SPRESS
!
```

APPENDIX B

PROWESS RAMSIN file

```
&PARA
   IPARALLEL=1,

   NMACH=6, HOSTS='par7','par6','par5','par4','par3','par2','par1',
   HPERF=1.1, 1.2, 1.3, 1.4, 1.5, 1.6, 1.7,
   HPERF=1.0, 1.0, 1.0, 1.0, 1.0, 1.0, 1.0,
   CPROG='/par0/u1/prowess/system/bin/4an',
   CNAME='/par0/u1/prowess/system/fore/RAMSIN.op',
   CVTAB='/par0/u1/prowess/system/fore/VTABLE',

/ $END


 $MODEL_GRIDS

! Simulation title (64 chars)
  EXPNME  =     'Version 3b sample',
                                           ! -1=diagnostic, 0=normal run
   IOTYPE   = 0,

   RUNTYPE = 'INITIAL',     ! type of run: MAKESFC, INITIAL, HISTORY, or MAKEVFILE

   TIMEUNIT = 'h',                       ! 'h','m','s' - Time units of
                                         !   TIMMAX, TIMSTR, VTIME

   TIMMAX=    20.0,                       ! Final time of simulation


   NGRIDS  =   4,                            ! Number of grids to run
                                             !
   NNXP     =  34,  34, 38, 42,                ! Number of x gridpoints
   NNYP     =  30,  38, 38, 58,                ! Number of y gridpoints
   NNZP     =  30,  30, 30, 30,                ! Number of z gridpoints

   NNZG     =  11,11,11,11,                  ! Number of soil gridpoints

   NXTNEST =   1, 1, 2, 3,                   ! Grid number which is the next
                                             !   coarser grid

      ! Coarse grid specifications

   IHTRAN   =       1,                    ! 0-Cartesian, 1-Polar stereo
   DELTAX   =  72000.,
   DELTAY   =  72000.,                    ! X and Y grid spacing

   DELTAZ   =     75.,                   ! Z grid spacing (set to 0. to use ZZ)
   DZRAT    =     1.25,                   ! vertical grid stretch ratio
   DZMAX    =     1000.,                  ! maximum delta Z for vertical stretch

   ZZ=0., 25., 75., 150., 250., 500., 750., 1000., 1500., 2000., 2500.,
      3250., 4000., 5000., 6000.,
                                          ! Vertical levels if DELTAZ = 0

   DTLONG   =      90.,                   ! Coarse grid long timestep
   NRATIO   =       4,                    ! Small timestep ratio

   IMONTH1 =    01,       ! Month
   IDATE1   =   17,      ! Day
   IYEAR1   =   97,      ! Year
   STRTIM   =   12.0,      ! GMT of model TIME = 0.
                                          ! Nest ratios between this grid
                                          !  and the next coarser grid.
   NSTRATX =   1, 4, 3, 4,                ! x-direction
   NSTRATY =   1, 4, 3, 4,                ! y-direction
   NNDTRAT =   1, 2, 2, 2,                ! time

   NESTZ = 0,                             ! contort coarser grids if negative
   NSTRATZ=4,4,3,3,3,3,2,2,2,2,1,1,1,1,   !


   POLELAT   =  30.0,                      ! Latitude of pole point
   POLELON  =   -83.0,                    ! Longitude of pole point

   CENTLAT=    30.0,28.5,28.5,28.6,
   CENTLON=    -83.0,-82.0,-81.0,-80.75,

                                          ! Grid point on the next coarser
```

```
                                              ! nest where the lower southwest
                                              ! corner of this nest will start.
                                              ! IF NINEST or NJNEST = 0, use CENTLAT/LON
   NINEST   =   1,  0, 0, 0,                  ! i-point
   NJNEST   =   1,  0, 0, 0,                  ! j-point
   NKNEST   =   1,  1, 1, 1,                  ! k-point

   NNSTTOP =    1,    1,    1,   1,             ! Flag (0-no or 1-yes) if this
   NNSTBOT =    1,    1,    1,   1,             ! nest goes the top or bottom of the
                                                ! coarsest nest.

   GRIDU    =  0.,   0.,   0.,   0.,             ! u-component for moving grids
   GRIDV    =  0.,   0.,   0.,   0.,             ! v-component for moving grids
                                                 !  (still not working!)

 $END


 $MODEL_FILE_INFO


               ! History file input

 TIMSTR=   1500.,        ! time of history start (see TIMEUNIT)
 HFILIN = 'cg5.h1500s',    ! input history file name

               ! History/analysis file output

 IOUTPUT=       1,            ! 0-no files, 1-save in ASCII, 2-save in binary
 HFILOUT='hist/f.h',                      ! history file prefix
 AFILOUT='f.a',                        ! analysis file prefix
 HFUNITS='d',      AFUNITS='d',        ! history/anal file units (M,m,H,h,S,s)
 FRQHIS  =72000.,   FRQANL  =3600.,     ! history/anal file frequency

               ! Variable initialization input

 INITIAL =   2,              ! Initial fields - 1=horiz.homogeneous, 2=variable


 VARFIL(1)='isan/pv17-jan-97-00',  VTIME(1)=00.,
 VARFIL(2)='isan/pv17-jan-97-06',  VTIME(2)=06.,
 VARFIL(3)='isan/pv17-jan-97-12',  VTIME(3)=12.,
 VARFIL(4)='isan/pv17-jan-97-18',  VTIME(4)=18.,
 VARFIL(5)='isan/pv17-jan-97-24',  VTIME(5)=24.,


 IVWIND =       0,           ! initial winds ( only 0 works)

 NUDLAT    =    5,           ! number of points in the lateral bnd region
 TNUDLAT   =    900.,        ! nudging time scale (s) at lateral boundary
 TNUDCENT  =    0.,      ! nudging time scale (s) in center of domain
 TNUDTOP   =    0.,      ! nudging time scale (s) at top of domain
 ZNUDTOP   =    15000.,      ! nudging at top of domain above this height (m)

               ! Printed output controls

  FRQPRT   =   21600.,     ! Printout frequency
  FRQIPR   =   99930.,     ! Integral print frequency
  FRQIST   =   99900.,     ! Integral store frequency

  ISTPFL   =        1,     ! Timestep message frequency flag
  INITFLD  =        0,     ! Initial field print flag 0=no print, 1=print
  INPRTFL  =        1,     ! Namelist print flag 0=no print, 1=print

                ! Input topography variables

   SFCFILES = '/par0/ul/prowess/system/fore/sfc2',            ! File path and prefix for
surface characteristic
                                ! files.

   ITOPTFLG = 1,1,1,1,            ! 2 - Fill data in "ruser"
   IPCTLFLG = 1,1,1,1,            ! 1 - Interp data from latlon dataset
   ISSTFLG  = 1,0,0,0,            ! 0 - Interpolate from coarser grid
   IVEGTFLG = 1,1,1,1,


                                !
                                ! The following only apply for IxxxxFLG=1
                                !
```

```
 ITOPTFN = '/u1/prowess/system/data/rams/topo10m/H',
           '/u1/prowess/system/data/rams/topo30s/U',      ! Input topography file name
           '/u1/prowess/system/data/rams/topo30s/U',      ! Input topography file name
           '/u1/prowess/system/data/rams/topo30s/U',      ! Input topography file name

 IPCTLFN = '/u1/prowess/system/data/rams/pctl10m/L',
           '/u1/prowess/system/data/rams/pctl10m/L',
           '/u1/prowess/system/data/rams/pctl10m/L',
           '/u1/prowess/system/data/rams/pctl10m/L',

 ISSTFN  = '/u1/prowess/system/data/rams/sst/SJUL',

 IVEGTFN  = '/u1/prowess/system/data/rams/ndvi/V',
            '/u1/prowess/system/data/rams/ndvi/V',
            '/u1/prowess/system/data/rams/ndvi/V',
            '/u1/prowess/system/data/rams/ndvi/V',

 SILAVWT  = 0.0, 0., 0.,0.,             ! Weighting of topo silhouette averaging
 TOPTWVL  = 4.0, 4., 4.,4.,             ! Topo wavelength cutoff in filter
 PCTLWVL  = 2.0, 2., 2.,2.,             ! Land pct wavelength cutoff in filter
 SSTWVL   = 2.0, 2., 2.,2.,             ! Land pct wavelength cutoff in filter

 MKCOLTAB = 0,          ! make microphysics collection table: 0 = no, 1 = yes
 COLTABFN = '/par0/u1/prowess/system/rams3b/data/micro/ct2.0',    ! collection table
filename to read or write
 EVPTABFN = '/par0/u1/prowess/system/rams3b/data/micro/et2.0',    ! evaporation table
filename to read

$END


$MODEL_OPTIONS

 NADDSC    =    0,0,0,0,     ! Number of additional scalar species (<= 5)


 NTOPSMTH  =        0,   ! Number of passes for topography smoother
 IZFLAT  =          0,   ! Width of flat margin around domain (in grid points)

    ! Numerical schemes

 ITMDIFF =          3,   ! 1=forward, 2=leapfrog, 3=hybrid
 NONHYD   =         1,   ! nonhydrostatic=1, hydrostatic=0
 SSPCT    =        0.,   ! Sound speed fraction for the nonhydrostatic model
 IMPL     =         1,   ! Implicit flag for acoustic model  -  0=off, 1=on
 ICNTEQ   =         2,   ! Hyd - continuity equation - 1 -incomp, 2 -anelastic
 WTKD     =        0.,   ! Klemp/Durran - current timestep weighting

 ICORFLG =          1,   ! Coriolis flag/2D v-component  -  0=off, 1=on

 IBCTOP =           0,   ! top boundary condition
                         ! 0-wall on top(nonhyd)        2-prognostic sfc prs(hyd)
                         ! 1-Klemp-Durran(nonhyd/hyd)  3-material surface(hyd)


 IBND     =         1,   ! Lateral boundary condition flags
 JBND     =         1,   ! 1-Klemp/Wilhelmson, 2-Klemp/Lilly, 3-Orlanski
                         ! 4-cyclic
 CPHAS    =       20.,   ! Phase speed if IBND or JBND = 1
 LSFLG    =         0,   ! Large-scale gradient flag for variables other than
                         ! normal velocity:
                         ! 0 = zero gradient inflow and outflow
                         ! 1 = zero gradient inflow, radiative b.c. outflow
                         ! 2 = constant inflow, radiative b.c. outflow
                         ! 3 = constant inflow and outflow
 NFPT     =         0,   ! Rayleigh friction - number of points from the top
 DISTIM   =       60.,   !                    - dissipation time scale

 TIMSCL   =        0.,   ! Initial wind spin-up - time scale
 KSPIN    =        33,   !                      - below this level (velocity)
 KMSPIN   =        10,   !                      - below this level (momentum)

 IPRSPLT =          0,   ! precipitation time-split scheme - 0=off, 1=on
 IADVL    =         2,   ! Order of advection - Leapfrog - 2 or 4
 IADVF    =         2,   ! Order of advection - Forward - 2 or 6
 IPGRAD   =         1,   ! Pressure gradient scheme for topo.: 1-transform
                         !                                     2-interpolate
 FILT4    =      000.,   ! Fourth order filter coefficient (0 - off)
                         !    ( > 0  timestep at which 2 delta waves are
                         !    totally removed)
 FXLONG   =    0.0000,   ! Long filter coefficient 0=off
```

```
FYLONG  =    0.0000, ! Long filter coefficient 0=off

    ! Radiation parameters

ISWRTYP =     1,     ! Shortwave radiation type 0-none, 2-Mahrer/Pielke, 1-Chen
ILWRTYP =     1,     ! Longwave radiation type 0-none, 2-Mahrer/Pielke, 1-Chen
RADFRQ  = 1200.,      ! Frequency of radiation tendency update in seconds
LONRAD  =     1,     ! Longitudinal variation of shortwave  (0-no, 1-yes)

    ! Cumulus parameterization parameters

NNQPARM =   1,    1,  1,  0,              ! convective parameterization flag
                                          !  0-off, 1-on
CONFRQ  = 1200.,     ! Frequency of conv param. updates in seconds
WCLDBS  =  .001,     ! vertical motion needed at cloud base for convection

    ! Surface layer and soil parameterization

ISFCL   =      1,    ! surface layer/soil/veg model
                     ! 0-specified surface layer gradients
                     ! 1-soil/vegetation model

NVGCON  =       1,      ! Vegetation type
                        ! 1 -- Crop/mixed farming            2 -- Short grass
                        ! 3 -- Evergreen needleleaf tree     4 -- Deciduous needleleaf tree
                        ! 5 -- Deciduous broadleaf tree      6 -- Evergreen broadleaf tree
                        ! 7 -- Tall grass                    8 -- Desert
                        ! 9 -- Tundra                       10 -- Irrigated crop
                        !11 -- Semi-desert                  12 -- Ice cap/glacier
                        !13 -- Bog or marsh                 14 -- Inland water
                        !15 -- Ocean                        16 -- Evergreen shrub
                        !17 -- Deciduous shrub              18 -- Mixed woodland
TSEASN  =   298.,       ! Average seasonal temp
TVGOFF  =     0.,       ! Initial veg temp offset
VWTRCON =      .000,    ! Initial veg water storage (not working)

UBMIN   =   0.25,       ! Minimum U value to use in computing U_*
PCTLCON =  1.0,         ! constant land percentage if for all domain
NSLCON  =    6,         ! constant soil type if for all domain
                      !  1=sand            2=loamy sand      3=sandy loam
                      !  4=silt loam       5=loam            6=sandy clay loam
                      !  7=silty clay loam 8=clay loam       9=sandy clay
                      ! 10=silty clay     11=clay           12=peat

ZROUGH  =  0.05,        ! constant roughness if for all domain
ALBEDO  =   0.2,        ! constant albedo when not running soil model
SEATMP  = 280.,         ! constant water surface temperature

DTHCON  =  -0.,        ! constant surface layer temp gradient for no soil
DRTCON  = .000,         ! constant surface layer moist gradient for no soil
SOILDZ  =   0.,         ! soil model grid spacing
SLZ    = -.50,-.40,-.30,-.25,-.20,-.16,-.12,-.09,-.06,-.03,  0.,! soil grid levels
SLMSTR  =  0.35, 0.35, 0.35, 0.35, 0.35,               ! initial soil moisture
           0.35, 0.35, 0.35, 0.35, 0.35, 0.35,
STGOFF=  5., 5., 5., 5., 3.5,  2.,  .5, -1.,-1.5,-1.8, -2.,
                        ! Initial soil temperature offset from lowest
                        ! atmospheric level


    ! Eddy diffusion coefficient parameters

IDIFFK = 1,1,1,1,            ! K flag:
                             !    1 - Horizontal deformation/ Vertical Mellor-Yamada
                             !    2 - Anisotropic deformation (horiz and vert differ)
                             !    3 - Isotropic deformation (horiz and vert same)
                             !    4 - Deardorff TKE (horiz and vert same)
CSX = .20,.20,.20,.20,.20, ! Adjustable parameter, deformation horiz. K's coefficient
CSZ = .20,.20,.20,.20,.20, ! Adjustable parameter, deformation vert. K's coefficient
XKHKM = 3.,3.,3.,3.,3.,      ! Ratio of horizontal K_h to K_m for deformation
ZKHKM = 3.,3.,3.,3.,3.,      ! Ratio of vertical K_h to K_m for deformation
AKMIN= 1.0,.75,1.0,2.0,1.,    ! Ratio of minimum horizontal eddy viscosity coefficient
                             !    to typical value from deformation K

    ! Microphysics

  NLEVEL  =   3,    3, 3,3,            ! moisture complexity level
!  NLEVEL  =   1,    1, 1,1,            ! moisture complexity level
  INUCPRG =   0,    0, 0,0,            ! Prognose ice nuclei  (0-no, 1-yes)

!  ICLOUD =   0,    0,  0,0,            ! Microphysics flags
```

```
!    IRAIN  =   0,    0,  0,0,              !------------------
!    IPRIS  =   0,    0,  0,0,              !  0 - no species
!    ISNOW  =   0,    0,  0,0,              !  1 - diagnostic concen.
!    IAGGR  =   0,    0,  0,0,              !  2 - specified mean diameter
!    IGRAUP =   0,    0,  0,0,              !  3 - specified y-intercept
!    IHAIL  =   0,    0,  0,0,              !  4 - specified concentration
    ICLOUD =   4,    4,  4,4,              ! Microphysics flags
    IRAIN  =   2,    2,  2,2,              !------------------
    IPRIS  =   5,    5,  5,5,              !  0 - no species
    ISNOW  =   0,    0,  0,0,              !  1 - diagnostic concen.
    IAGGR  =   2,    2,  2,2,              !  2 - specified mean diameter
    IGRAUP =   0,    0,  0,0,              !  3 - specified y-intercept
    IHAIL  =   2,    2,  2,2,              !  4 - specified concentration
                                           !  5 - prognostic concentration

    CPARM  =  .3e9,  .3e9, .3e9,  .3e9,    ! Microphysics parameters
    RPARM  = .1e-2, .1e-2,.1e-2, .1e-2,    !------------------------
    PPARM  =    0.,    0.,   0.,    0.,    ! Characteristic diameter,
    SPARM  = .1e-2, .1e-2,.1e-2, .1e-2,    !    number concentration, or
    APARM  = .1e-2, .1e-2,.1e-2, .1e-2,    !    y-intercept
    GPARM  = .1e-2, .1e-2,.1e-2, .1e-2,
    HPARM  = .3e-2, .3e-2,.3e-2, .3e-2,

    AMI0    =  1.e-12,               ! minimum crystal mass (kg)

!   gnus for: cloud rain pris snow aggr graup hail
    GNU =       2.,   2.,  2.,  2.,  2.,   2.,  2.,    ! gamma shape parms

$END

$MODEL_SOUND
     ! Sounding specification

          ! Flags for how sounding is specified

  IPSFLG=1,     ! specifies what is in PS array
                ! 0 - pressure (mb), 1 - heights (m), PS(1)=sfc press(mb)

  ITSFLG=2,     ! specifies what is in TS array
                ! 0 - temp(C), 1 - temp(K), 2 - pot. temp(K)

  IRTSFLG=3,    ! specifies what is in RTS array
                ! 0 - dew pnt.(C), 1 - dew pnt.(K), 2 - mix rat(g/kg)
                ! 3 - relative humidity on %, 4 - dew pnt depression(K)

  IUSFLG=0,     ! specifies what is in US and VS arrays
                ! 0 - u,v component(m/s), 1 - umoms-direction, vmoms-speed

  IUSRC = 0,    !  source of wind profile:
                !  0  - umoms, vmoms, valid at sounding levels (PS)
                !  -1 - usndg, vsndg, valid at model levels    (Z)

  HS = 0.,

  PS = 1000.,1000.,2000.,3000.,3500.,4500.,7000.,10000.,15000.,20000.,25000.,

  TS =  300.,302.,304.,306.,308.,310.,314.,320.,370.,420.,470.,

  RTS =  60.,60.,60.,60.,10.,10.,10.,10.,10.,10.,10.,

  US =  3.,3.,3.,3.,3.,3.,3.,3.,3.,3.,3.,

  VS =  0.,0.,0.,0.,0.,0.,0.,0.,0.,0.,0.,

  USNDG = 0.,    ! Wind components if IUSRC= -1
  VSNDG = 0.,    !

  KMEAN1 = 0,    !  lower model level for calculation of (umean,vmean)
  KMEAN2 = 0,    !  upper model level for calculation of (umean,vmean)

  UMEAN = 0.0,   !  u-component for Galilean transformation
  VMEAN = 0.0,   !  v-component for Galilean transformation

 $END

 $MODEL_PRINT
          ! Specifies the fields to be printed during the simulation

  NPLT  =  6,              ! Number of fields to be printed at each time
                           !    for various cross-sections (limit of 50)
```

```
 IPLFLD = 'UP','VP','WP','THETA','TKE','RT',
                             ! Field names - see table below
!!  PLFMT(1) = '10PF7.2',      ! Format specification if default is unacceptable

 IXSCTN = 3,3,3,3,3,3,3,3,3,3,3,3,
!  IXSCTN = 2,2,2,2,2,2,2,2,2,2,
                             ! Cross-section type (1=XZ, 2=YZ, 3=XY)
 ISBVAL = 2,2,2,2,2,2,2,2,2,2,2,2,
                             ! Grid-point slab value for third direction

 ! The following variables can also be set in the $PRNT namelist:  IAA,
 ! IAB, JOA, JOB, NAAVG, NOAVG, PLTIT, PLCONLO, PLCONHI, and PLCONIN.

 $END

C     'UP'     - UP(M/S)       'RC'    - RC(G/KG)      'PCPT' - TOTPRE
C     'VP'     - VP(M/S)       'RR'    - RR(G/KG)      'TKE'  - TKE
C     'WP'     - WP(CM/S)      'RP'    - RP(G/KG)      'HSCL' - HL(M)
C     'PP'    - PRS(MB)       'RA'    - RA(G/KG)      'VSCL' - VL(M)
C     'THP'   - THP(K)
C     'THETA'- THETA(K)       'RL'    - RL(G/KG)      'TG'    - TG (K)
C     'THVP' - THV'(K)        'RI'    - RI(G/KG)      'SLM'   - SLM (PCT)
C     'TV'    - TV(K)         'RCOND'- RD(G/KG)       'CONPR'- CON RATE
C     'RT'    - RT(G/KG)      'CP'    - NPRIS         'CONP' - CON PCP
C     'RV'    - RV(G/KG)      'RTP'   - RT'(G/KG)     'CONH' - CON HEAT
C                                                     'CONM' - CON MOIS
C     'THIL' - Theta-il (K)    'TEMP' - temperature (K)
C     'TVP'  - Tv' (K)         'THV'  - Theta-v     (K)
C     'RELHUM'-relative humidity (%)         'SPEED'- wind speed (m/s)
C     'FTHRD'- radiative flux convergence ()
C     'MICRO'- GASPRC
C     'Z0'    - Z0 (M)         'ZI'   - ZI (M)        'ZMAT' - ZMAT (M)
C     'USTARL'-USTARL(M/S) 'USTARW'-USTARW(M/S) 'TSTARL'-TSTARL (K)
C     'TSTARW'-TSTARW(K)    'RSTARL'-RSTARL(G/G) 'RSTARW'-RSTARW(G/G)
C     'UW'    - UW  (M*M/S*S)                        'VW'    - VW (M*M/S*S)
C     'WFZ'   - WFZ (M*M/S*S)                        'TFZ'   - TFZ (K*M/S)
C     'QFZ'   - QFZ (G*M/G*S)                        'RLONG'- RLONG
C     'RSHORT'-RSHORT


 $ISAN_CONTROL
   MSTAGE  = 1,  1,  1,              ! Main switches for
                                     ! pressure, isentropic, "varfile" processing

   NATIMES = 1,                   ! Number of times on which to perform analysis

   IAHOUR  = 24,                 ! Hours to analyze
   IADATE  = 17,                 ! Dates
   IAMONTH = 01,     ! Months
   IAYEAR  = 97,    ! Years

   GUESS1ST='PRESS',

                 !     NCAR archived data file names

   IAPR    = '../data/ip17-jan-97-24' ,

   IARAWI  = ' ' ,          ! Archived rawindsonde file name

   IASRFCE = ' ' ,          ! Archived surface obs file name

                  ! File names and dispose flags

   IFNPRS = 'isan/pp',  ! Pressure file name prefix
   IOFLGP= 1,                ! Dispose flag:  0 = no write, 1 = write

   IFNISN = 'isan/pi',  ! Isentropic file name prefix
   IOFLGI= 1,                ! Dispose flag:  0 = no write, 1 = write

   IFNSIG = 'isan/ps',  ! Sigma-z file name prefix
   IOFLGS= 1,                ! Dispose flag:  0 = no write, 1 = write

   IFNVAR = 'isan/pv',  ! "Variable initialization" file name prefix
   IOFLGV= 1,                ! Dispose flag:  0 = no write, 1 = write


 $END
```

```
$ISAN_PRESSURE

                  !---------------------------------
                  !   Pressure grid information:
                  !---------------------------------
   NPRX=93,              ! number of grid points in x (lon) direction
   NPRY=65,              ! number of grid points in y (lat) direction
   NPRZ=19,              ! number of pressure levels


   WPLON =  -140.0,      ! West longitude bound of pressure data access
   SPLAT =    20.0,      ! South latitude bound
                         ! Latitude and longitude bounds are north and east
                         !   if positive, south and west if negative.


  SPCNPRX = 2.5,         ! East-west grid spacing of pressure data
  SPCNPRY = 1.25,        ! North-south spacing

                         ! Pressure levels (mb) in input dataset to access
  LEVPR  = 1000,950,900,850,800,750,700,650,600,
             550,500,450,400,350,300,250,200,150,100,

$END

-------------------------------------------
     Isentropic and sigma-z processing
-------------------------------------------

$ISAN_ISENTROPIC

                  !---------------------------------
                  !     Specify isentropic levels
                  !---------------------------------

  NISN    =    32,       ! number of isentropic levels
  LEVTH   =  280,282,284,286,288,290,292,294,296,298,300,303,306,309,312,
             315,318,321,324,327,330,335,340,345,350,355,360,380,400,420,
             440,460,

                  !---------------------------------
                  !   Analyzed grid information:
                  !---------------------------------

  NIGRIDS =  3,          ! number of RAMS grids to analyze

  TOPSIGZ =  20000.,     ! sigma-z coordinates to about this height

  HYBBOT  = 4000.,       ! Bottom (m) of blended sigma-z/isentropic layer in varfiles
  HYBTOP  = 6000.,       ! Top (m) of blended sigma-z/isentropic layer

  SFCINF  = 1000.,       ! Vertical influence of surface observation analysis

  SIGZWT  =    1.,       ! Weight for sigma-z data in varfile:
                         !     0.= no sigz data, 1.=full weight from surface to HYBBOT

  NFEEDVAR =    1,       ! 1 = feed back nested grid varfile info, 0 = don't

                  !---------------------------------
                  !   Observation number limits:
                  !---------------------------------

  MAXSTA=150,               ! maximum number of rawindsondes (archived + special)
  MAXSFC=1000,              ! maximum number of surface observations

  IARCSND =       1,        ! Input archived soundings ? (0-no, 1-yes)
  IARCSFC =       1,        ! Input archived surface obs ?
  ISPCSND =       0,        ! Input special soundings ?
  ISPCSFC =       0,        ! Input special surface obs ?

  NONLYS  =       0,        ! Number of stations only to be used
  IDONLYS ='76458',         ! Station ID's used

  NOTSTA  =       0,        ! Number of stations to be excluded
  NOTID   ='r76458',        ! Station ID's to be excluded
                            !   Prefix with 'r' for rawindsonde, 's' for surface


  STASEP  =     .001,       ! Minimum surface station separation in degrees.
                            !    Any surface obs within this distance
```

```
                              !    of another obs will be thrown out unless it has
                              !    less missing data, in which case the other obs
                              !    will be thrown out.

 ISTAPLT =      0,            ! If ISTAPLT = 1, soundings are plotted;
 ISTAREP =      0,            ! If ISTAREP = 1, soundings are listed;
                              !    no objective analysis is done.
                              ! If ISTAREP/ISTAPLT = 0, normal processing is done


 IUPPER  =      1,            ! 1-Do upper air analysis, 0-Only do surface

 IGRIDFL =      1,            ! Grid flag = 0, if no grid point data, only obs
!!!   IGRIDFL =      3,          ! Grid flag = 0, if no grid point data, only obs
                              !             1, if all grid point data and obs
                              !             2, if partial grid point and obs
                              !             3, if only grid data


 GRIDWT  =       .01, .01, .01,
                              ! Relative weight for the gridded pressure data compared
                              !   to the observational data in the objective analysis


 GOBSEP  =    5.0,            ! Grid-observation separation (degrees)
 GOBRAD  =    5.0,            ! Grid-obs proximity radius (degrees)

 WVLNTH  =  1200., 900., 600.,
                              ! Used in S. Barnes objective analysis.
                              !    Wavelength in km to be retained to the RESPON
                              !    percent from the data to the upper air grids.
 SWVLNTH =  750., 300.,  150.,
                              ! Wavelength for surface objective analysis

 RESPON  =    .90, .9,   .9,
                              ! Percentage of amplitude to be retained.


$END
------------------------------------------
     Graphical processing
------------------------------------------

$ISAN_GRAPH

        ! Main switches for plotting

IPLTPRS  =   0,      ! Pressure coordinate horizontal plots
IPLTISN  =   1,      ! Isentropic coordinate horizontal plots
IPLTSIG  =   1,      ! Sigma-z coordinate horizontal plots
IPLTSTA  =   0,      ! Isentropic coordinate "station" plots
        !---------------------------------------
        ! Pressure plotting information
        !---------------------------------------
ILFT1I  =   0,      ! Left boundary window
IRGT1I  =  18,      ! Right boundary window
IBOT1J  =   3,      ! Bottom boundary window
ITOP1J  =  13,      ! Top boundary window
                    !    Window defaults to entire domain if one equals 0.

NPLEV   =   2,               ! Number of pressure levels to plot
IPLEV   = 1000,500,
                             ! Levels to be plotted
NFLDU1  =   4,               ! Number of fields to be plotted
IFLDU1  =   'U','THETA','GEO','RELHUM',          ! Field names
CONU1   = 0.,0.,0.,0.,       ! Field contour increment
IVELU1  = 2,0,0,0,           ! Velocity vector flag


        !---------------------------------------
        ! Isentropic plotting information
        !---------------------------------------
ILFT3I  =   0,      ! Left boundary window
IRGT3I  =  18,      ! Right boundary window
IBOT3J  =   3,      ! Bottom boundary window
ITOP3J  =  13,      ! Top boundary window
                    !    Window defaults to entire domain if one equals 0.

                    ! Upper air plots:
```

```
IUP3BEG = 340,      ! Starting isentropic level for plotting
IUP3END = 4000,      ! Ending isentropic level
IUP3INC =  60,      ! Level increment

NFLDU3  =   4,                 ! Number of fields to be plotted
IFLDU3  =   'U','PRESS','MONTSTR','RELHUM',          ! Field names
CONU3   = 0.,0.,               ! Field contour increment
IVELU3  = 1,0,                 ! Velocity vector flag


        !-------------------------------------
        ! Surface plotting information
        !-------------------------------------
! Uses isentropic plotting window info

NFLDS3  =   4,                 ! Number of surface fields to plot
IFLDS3  =   'U','TEMP','PRESS','RELHUM',          ! Field names
CONS3   = 0.,0.,0.,0.,0.,      ! Field contour increment
IVELS3  = 1,0,0,0,0,           ! Velocity vector flag


        !-------------------------------------
        ! Sigma-z plotting information
        !-------------------------------------
! Uses isentropic plotting window info

ISZBEG = 2,      ! Starting sigma-z level for plotting
ISZEND = 26,      ! Ending sigma-z level
ISZINC = 6,      ! Level increment

NFLDSZ  =   4,                 ! Number of fields to be plotted
IFLDSZ  =   'U','PRESS','THETA','RELHUM',          ! Field names
CONSZ   = 0.,0.,               ! Field contour increment
IVELSZ  = 1,0,                 ! Velocity vector flag



        !-------------------------------------
        ! "Station" plotting information
        !-------------------------------------
NPLTRAW = 9,            ! Approximate number of raw rawinsonde plots per
                        !    frame. 0 turns off plotting.

NSTIS3  =   3,          ! number of station surface plots
ISTIS3  =  'PRESS','TEMP','RELHUM',     ! field names


        !-------------------------------------
        ! Cross-section plotting information
        !-------------------------------------
NCROSS3 =    0,                  ! number of cross section slabs
ICRTYP3 =   2,1,                 ! type of slab: 1=E-W, 2=N-S
ICRA3   =   1,1,                 ! left window
ICRB3   =   35,43,               ! right window
ICRL3   =   22,25,               ! cross section location
NCRFLD3 =   3,                   ! number of plots on each cross section
ICRFLD3 =  'MIXRAT','RELHUM','THETAE',     ! field names
THCON3  =   5.,5.,5.,                      ! contour interval of isentropes
ACON3   =   0.,0.,0.,                      ! contour interval of other field

$END
!----------------------------------
!   Field values for graphical stage
!----------------------------------
!
!     Pressure         Isentropic    Station       Sigma-z
!--------------------------------------------------------------------------
!     U                U             U             U
!     V                V             V             V
!     TEMP             PRESS         PRESS         PRESS
!     GEO              GEO           TEMP          THETA
!     RELHUM           RELHUM        RELHUM        RELHUM
!     MIXRAT           MIXRAT        MIXRAT
!     THETA            THETA
!     SPEED            SPEED
!     ENERGY           ENERGY
!     THETAE           THETAE
!     SPRESS           SPRESS
!
```

APPENDIX C

ERDAS HYPACT_IN file

```
 &hypact_in
 hypref='/u1/met/9701171200.alt3/RAMS/f.a                                                                  ',
freqpwrt=  600.0000000    ,
hpartfile='./test/H.                                    ',
dtpart= 120.00000000    ,
maxpart=      100000,
npartbl=       10000,
freqavg=  600.0000000    ,
npsources=          21,
emission=  305.7910156    ,  1242.040039    ,  279.9200134    ,  297.2650146    ,
641.5090332    ,  695.7250366    ,  629.8619995    ,  655.7630615    ,  675.3580322    ,
3182.340088    ,  3350.410156    ,  672.8680420    ,  637.9080200    ,  598.8270264    ,
593.5370483    ,  572.7090454    ,  504.3070374    ,  429.7100220    ,  1379.640015    ,
1599.430054    ,  3960.960205    , 0.0000000000E+00, 0.0000000000E+00, 0.0000000000E+00,
0.0000000000E+00, 0.0000000000E+00, 0.0000000000E+00, 0.0000000000E+00, 0.0000000000E+00,
0.0000000000E+00, 0.0000000000E+00, 0.0000000000E+00, 0.0000000000E+00, 0.0000000000E+00,
0.0000000000E+00, 0.0000000000E+00, 0.0000000000E+00, 0.0000000000E+00, 0.0000000000E+00,
0.0000000000E+00, 0.0000000000E+00, 0.0000000000E+00, 0.0000000000E+00, 0.0000000000E+00,
0.0000000000E+00, 0.0000000000E+00, 0.0000000000E+00, 0.0000000000E+00, 0.0000000000E+00,
0.0000000000E+00,
szpwr=  1.000000000    ,
szmin=  1.000000000    ,
szmax=  1.000000000    ,
irelstrt=      163200,     163200,     163200,     163200,     163200,     163200,     163200,
163200,     163200,     163200,     163200,     163200,     163200,     163200,     163200,
163200,     163200,     163200,     163200,     163200,     163200,          0,          0,
0,          0,          0,          0,          0,          0,          0,          0,
0,          0,          0,          0,          0,          0,          0,          0,
0,          0,          0,          0,          0,          0,          0,          0,
0,          0,          0,
ireldur=          1,          1,          1,          1,          1,          1,          1,
1,          1,          1,          1,          1,          1,          1,          1,
1,          1,          1,          1,          1,          1,          0,          0,
0,          0,          0,          0,          0,          0,          0,          0,
0,          0,          0,          0,          0,          0,          0,          0,
0,          0,          0,          0,          0,          0,          0,          0,
0,          0,          0,
isimend=     203000,
istrtdays=          0,          0,          0,          0,          0,          0,
0,          0,          0,          0,          0,          0,          0,          0,
0,          0,          0,          0,          0,          0,          0,          0,
0,          0,          0,          0,          0,          0,          0,          0,
0,          0,          0,          0,          0,          0,          0,          0,
0,          0,          0,          0,          0,          0,          0,          0,
0,          0,          0,          0,
idurdays=          0,          0,          0,          0,          0,          0,          0,
0,          0,          0,          0,          0,          0,          0,          0,
0,          0,          0,          0,          0,          0,          0,          0,
0,          0,          0,          0,          0,          0,          0,          0,
0,          0,          0,          0,          0,          0,          0,          0,
0,          0,          0,          0,          0,          0,          0,          0,
0,          0,          0,
ienddays=          0,
tricoord= 0.0000000000E+00,
srcx= -80.55101776    , -80.55413818    , -80.55320740    , -80.55086517    , -80.54810333
, -80.54810333    , -80.54810333    , -80.54810333    , -80.54810333    , -80.54810333    , -
80.54810333    , -80.54810333    , -80.54810333    , -80.54810333    , -80.54810333    , -
80.54810333    , -80.54810333    , -80.54810333    , -80.54810333    , -80.54810333    , -
80.54810333    , 0.0000000000E+00, 0.0000000000E+00, 0.0000000000E+00, 0.0000000000E+00,
0.0000000000E+00, 0.0000000000E+00, 0.0000000000E+00, 0.0000000000E+00, 0.0000000000E+00,
0.0000000000E+00, 0.0000000000E+00, 0.0000000000E+00, 0.0000000000E+00, 0.0000000000E+00,
0.0000000000E+00, 0.0000000000E+00, 0.0000000000E+00, 0.0000000000E+00, 0.0000000000E+00,
0.0000000000E+00, 0.0000000000E+00, 0.0000000000E+00, 0.0000000000E+00, 0.0000000000E+00,
0.0000000000E+00, 0.0000000000E+00, 0.0000000000E+00, 0.0000000000E+00, 0.0000000000E+00,
srcy=  28.42615509    ,  28.42622375    ,  28.42408943    ,  28.42531013    ,  28.42695618
,  28.42695618    ,  28.42695618    ,  28.42695618    ,  28.42695618    ,  28.42695618    ,
28.42695618    ,  28.42695618    ,  28.42695618    ,  28.42695618    ,  28.42695618    ,
28.42695618    ,  28.42695618    ,  28.42695618    ,  28.42695618    ,  28.42695618    ,
28.42695618    , 0.0000000000E+00, 0.0000000000E+00, 0.0000000000E+00, 0.0000000000E+00,
0.0000000000E+00, 0.0000000000E+00, 0.0000000000E+00, 0.0000000000E+00, 0.0000000000E+00,
0.0000000000E+00, 0.0000000000E+00, 0.0000000000E+00, 0.0000000000E+00, 0.0000000000E+00,
0.0000000000E+00, 0.0000000000E+00, 0.0000000000E+00, 0.0000000000E+00, 0.0000000000E+00,
0.0000000000E+00, 0.0000000000E+00, 0.0000000000E+00, 0.0000000000E+00, 0.0000000000E+00,
0.0000000000E+00, 0.0000000000E+00, 0.0000000000E+00, 0.0000000000E+00, 0.0000000000E+00,
srcz=  349.8999939    ,  449.8999939    ,  508.2500000    ,  524.9499512    ,  550.0000000
,  583.4500122    ,  614.4500122    ,  643.0000000    ,  671.5499878    ,  742.9499512    ,
```

```
856.3499756    , 925.0999756    , 950.0999756    , 975.0999756    , 1000.949951    ,
1028.599976    , 1057.199951    , 1085.750000    , 1200.000000    , 1450.099976    ,
2050.100098    , 0.0000000000E+00, 0.0000000000E+00, 0.0000000000E+00, 0.0000000000E+00,
0.0000000000E+00, 0.0000000000E+00, 0.0000000000E+00, 0.0000000000E+00, 0.0000000000E+00,
0.0000000000E+00, 0.0000000000E+00, 0.0000000000E+00, 0.0000000000E+00, 0.0000000000E+00,
0.0000000000E+00, 0.0000000000E+00, 0.0000000000E+00, 0.0000000000E+00, 0.0000000000E+00,
0.0000000000E+00, 0.0000000000E+00, 0.0000000000E+00, 0.0000000000E+00, 0.0000000000E+00,
0.0000000000E+00, 0.0000000000E+00, 0.0000000000E+00, 0.0000000000E+00, 0.0000000000E+00,
xsize=  470.3999939    , 705.7999878    , 789.0000000    , 808.2000122    , 833.7999878
,  862.0000000    , 883.0000000    , 898.0000000    , 909.2000122    , 921.2000122    ,
894.5999756    , 848.7999878    , 826.0000000    , 799.4000244    , 767.4000244    ,
727.5999756    , 679.4000244    , 622.2000122    , 399.7999878    , 399.7999878    ,
399.7999878    , 0.0000000000E+00, 0.0000000000E+00, 0.0000000000E+00, 0.0000000000E+00,
0.0000000000E+00, 0.0000000000E+00, 0.0000000000E+00, 0.0000000000E+00, 0.0000000000E+00,
0.0000000000E+00, 0.0000000000E+00, 0.0000000000E+00, 0.0000000000E+00, 0.0000000000E+00,
0.0000000000E+00, 0.0000000000E+00, 0.0000000000E+00, 0.0000000000E+00, 0.0000000000E+00,
0.0000000000E+00, 0.0000000000E+00, 0.0000000000E+00, 0.0000000000E+00, 0.0000000000E+00,
0.0000000000E+00, 0.0000000000E+00, 0.0000000000E+00, 0.0000000000E+00, 0.0000000000E+00,
ysize=  470.3999939    , 705.7999878    , 789.0000000    , 808.2000122    , 833.7999878
,  862.0000000    , 883.0000000    , 898.0000000    , 909.2000122    , 921.2000122    ,
894.5999756    , 848.7999878    , 826.0000000    , 799.4000244    , 767.4000244    ,
727.5999756    , 679.4000244    , 622.2000122    , 399.7999878    , 399.7999878    ,
399.7999878    , 0.0000000000E+00, 0.0000000000E+00, 0.0000000000E+00, 0.0000000000E+00,
0.0000000000E+00, 0.0000000000E+00, 0.0000000000E+00, 0.0000000000E+00, 0.0000000000E+00,
0.0000000000E+00, 0.0000000000E+00, 0.0000000000E+00, 0.0000000000E+00, 0.0000000000E+00,
0.0000000000E+00, 0.0000000000E+00, 0.0000000000E+00, 0.0000000000E+00, 0.0000000000E+00,
0.0000000000E+00, 0.0000000000E+00, 0.0000000000E+00, 0.0000000000E+00, 0.0000000000E+00,
0.0000000000E+00, 0.0000000000E+00, 0.0000000000E+00, 0.0000000000E+00, 0.0000000000E+00,
zsize=  100.0000000    , 100.0000000    , 16.69998169    , 16.70001221    , 33.40002441
,  33.50000000    , 28.50000000    , 28.59997559    , 28.50000000    , 114.2999878    ,
112.5000000    , 25.00000000    , 25.00000000    , 25.00000000    , 26.70001221    ,
28.60003662    , 28.59997559    , 28.50000000    , 200.0000000    , 300.1999512    ,
899.8000488    , 0.0000000000E+00, 0.0000000000E+00, 0.0000000000E+00, 0.0000000000E+00,
0.0000000000E+00, 0.0000000000E+00, 0.0000000000E+00, 0.0000000000E+00, 0.0000000000E+00,
0.0000000000E+00, 0.0000000000E+00, 0.0000000000E+00, 0.0000000000E+00, 0.0000000000E+00,
0.0000000000E+00, 0.0000000000E+00, 0.0000000000E+00, 0.0000000000E+00, 0.0000000000E+00,
0.0000000000E+00, 0.0000000000E+00, 0.0000000000E+00, 0.0000000000E+00, 0.0000000000E+00,
0.0000000000E+00, 0.0000000000E+00, 0.0000000000E+00, 0.0000000000E+00, 0.0000000000E+00,
ihfall=          0,
ihturb=          1,
 sourcetype(1)='lag/1/ellipse/total',
 sourcetype(2)='lag/1/ellipse/total',
 sourcetype(3)='lag/1/ellipse/total',
 sourcetype(4)='lag/1/ellipse/total',
 sourcetype(5)='lag/1/ellipse/total',
 sourcetype(6)='lag/1/ellipse/total',
 sourcetype(7)='lag/1/ellipse/total',
 sourcetype(8)='lag/1/ellipse/total',
 sourcetype(9)='lag/1/ellipse/total',
 sourcetype(10)='lag/1/ellipse/total',
 sourcetype(11)='lag/1/ellipse/total',
 sourcetype(12)='lag/1/ellipse/total',
 sourcetype(13)='lag/1/ellipse/total',
 sourcetype(14)='lag/1/ellipse/total',
 sourcetype(15)='lag/1/ellipse/total',
 sourcetype(16)='lag/1/ellipse/total',
 sourcetype(17)='lag/1/ellipse/total',
 sourcetype(18)='lag/1/ellipse/total',
 sourcetype(19)='lag/1/ellipse/total',
 sourcetype(20)='lag/1/ellipse/total',
 sourcetype(21)='lag/1/ellipse/total',
numparts=        200,       200,       200,       200,       200,       200,       200,
200,       200,       200,       200,       200,       200,       200,       200,
200,       200,       200,       200,       200,       200,       0,         0,
0,         0,         0,         0,         0,         0,         0,         0,
0,         0,         0,         0,         0,         0,         0,         0,
0,         0,         0,         0,         0,         0,         0,         0,
0,         0,         0,
rotation= 0.0000000000E+00,
mxcg=        400,
mycg=        400,
mzcg=         40,
delxcg=  600.000000    ,
delycg=  600.000000    ,
delzcg=  75.00000000    ,
centxcg= -80.56600    ,
```

```
centycg=  28.00     ,
ixyslab=           4,
ixzslab=           100,
iyzslab=           0,
&end
```

APPENDIX D

PROWESS HYPACT_IN file

```
&HYPACT_IN
hypref='/u1/met/970117.12/RAMS/f.a',
freqpwrt=600.,   iavgout=1,
hpartfile='./test/H.',
dtpart=120.,
maxpart=46000, npartbl=46000,
freqavg=600.,
ihturb=1,
iadvord=2,
nspecies=0,
npsources=2,
irelstrt=163000,163000,060000,060000,060000,
istrtdays=    0,      0,      0,      0,      0,
ireldur =000500,000500,002000,002000,002000,
idurdays=     0,      0,      0,      0,      0,
isimend =203000,
ienddays=     0,
numparts=3000,3000,400,400,400,
emission=1.,1.,1.,1.,1.,
tricoord=-4.,42.,-3.,43.,-2.,41.,
          2.,4.,6.,3.,5.,7.,
          2.,4.,6.,3.,5.,7.,
srcy=28.448,28.448,
srcx=-80.566,-80.566,
srcz=600.,1800.,
xsize=600.,600.,3000.,3000.,
ysize=600.,600.,6000.,6000.,
zsize= 400.,400.,100.,100.,
sourcetype(1)='lag/1/ellipse/total',
sourcetype(2)='lag/1/ellipse/total',
sourcetype(3)='lag/1/ellipse/total',
sourcetype(4)='lag/2/rectangle/total',
sourcetype(5)='both/3/ellipse/scaled',
rotation=0.,0.,30.,30.,45.,45.,
ihfall=0,
szpwr=1.,1.,1.,1.,1.,
szmin=1.,1.,1.,1.,1.,
szmax=1.,1.,1.,1.,1.,
mxcg=400,
mycg=400,
mzcg=40,
delxcg=600.,
delycg=600.,
delzcg=75.,
centycg=28.00,
centxcg=-80.566,
ixyslab=4,
ixzslab=100,
iyzslab=0,
&end
```

NOTICE

REPORT DOCUMENTATION PAGE			Form Approved OMB No. 0704-0188

1. AGENCY USE ONLY (Leave blank)	2. REPORT DATE July 2000	3. REPORT TYPE AND DATES COVERED Contractor Report

4. TITLE AND SUBTIITLE Delta II Explosion Plume Analysis Report	5. FUNDING NUMBERS C-NAS10-96018
6. AUTHOR(S) Randolph J. Evans	
7. PERFORMING ORGANIZATION NAME(S) AND ADDRESS(ES) ENSCO, Inc., 1980 North Atlantic Avenue, Suite 230, Cocoa Beach, FL 32931	8. PERFORMING ORGANIZATION REPORT NUMBER 00-004
9. SPONSORING/MONITORING AGENCY NAME(S) AND ADDRESS(ES) NASA, John F. Kennedy Space Center, Code AA-C-1, Kennedy Space Center, FL 32899	10. SPONSORING/MONITORING AGENCY REPORT NUMBER CR-2000-208582
11. SUPPLEMENTARY NOTES Subject Cat.: #47 (Meteorology and Climatology)	
12A. DISTRIBUTION/AVAILABILITY STATEMENT Unclassified - Unlimited	12B. DISTRIBUTION CODE

13. ABSTRACT (Maximum 200 Words)

A Delta II rocket exploded seconds after liftoff from Cape Canaveral Air Force Station (CCAFS) on 17 January 1997. The cloud produced by the explosion provided an opportunity to evaluate the models which are used to track potentially toxic dispersing plumes and clouds at CCAFS. The primary goal of this project was to conduct a case study of the dispersing cloud and the models used to predict the dispersion resulting from the explosion. The case study was conducted by comparing mesoscale and dispersion model results with available meteorological and plume observations.

The models used in the study are part of the Eastern Range Dispersion Assessment System (ERDAS) and include the Regional Atmospheric Modeling System (RAMS), HYbrid Particle And Concentration Transport (HYPACT), and Rocket Exhaust Effluent Dispersion Model (REEDM).

The primary observations used for explosion cloud verification of the study were from the National Weather Service's Weather Surveillance Radar 1988-Doppler (WSR-88D). Radar reflectivity measurements of the resulting cloud provided good estimates of the location and dimensions of the cloud over a four-hour period after the explosion.

The results indicated that RAMS and HYPACT models performed reasonably well. Future upgrades to ERDAS are recommended.

14. SUBJECT TERMS Dispersion, Diffusion, Mesoscale Modeling, Launch Plume, Rocket Explosion, Weather Radar, RAMS, HYPACT, ERDAS, REEDM, Hazardous Material, Toxic Cloud	15. NUMBER OF PAGES 104 16. PRICE CODE

17. SECURITY CLASSIFICATION OF REPORT	18. SECURITY CLASSIFICATION OF THIS PAGE	19. SECURITY CLASSIFICATION OF ABSTRACT	20. LIMITATION OF ABSTRACT
UNCLASSIFIED	UNCLASSIFIED	UNCLASSIFIED	NONE